Quantized Scalar Fields Under the Influence of Moving Mirrors and Anisotropic Curved Spacetime

Michael R.R. Good

A dissertation submitted to the faculty of the University of North Carolina at Chapel Hill in partial fulfillment of the requirements for the degree of Doctor of Philosophy in the Department of Physics and Astronomy.

Chapel Hill
2011

Approved by:

Charles R. Evans

Paul R. Anderson

Y. Jack Ng

J. Christopher Clemens

Jonathan Engel

Abstract

MICHAEL R.R. GOOD: Quantized Scalar Fields Under the Influence of Moving Mirrors and Anisotropic Curved Spacetime.
(Under the direction of Charles R. Evans and Paul R. Anderson.)

This thesis develops three main topics. First, the moving mirror model is examined where particle and energy creation occur for a minimally coupled, quantized massless scalar field. New exactly solvable trajectories are introduced such that the Bogolubov transformation coefficients are found and energy flux is calculated. The integrated solutions are verified on the past and future hypersurfaces using a split-mode technique. The time-dependent acceleration responsible for thermal radiation is revealed.

The second main part involves calculations of spectral time evolution analysis of those trajectory solutions which are asymptotically inertial and unitary by construction. Quanta summing, energy flux integration and energy packet summations are compared and verified.

The third main piece involves renormalization counterterms for the field fluctuations and energy density terms in curved spacetime using a quantized scalar field with arbitrary mass and general curvature coupling. Adiabatic regularization is used to generate the counterterms for $\langle \phi^2 \rangle$ and the energy density in a general Bianchi Type I anisotropic spacetime. The results are verified in both the isotropic and conformal coupling limits.

Acknowledgments

Table of Contents

Chapter 1

Introduction

It took nearly 22 years after Casimir [1] first ushered in his celebrated effect before a dynamic version was conceived by Moore [2]. Hawking's seminal paper [3] motivated the coming realization that the dynamical Casimir effect (DCE) was intimately related to the physics of black hole radiation. Independent of Moore's work, DeWitt noticed that accelerated neutral conductors radiate particles[4]. As a follow up to DeWitt and Moore's program, Davies and Fulling[5][6] found that essential features of quantum field theory in curved spacetime can be explored using a specific example of the DCE, without the complication of curved geometry. Thus the first 'moving mirror' trajectory was created and used to uncover the interesting aspects of black hole formation and evaporation.

The moving mirror model [5],[6] describes the disturbance of a field by an accelerated boundary which results in the appearance of energy and particles. The mirror model is closely and fundamentally related to black hole evaporation because both effects are the result of the amplification of quantum field fluctuations. In the black hole case this is due to strongly time dependent gravitational fields while in the mirror case this is due to strongly time dependent accelerations. Acceleration

radiation without a boundary-the Unruh effect[7], has a strong and intimate relevance to these phenomena. As the mirror model matured [8] [9] [10] [11] [12], it became apparent that accelerating boundaries could be used to understand entropy production [13],[14], the relationship between particles and energy[15], and thermodynamical paradoxes [16] [17] [18], among other topics. The DCE's kinship to the celebrated and experimentally well-confirmed Casimir effect is understood within the framework of quantum field theory in curved spacetime (see the textbooks: [4][19][20][21][22][23]). The DCE has the exciting potential to be measured,[24] [25], while there have been serious proposals that it has already been seen [26]. At the time of this writing, researchers are claiming to have measured the DCE via a superconducting circuit in which a superconducting quantum interference device (SQUID) effectively acts as a moving mirror [27].

The importance of vacuum polarization and particle creation in the presence of moving boundaries exemplified by the DCE is highlighted by the attention it has received on numerous fronts [28]. Notably, moving mirrors are used because they are a simple way to understand the gravitational field. In flat spacetime the mirror plays a role similar to a time-dependent background geometry, distorting field modes like in the gravitational case. This close kinship has been used to understand the nature of the black hole evaporation calculation by offering a simpler framework in which to proceed.

1.1 Davies-Fulling Effect

The simplest theoretical manifestation of the DCE is that of the moving mirror model in (1+1) dimensional flat spacetime. This was first investigated by Moore in 1970 [2] and later by DeWitt in 1975 [4]. However, Davies and Fulling were the first to show

that with the right trajectory a Planck spectrum in analogy with the Planck spectrum that Hawking found for black hole evaporation can be obtained. The problem Davies and Fulling [5][6] laid out was the creation of particles and energy in a two dimensional quantum theory of a massless scalar field influenced by the motion of a perfectly reflecting boundary. This model is technically simple and sheds light on the evaporation process of black holes. Davies and Fulling sought to untangle the local, operational association of particles and the formal, global-dependent definition of particles. One of their goals was to understand and extract an intuitive notion of particles, and in addition, investigate carefully the connection between particles and energy in quantum field theory.

Their two major papers are widely credited for the discovery of the moving mirror-black hole connection[5][6]. Most of the calculational framework for the moving mirror model resides here and among the major advances of these papers were the well-known solutions for the stress energy tensor of the quantum field, the quantum field two point function, and the basic conclusion that moving mirrors may produce energy and particles. They were the first to conclude that late time asymptotic behavior ($t \to \infty$) involving infinite acceleration for a boundary trajectory, i.e. $\alpha \to \infty$, ($z \to -t - Ae^{-2\kappa t} + B$) results in black body radiation in two dimensions with $T = \kappa/2\pi$.

There are a number of deficiencies of the Davies-Fulling model and trajectory, despite its pioneering and significant results. The original calculations ignore integral boundary terms and make use of questionable approximations. Fulling [29] points out that the hard-to-justify calculations proved to be 'embarrassing' but that the basic conclusions are not changed. Calogeracos [30] [31] [32] has helped to point out much of the calculational issues involving the Bogolubov coefficients in the original Davies-Fulling calculation. While Walker [15] and Grove [33] have followed up

with detailed treatments intended to correct, polish and expand on the original calculations involving the energy-particle connection, creation and detection. Walker suggests that the simple formula for summing quanta to find total energy will not be valid if the trajectory has an asymptote. Grove contends that particle flux is coincident with energy flux in the moving mirror model.

I also revisit the Davies-Fulling trajectory in order to compute correctly the beta coefficients for the original Davies-Fulling trajectory in Section 3.3.3. This form is a specific realization of the original late time form and I have confirmed the late-time trajectory approaches thermal character in the high frequency limit.

One limitation of the Davies-Fulling trajectory, by its very construction, is that it is a late-time trajectory. Without an early-time form, one cannot compute particle or energy creation during this interesting region of motion. I have addressed this limitation of the Davies-Fulling trajectory through the creation of three distinct 'all-time' trajectories. These new trajectories have motions which are exactly known for early times. These static-start future-horizon mirrors are discussed in Section 3.5 and, in addition, contain new and interesting physical content not associated with the original Davies-Fullling mirror. For instance, one trajectory has an extended pulse of positive energy flux during a phase of its motion, (subsection 3.5.2). I have also solved for the Bogolubov transformation coefficients using no approximations.

Another weakness in the calculations done by Davies and Fulling is that the Bogolubov transformation coefficients were computed by only integrating over part of I^{+}[1]. Walker and Davies state that asymptotically null trajectories are associated with "... a crop of problems to do with the completeness of the field modes on I^{+}..." [34].

---

[1] I^{+} is future null infinity with fixed $t - x$, or $v \to +\infty$. I^{-} is past null infinity with fixed $t + x$ or $u \to -\infty$.

Carlitz and Willey[11] have pointed out a correct way to deal with the completeness, orthogonality and normalization conditions for the modes of a trajectory that emits a constant energy flux for all times. I have addressed the issue of modes in the Davies-Fulling model and trajectory motion by use of the correct set of modes to avoid completeness problems on I^+ in conjunction with the three static-start future horizon mirrors.

Walker and Davies have claimed that the ultimately unphysical character of asymptotically null trajectories in their model [34] is motivation for finding asymptotically inertial trajectories. Calogeracos points out that his results [31] offer a guide to what can be realistically expected in the case where a mirror does not have its velocity forever increasing (a spliced trajectory was used to stop the acceleration). There are several advantages to and motivations for considering asymptotically inertial trajectories, which we will spell out in detail.

In an effort to avoid the inherently unphysical nature of asymptotically null trajectories of the Davies-Fulling model, I have utilized the advantages of asymptotically inertial trajectories in two, exactly solvable, unspliced (no artificial joining of distinct trajectories), relativistic mirror motions in Chapter 3. These mirror trajectories are also introduced in order to investigate the dynamical nature of the onset of particle and energy creation. In particular we emphasize that there is finite energy production with these trajectories. These trajectories have made it possible to obtain time dependent spectra using wavepacket localization of the Bogolubov coefficients as discussed in Section 1.4.

1.2 Walker-Davies and Carlitz-Willey Trajectories

A trajectory which has received little attention, but nevertheless is of significant interest was presented by Walker and Davies in 1982.[34] They consider a mirror trajectory that is asymptotically inertial (static in fact) in the far past and future. The main results are a finite, exactly-known total energy, and finite particle creation count, $\langle N \rangle$ (which is not exactly known). This is the first and only asymptotically inertial mirror trajectory that we know of in the literature. We distinguish the static future motion of the mirror by calling mirrors of this type, Future Asymptotically Static Trajectories, (FAST). It is also the first and only finite energy result from a non-spliced mirror trajectory. With this FAST mirror, Walker and Davies avoid late time approximations and problems with completeness of the field modes on the future null surface.

There are a few disadvantages, however, in using the Walker-Davies trajectory. The trajectory function $z(t)$, which is important for calculating the acceleration and the ray-tracing function, is unknown. The transcendental inversion necessary to find this form is hard to obtain analytically. This complexity makes it difficult to compute energy flux or total energy in the standard way.

If one looks at Figure 2 of [34], one notices there is a period in which the mirror emits a negative flux of energy. This raises the interesting question of whether or not the total energy emitted by this mirror as computed by integrating over the energy flux emitted is the same as the total energy by summing the energies of all the particles created. I have confirmed that this is true, as was originally formulated in general by Walker [15]. The Walker-Davies Bogolubov transformation coefficients are consistent with the total energy result, which is confirmed by explicitly performing the summation of particle energies. This is done by verifying the consistency of the beta coefficients and total energy of the solution in Walker-Davies through the use of numerically summing quanta. Confirmation of the original Walker-Davies

Bogolubov coefficients and total energy are given in Chapter 3, Section 3.4.

I have introduced two new trajectories that are also asymptotically inertial and instead of asymptotically static like the Walker-Davies mirror, have asymptotically constant velocities. One mirror reaches an arbitrary constant velocity (between zero and the speed of light) and the other asymptotically approaches the speed of light. Called COnstant-velocity ASymptotic Trajectories (COAST mirrors), these new solutions, as opposed to the FAST Walker-Davies solution, are expressed as functions of $z(t)$ rather than $t(z)$ and consequently, a closed form for the proper acceleration is given. A form for one of the trajectory's ray-tracing function has been found that allows energy flux to be calculated.

Carlitz and Willey's 1987 seminal paper [11] computes particle creation for a mirror trajectory that emits a constant energy flux. The result is a thermal spectrum for all times. Their solution is important because they compute the Bogolubov transformation coefficients exactly and analytically. They use a combination of null coordinate integrals and a left-right construction for the past null integration surface. Their result, which most mimics an eternal black hole that thermally evaporates for all times at a fixed temperature, does not utilize any late time approximations. They went further and studied stimulated emission, stress-energy tensor correlations, and the density matrix.

The biggest shortcoming in the Carlitz-Willey paper is that there is no expression for the trajectory itself. Despite finding the Bogolubov transformation coefficients, no analytic is given for finding the proper acceleration of the trajectory. It would be useful to understand analytically the time-dependence of the Carlitz-Willey trajectory. I have solved for the explicit form of their trajectory and the time-dependent proper acceleration that results in a constant energy flux. I also have provided the

7

transcendental inversion necessary to obtain the ray-tracing function from the trajectory function.

The Carlitz-Willey trajectory has constant particle emission or energy flux. I have expanded on their model by the introduction of mirror trajectories, which are in some ways similar, but for which the early-time particle production rate is dynamic. In addition Carlitz and Willey solved for the eternal Planck spectrum using the density matrix formulation. I add to their valuable contribution by using a method of particle localization which removes occupation number divergences. I have found that spectrum is Planckian. This is discussed in Chapter 4.

1.3 Asymptotically Inertial Mirrors

Although the advantages of asymptotically inertial trajectories were foreseen, ([35], [32], [13]) no examples besides the Walker-Davies mirror exist. Wilczek has qualitatively considered the class of mirror trajectories depicted in Figure 3.1 and Section 3.4, where the mirrors eventually stop accelerating. He noted that as all rays eventually intersect the mirror, and get reflected to I^+, a pure state is obtained on I^+. The mirror can emit radiation that can look thermal for an arbitrarily long time. When the mirror stops accelerating there is no longer any radiation emitted and the transition to zero acceleration can be done smoothly, so that only a small burst accompanies it. The burst can have a magnitude that is essentially independent of the length of the interval over which thermal radiation has occurred. He emphasizes that this burst (which is negative energy flux emission) is the price paid for quantum purity.[35]

Calogerocos in 2001 [32] makes the clear distinction between type (1) (asymptotically inertial) trajectories where the mirror ends its acceleration and type (2) (diverging acceleration) mirrors where acceleration reaches an infinite singularity in the future. There are two subsets of type (1) mirrors, COnstant-velocity ASymptotic Trajectories (COAST mirrors), and asymptotically zero velocity trajectories, Future Asymptotically Static Mirrors (FAST mirrors). COAST mirrors end their motion with a constant, coasting velocity, ξ, while FAST mirrors come to a complete stop. Calogeracos has also pointed out the many advantages in considering asymptotically inertial trajectories, type (1) mirrors: First, acceleration continuing for an infinite time leads to serious problems (mathematical singularities, infinite energy that has to be imparted to the mirror, etc). Second, the mirrors rest frame eventually (after acceleration stops) becomes an inertial frame and the standard description in terms of IN and OUT states is possible. A freedom to choose either the lab frame or the mirrors rest frame to describe emitted photons is possible. Third, one can make unambiguous statements pertaining to particle production at times $t \to \pm\infty$ when the acceleration vanishes.[32]

COAST mirrors, as a subset of type (1) trajectories, model black hole evaporation which does not 'finalize'. Although particle production eventually stops, and positive frequencies at late times are indeed reflected into positive frequencies at early times, the frequencies of the modes are highly redshifted. Thus, as pointed out by Wilczek [35], at late times a left over remnant will exist that delays particles for a long time and saps their energy, causing these highly redshifted late time modes. For FAST mirrors, (asymptotically static), particles emitted at late times, which intersect the mirror during its second period of rest, behave as if passing through the origin of empty space in the analogue black hole problem. Thus FAST mirror trajectories provide a model for a black hole that completely evaporates.[35] Both the COAST

9

and FAST mirror constructions incorporate pure initial states that evolve into a pure final states.

Asymptotically inertial mirrors echo a backreaction-type effect. In black hole evaporation, the total energy radiated is given by integrating the luminosity over the entire radiation time. The importance of backreaction effects of radiated black hole energy on the background geometry is justified by the necessity to have a finite integrated energy emitted per unit time (luminosity $\sim$ erg/s). Ignore backreaction and the black hole will emit forever giving a divergent total energy result. This situation is in contradiction with the finite amount of energy contained inside the black hole. Therefore, the primary consequence of backreaction should be to provide a finite result for the total radiated energy. Modification of the exponential trajectory in the moving mirror model to obtain an asymptotically inertial motion in the past and future has some similarities with black hole radiation backreaction. Unitary by construction, because all the incident waves from I_R^- are reflected to I_R^+, this class of trajectories has $\langle T_{uu} \rangle \to 0$ in the asymptotic past and future. It is known that an interesting feature of this class of mirrors is that their emitted flux is not always positive [23].

I have introduced the first asymptotic constant velocity trajectories for which the Bogolubov transformation coefficients have been computed analytically and exactly. These trajectories are smooth, continuous and therefore no δ-function pulses are emitted. These COAST mirrors (two of them) are discussed in Section 3.4. I have computed the COAST mirror's energies, their Bogolubov coefficients and other revelant quantities. I find that for an extended part of their trajectories, negative energy flux is emitted. These COAST mirror radiate a total positive finite amount of energy. I present time evolved spectral analyses of the radiation emitted by the mirrors following these trajectories in Chapter 4.

1.4 Wavepacket Quantization

Wavepackets were used by Hawking in his original calculation of black hole radiation [3]. Wave packetization for the moving mirror model was used to compute a finite spectrum in [36]. The localization procedure utilized there has a 'double' packetization approach on both mode frequencies, *in* and *out*. The meaning of these mode frequencies is clarified in Chapter 2. Avoiding the infinite expression for the total number of particles obtained by the standard monochromatic modes, the wavepacket quantization technique was applied to the originally [5] calculated Davies-Fulling Bogolubov coefficients. Regardless of the fact that these beta Bogolubov coefficients were obtained with obscure approximations[29], the divergences are eliminated using wavepackets. As a method for localizing the global Bogolubov coefficients or localizing the modes, wave packetization has been fruitful for obtaining finite results [23].

However, there are shortcomings in the approaches so far for wavepacket localization to the moving mirror model. Wavepackets were applied to the those transformation coefficients which utilized obscure approximations in the case of the late-time Davies-Fulling trajectory [5]. There has been no association of wavepackets with a localized energy production. This is important for confirming the particle/energy connection. So far the use of wavepackets has been strictly limited in its application to the Davies-Fulling late-time form. Wavepackets have not been (numerically or analytically) utilized to localize energy or particles at early times in the moving mirror model. There has been no effort to confirm total energy production from a moving mirror using localization of particles, as well as no effort to confirm the Planck spectrum for the constant flux trajectory.

I apply wave packet localization introduced in Section 4.1 to the COAST mirrors

introduced in Chapter 3 to time evolve their spectra. I apply wavepackets to the correct transformation coefficients in the asymptotically inertial mirror cases and I use wavepackets to confirm total energy production. I extend the concept of wavepackets to an energy packet. I have found a relationship between applying packetization to either modes or Bogolubov transformation coefficients. The first derivation of the Planck spectrum using wavepackets for the constant flux mirror (Carlitz and Willey trajectory) is given. This work is discussed in Chapter 4.

1.5   Adiabatic Regularization in Bianchi Type I

Quantum effects may be of practical importance to cosmology in the context of a hypothetical anisotropic early stage of the universe. It has been shown that particle production can dissipate anisotropy [37] [38] [39] [40] [41] [42]. One way to compute the dissipation of anisotropy due to particle production is to solve the semiclassical backreaction equations. This requires the use of a renormalized energy-momentum tensor.

There are a number of different schemes to regularize and renormalize the formally divergent stress tensor and other quantities that involve squares or higher powers of fields or their derivatives evaluated at a single point of spacetime. There is dimensional regularization, zeta-function regularization, point-splitting regularization and adiabatic regularization [19]. In this thesis we employ zeta-function regularization for the static Casimir effect in Chapter 2 and adiabatic regularization in Chapter 5. Adiabatic regularization is arguably one of the the most efficient methods for calculating the finite expectation values of quadratic field quantities, rather than just the form of the divergences. It involves a mode-by-mode subtraction technique and is useful for numerical calculations.

Adiabatic regularization was first introduced by Parker [43] in an attempt to understand particle number expectation values, it was then later generalized and applied to the stress tensor in several other papers: Fulling-Parker (1974) [44], Fulling-Parker-Hu (1974)[45], Parker-Fulling (1974)[46]. Birrell [47] and Anderson-Parker [48] showed that adiabatic regularization gives the same results as point-splitting in homogeneous and isotropic spacetimes.

The basic approach to stress tensor renormalization involves expectation values of $T_{\mu\nu}$ which are calculated from formally divergent mode sums. An adiabatic vacuum state, $|0_A\rangle$, is defined using a WKB approximation. This characterizes the high frequency behavior of the quantum field and since the divergences in the original mode sum come from the high-frequency modes, they are the same divergences in $\langle 0_A|T_{\mu\nu}|0_A\rangle$. The original mode sum can be renormalized by subtracting it from the quantity $\langle 0_A|T_{\mu\nu}|0_A\rangle$ calculated to adiabatic order four. Applying this subtraction to the integrand of the original mode sum leaves finite integrals. The result determines the renormalized expectation value and is conserved. Fulling-Parker-Hu (FPH) [45] calculated the energy-momentum tensor for a conformally coupled scalar field in an arbitrary Bianchi Type I anisotropic metric. They used adiabatic regularization to find the divergent counterterms for the energy density.

I have computed the renormalization counterterms for the field fluctuations, $\langle \phi^2 \rangle$, in an arbitrary Bianchi Type I anisotropic spacetime. In the isotropic limit I have checked my results by comparing with those of Ref. [49]. In addition, this calculation has been done with arbitrary mass and general coupling. I have computed an analytical approximation for $\langle \phi^2 \rangle$ in a limited class of anisotropic metrics. This calculation is verified in the isotropic limit in accordance with [49]. I have also computed the renormalization counterterms for the energy density of a scalar field with general coupling and arbitrary mass. I have checked in the limit of conformal coupling

that my results agree with those of FPH. I have also checked that for general coupling, my expressions agree with Bunch in the isotropic limit [50]. These calculations are presented in Chapter 5.

Chapter 2

Elements of Quantum Field Theory

2.1 Background: Quantum Field Theory

2.1.1 Massless Scalar Field in (1+1) Dimensional Flat Spacetime

In order to offer the relevant background for our subsequent discussion of the moving mirror model and cosmological particle creation, this section presents some basics of quantum field theory. Particular emphasis is on the normalization conventions and (1+1) dimensions. This treatment does not include the imposition of the mirror or curved space, but nevertheless remains relevant for future reference. Those readers who are adequately familiar with quantum field theory in Minkowski space will still gain utility from the explicit and simplified treatment of the formulas relevant for the free, massless, real, scalar field in (1+1) dimensions.

The simplest, non-trivial quantum field theory that can be constructed is that of a massless scalar field with Lagrangian

$$\mathcal{L} = \frac{1}{2}(\partial_\mu \psi)^2 = \frac{1}{2}\eta^{\mu\nu}\partial_\mu \psi \partial_\nu \psi \; , \tag{2.1}$$

where $\eta_{\mu\nu}$ is the Minkowski metric,

$$\eta_{\mu\nu} = \begin{bmatrix} 1 & 0 \\ 0 & -1 \end{bmatrix} , \tag{2.2}$$

in (1+1) dimensions. After varying the action, $S = \int \mathcal{L} d^2 x$, and setting $\delta S = 0$, the field equation is derived from the Euler-Lagrange equations,

$$\partial_\mu \frac{\partial \mathcal{L}}{\partial(\partial_\mu \psi)} = \frac{\partial \mathcal{L}}{\partial \psi} , \tag{2.3}$$

and is shown to be in this case

$$\Box \psi = \partial_t^2 \psi - \partial_x^2 \psi = 0 . \tag{2.4}$$

This is the massless Klein-Gordon field equation in (1+1) dimensions. Varying the action with respect to the metric, gives the energy-momentum-stress tensor (stress tensor)

$$T_{\mu\nu} = (\partial_\mu \psi)(\partial_\nu \psi) - \frac{1}{2}\eta_{\mu\nu}\eta^{\lambda\delta}(\partial_\lambda \psi)(\partial_\delta \psi) . \tag{2.5}$$

Explicitly, one gets for the energy density, $T_{tt} = \frac{1}{2}[(\partial_t \psi)^2 + (\partial_x \psi)^2]$, and the other components of the energy-momentum tensor

$$T_{\mu\nu} = \frac{1}{2} \begin{bmatrix} (\partial_t \psi)^2 + (\partial_x \psi)^2 & \partial_t \psi \partial_x \psi + \partial_x \psi \partial_t \psi \\ \partial_t \psi \partial_x \psi + \partial_x \psi \partial_t \psi & (\partial_t \psi)^2 + (\partial_x \psi)^2 \end{bmatrix} . \tag{2.6}$$

When the field is expanded in terms of the field modes, ϕ_ω,

$$\psi = \int_{-\infty}^{\infty} dk \, [a_k \phi_\omega + a_k^\dagger \phi_\omega^*] , \tag{2.7}$$

16

where a and $a^\dagger$ are annihilation and creation operators, respectively. The modes are orthogonal and normalized according to the (1+1) dimensional scalar product

$$(\phi_1, \phi_2) = -i \int_t dx \, [\phi_1 \partial_t \phi_2^* - \phi_2^* \partial_t \phi_1] \equiv i \int_{-\infty}^{\infty} dx \, \phi_2^* \overset{\leftrightarrow}{\partial_t} \phi_1 = \delta(\omega_1 - \omega_2) \,, \qquad (2.8)$$

where we have introduced the $\overset{\leftrightarrow}{\partial}$ notation for simplicity. Here t denotes a spacelike hypersurface of simultaneity at instant t. For more on the constant t hypersuface, see Parker 2009 [20]. The hypersurface is a Cauchy surface. A Cauchy surface is any subset of spacetime which is intersected by every non-spacelike, causal curve, exactly once. Quantization proceeds in the canonical way by treating the field as an operator and imposing equal time commutation relations,

$$[\psi(t, x), \psi(t, x')] = [\pi(t, x), \pi(t, x')] = 0 \,, \qquad [\psi(t, x), \psi(t, x')] = i\delta(x - x') \,, \quad (2.9)$$

with $\pi \equiv \frac{\partial \mathcal{L}}{\partial(\partial_t \psi)} = \partial_t \psi$. The expansion of the field in terms of modes allows us to express the commutation relations as,

$$[a_k, a_{k'}] = [a_k^\dagger, a_{k'}^\dagger] = 0 \,, \qquad [a_k, a_{k'}^\dagger] = \delta(k - k') \,. \qquad (2.10)$$

Flat Spacetime Without A Mirror

In flat spacetime with no boundaries (see Fig 2.1), the right moving modes $(+k)$ take the form of positive and negative frequency solutions, respectively,

$$\phi_\omega = \frac{1}{\sqrt{4\pi\omega}} e^{-i\omega(t-x)}, \qquad \phi_\omega^* = \frac{1}{\sqrt{4\pi\omega}} e^{i\omega(t-x)} \,. \qquad (2.11)$$

17
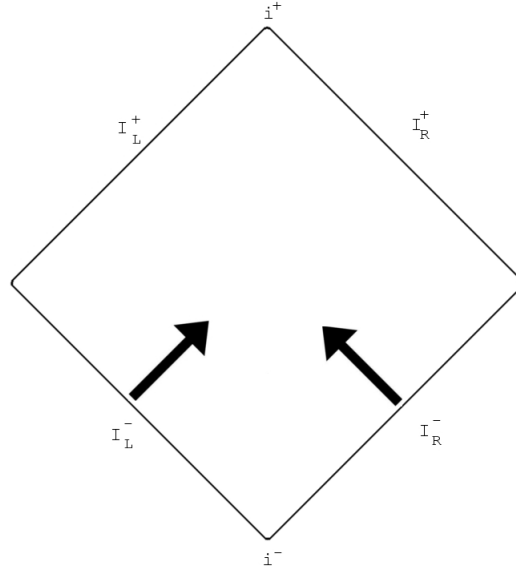
Figure 2.1: Penrose diagram in flat space without a mirror. The arrows indicate left and right moving field modes.

The left moving modes $(-k)$ with positive and negative frequencies are

$$\phi_\omega = \frac{1}{\sqrt{4\pi\omega}}e^{-i\omega(t+x)} \; , \qquad \phi_\omega^* = \frac{1}{\sqrt{4\pi\omega}}e^{i\omega(t+x)} \; . \tag{2.12}$$

For spacetimes of dimension n, the normalization factor is generalized to $[2\omega(2\pi)^{n-1}]^{-1/2}$[19].
The terms, 'positive' and 'negative' above, refer to the fact that applying the operator $\hat{E} \to i\partial_t$, gives a positive eigenvalue,

$$i\partial_t\phi_\omega = \omega\phi_\omega \; , \quad \omega > 0 \; , \tag{2.13}$$

for the 'positive' frequency ϕ_ω mode, and a negative eigenvalue

$$i\partial_t\phi_\omega^* = -\omega\phi_\omega^* \; , \quad \omega > 0 \; , \tag{2.14}$$

18

for the 'negative' frequency ϕ_ω^* mode. Notice that $\omega \geq 0$ always. Note also that the dispersion relation, $\omega = |\vec{k}|$ ($E = |\vec{p}|$), holds because the quanta are massless. As can be verified, the modes are normalized according to the scalar product, Equation (2.8).

Null Coordinates

It is often helpful to work in null coordinates, $u = t - x$, $v = t + x$ where the line element becomes $ds^2 = dudv$. Then the metric, from $ds^2 = \eta_{\mu\nu}dx^\mu dx^\nu$, is

$$\eta_{\mu\nu} = \frac{1}{2}\begin{bmatrix} 0 & 1 \\ 1 & 0 \end{bmatrix}. \tag{2.15}$$

The Klein-Gordon field equation then takes the form

$$\partial_u \partial_v \psi = 0 . \tag{2.16}$$

The scalar product is used to normalize the modes. If we choose a right moving set of solutions, $\phi_\omega \propto e^{-i\omega u}$, and integrate over the hypersurface taken to be the Cauchy surface $\mathcal{I}^- = \mathcal{I}_L^- \bigcup \mathcal{I}_R^-$, then the functions are normalized

$$i \int_{-\infty}^{\infty} du\ \phi_{\omega'}^*\ \overleftrightarrow{\partial}_u\ \phi_\omega = \delta(\omega - \omega') , \tag{2.17}$$

where the integration is done along $\mathcal{I}_L^-$ and the integration along $\mathcal{I}_R^-$ gives no contribution. For left moving modes, $\phi_\omega \propto e^{-i\omega v}$, the set of mode functions are also normalized on $\mathcal{I}^-$

$$i \int_{-\infty}^{\infty} dv\ \phi_{\omega'}^*\ \overleftrightarrow{\partial}_v\ \phi_\omega = \delta(\omega - \omega') , \tag{2.18}$$

where the integration is done along $\mathcal{I}_R^-$ with no contribution along $\mathcal{I}_L^-$. If we instead chose a future Cauchy surface to perform normalization, $\mathcal{I}^+ = \mathcal{I}_L^+ \bigcup \mathcal{I}_R^+$, then the right movers are integrated along $\mathcal{I}_L^+$, over u, with no contribution from the $\mathcal{I}_R^+$ side, (integration over v). The left movers are integrated over $\mathcal{I}_R^+$, over v and have no contribution from the $\mathcal{I}_L^+$ side (integration over u). See Fig. 2.1.

Simple expressions for the modes in null coordinates will prove useful for computing transformation coefficients between different modes. The positive and negative frequency modes take the simple right moving forms,

$$\phi_\omega = \frac{1}{\sqrt{4\pi\omega}} e^{-i\omega u} , \qquad \phi_\omega^* = \frac{1}{\sqrt{4\pi\omega}} e^{i\omega u} , \tag{2.19}$$

and one may also choose the left moving forms

$$\phi_\omega = \frac{1}{\sqrt{4\pi\omega}} e^{-i\omega v} , \qquad \phi_\omega^* = \frac{1}{\sqrt{4\pi\omega}} e^{i\omega v} . \tag{2.20}$$

In addition, the stress tensor components in null coordinates become

$$T_{\mu\nu} = \begin{bmatrix} (\partial_u \phi_\omega)^2 & \frac{1}{2}\partial_u \phi_\omega \partial_v \phi_w \\ \frac{1}{2}\partial_u \phi_\omega \partial_v \phi_w & (\partial_v \phi_\omega)^2 \end{bmatrix} . \tag{2.21}$$

2.1.2 Transformation Coefficients

The first set of modes,

$$\psi = \int_{-\infty}^{\infty} dk \, [a_k \phi_\omega + a_k^\dagger \phi_\omega^*] , \tag{2.22}$$

is not the only way to decompose the field. Consider a second set of modes which are complete and are also used to expand the field,

$$\psi = \int_{-\infty}^{\infty} dk' \, [b_{k'} \chi_{\omega'} + b_{k'}^\dagger \chi_{\omega'}^*] . \tag{2.23}$$

20

A new vacuum state and a new Fock space are defined through this second set. The two sets of modes are clearly distinguished by ϕ_ω and $\chi_{\omega'}$ and will sometimes only be distinguished by ω or ω' in the literature (and we will often follow suit). They can be expanded in terms of each other

$$\phi_\omega = \int_0^\infty d\omega' \left[\alpha_{\omega'\omega}^* \chi_{\omega'} - \beta_{\omega'\omega} \chi_{\omega'}^* \right], \qquad \text{and} \qquad (2.24)$$

$$\chi_{\omega'} = \int_0^\infty d\omega \left[\alpha_{\omega'\omega} \phi_\omega + \beta_{\omega'\omega} \phi_\omega^* \right], \qquad (2.25)$$

where normalization must be done to the transformation coefficients.

These transformations are called Bogolubov transformations and the coefficients, $\alpha_{\omega'\omega}$ and $\beta_{\omega'\omega}$ are the Bogolubov coefficients which are defined up to an arbitrary phase factor (unit complex number). We can use whatever definition we like, as in the end, the number, energy, entropy or any observable will be invariant of the definition after the modulus of the coefficient is squared. The transformation coefficients are evaluated as

$$\alpha_{\omega'\omega} = i \int_{-\infty}^\infty dv \, \chi_{\omega'}^* \overset{\leftrightarrow}{\partial}_v \phi_\omega \,, \qquad (2.26)$$

$$\beta_{\omega'\omega} = i \int_{-\infty}^\infty dv \, \chi_{\omega'}^* \overset{\leftrightarrow}{\partial}_v \phi_\omega^* \,. \qquad (2.27)$$

These expressions are for left-moving modes, where the Cauchy surface has been chosen to be the null past surface. For more on the convention for the Bogolubov coefficients used by Carlitz and Willey, see [11].

The physical meaning of the Bogolubov coefficients reveals itself by the fact that as long as $\beta \neq 0$, the Fock spaces based on the two choices of modes are different. In particular, the vacuum state for the ϕ_ω modes, $|0_{\phi_\omega}\rangle$, is not annihilated by $b_{\omega'}$, $b_{\omega'}|0_{\phi_\omega}\rangle = \beta_{\omega'\omega}|1_{\phi_\omega}\rangle \neq 0$ and the expectation value of the number operator, $N_\omega =$

$a_\omega^\dagger a_\omega$, in the vacuum state of the $\chi_{\omega'}$ modes is non-zero,

$$\langle 0_{\chi_{\omega'}} | N_\omega | 0_{\chi_{\omega'}} \rangle = \int_0^\infty d\omega' |\beta_{\omega'\omega}|^2 \neq 0 \ . \tag{2.28}$$

In this case, the vacuum of the $\chi_{\omega'}$ modes contains $\int d\omega' |\beta_{\omega'\omega}|^2$ particles in the ϕ_ω mode.

Different Bogolubov Coefficient Definitions

Birrell and Davies [19] use a different but equivalent definition for the Bogolubov coefficients. They use

$$\alpha_{\omega'\omega} = (\chi_{\omega'}, \phi_\omega) = i \int_{-\infty}^\infty dv \ \phi_\omega^* \overset{\leftrightarrow}{\partial_v} \chi_{\omega'} \ , \tag{2.29}$$

$$\beta_{\omega'\omega} = -(\chi_{\omega'}, \phi_\omega^*) = -i \int_{-\infty}^\infty dv \ \phi_\omega \overset{\leftrightarrow}{\partial_v} \chi_{\omega'} \ . \tag{2.30}$$

The difference only leads to a factor of $-i$ which should not cause confusion. The difference in definitions is an irrelevant phase factor. Switching from the Birrell and Davies to Carlitz and Willey definitions is done by, $\alpha \to \alpha^*$ and $\beta \to -\beta^*$. We have found the Carlitz-Willey convention to be more convenient.

2.1.3   The Model

The moving mirror model in (1+1) dimensions consists of a perfectly reflecting boundary in Minkowski space where the massless scalar field ϕ, described by

$$(\partial_t^2 - \partial_x^2)\phi = 0 \ , \tag{2.31}$$

and is required to vanish at the mirror,

$$\phi|_z = 0 \ . \tag{2.32}$$

The mirror is assumed to follow some timelike trajectory, $x = z(t)$. There are two ways of expressing the mode solutions for the field.[1]

$$\phi_\omega^{in} = \frac{i}{\sqrt{4\pi\omega}} [e^{-i\omega v} - e^{-i\omega p(u)}] \ , \qquad \text{or} \tag{2.33}$$

$$\phi_\omega^{out} = \frac{i}{\sqrt{4\pi\omega}} [e^{-i\omega f(v)} - e^{-i\omega u}] \ . \tag{2.34}$$

This field behavior results from satisfying both the field equation, Equation (2.31), and the boundary condition, Equation (2.32). Here

$$p(u) = 2t_u - u \ , \qquad u = t_u - z(t_u) \ , \tag{2.35}$$

$$f(v) = 2t_v - v \ , \qquad v = t_v + z(t_v) \ . \tag{2.36}$$

The procedure for calculating interesting observables, like the energy or particle number, starts with the choice of an appropriate trajectory, $z(t)$. The definition $u = t_u - z(t_u)$ is used to find $u(t)$, inverted to find $t(u)$, and plugged into $p(u) = 2t_u - u$ to find $p(u)$. A similar procedure works for $f(v)$ where one uses $v = t_v + z(t_v)$ to find $v(t)$, inverted to find $t(v)$, and plugged into $f(v) = 2t_v - v$ to find $f(v)$. One can also use $p^{-1}(u) = f(v)$. A key feature of these procedures relies on the ability to solve for the relevant, and often transcendental, function inversions. This transcendental inversion requirement has made it difficult to find exactly solvable

---

[1]If the mirror has a future asymptotically null trajectory to $v = v_{max}$ then for $v > v_{max}$ the modes that do not hit the mirror will have a different form. See for example Carlitz-Willey[11].

mirror trajectories. The function $p(u)$, commonly called the ray tracing function[51], characterizes the mirror trajectory and is incorporated in the modes, the two-point function, the energy flux, and the correlation functions.

Particles via Beta Bogolubov Coefficients

Null Coordinate Beta Integrals

The Bogoliubov beta coefficient integrals are[2]

$$\beta_{\omega'\omega} = i \int_{-\infty}^{\infty} dv \ \phi_{\omega'}^{in*} \overset{\leftrightarrow}{\partial_v} \phi_{\omega}^{out*} \ , \tag{2.37}$$

$$\beta_{\omega'\omega} = i \int_{-\infty}^{\infty} du \ \phi_{\omega'}^{in*} \overset{\leftrightarrow}{\partial_u} \phi_{\omega}^{out*} \ . \tag{2.38}$$

Using null coordinates while avoiding partial integration, we substitute the modes, Eqn. (2.33) and Eqn. (2.34), into the above integrals to obtain

$$\beta_{\omega'\omega} = (4\pi\sqrt{\omega\omega'})^{-1} \int_{-\infty}^{\infty} dv \ e^{i\omega'v} e^{i\omega f(v)} \left(\omega' - \omega f'(v)\right) \ , \tag{2.39}$$

$$\beta_{\omega'\omega} = (4\pi\sqrt{\omega\omega'})^{-1} \int_{-\infty}^{\infty} du \ e^{i\omega u} e^{i\omega' p(u)} \left(\omega' p'(u) - \omega\right) \ . \tag{2.40}$$

These integrals are used to solve for the 'beta' Bogolubov coefficients. The coefficients may be computed on both the past and future null surfaces, respectively. Note that the integrals are taken along their respective surface, simplifying the input of

---

[2]These formulas are valid for 'physical' mirrors which do not have asymptotically null trajectories. Those trajectories which start static but proceed with acceleration for infinite time will require an additional integral for the future surface of the form $\int_{v_{max}}^{\infty} dv$.

the modes Eqn's (2.33) and (2.34). In the presence of a horizon[3] the same form of the field modes will not be integrated over the entire future surface. Carlitz-Willey utilizes a 'work-around' for complete Cauchy surface integration and normalization by incorporating a new form for the field modes which are well defined for the modes that reflect and do not reflect due to horizons. For more on the past and future Cauchy surfaces see Fabbri [23] and for the remedy procedure see Carlitz and Willey [11]. The alpha Bogolubov coefficient may be obtained by a similar pair of integrals by simply switching the sign on ω. The particle occupation number per mode ω and ω' are respectively found by

$$\langle N_\omega \rangle = \int_0^\infty |\beta_{\omega'\omega}|^2 d\omega' \,, \tag{2.41}$$

and

$$\langle N_{\omega'} \rangle = \int_0^\infty |\beta_{\omega'\omega}|^2 d\omega \,. \tag{2.42}$$

The first equation is the occupation number for the quantity that is often called the 'out' particles for the 'in' vacuum state. Of course, it is a particle count per mode ω. The expectation value for the global quantity of total particles created is the double integral

$$\langle N \rangle = \int_0^\infty \int_0^\infty |\beta_{\omega'\omega}|^2 d\omega' d\omega \,. \tag{2.43}$$

This quantity is dimensionless. If acceleration continues forever, the total number diverges, usually because the particle occupation number, Eqn. (2.41), diverges.

---

[3]A horizon in the moving mirror model is a null asymptote made by a diverging acceleration mirror motion. If a mirror approaches the speed of light, the field modes traveling to the left will eventually be unable to reflect off of the mirror. As the acceleration diverges, the last null ray that will be able to reflect off of the mirror forms what is refered to as a horizon.

Total Energy from Summing Quanta

If the acceleration does not continue forever, then one may find the total energy produced by summing the quanta [15],

$$E = \int_0^\infty \omega \langle N_\omega \rangle d\omega \ .$$ (2.44)

Energy via Stress Tensor

Energy Flux from $p(u)$, $z(t_u)$, or $\dot{\alpha}(t_u)$

The energy flux produced by the mirror is [5]

$$\langle T_{uu} \rangle = \frac{1}{24\pi} \left[\frac{3}{2} \left(\frac{p''}{p'} \right)^2 - \frac{p'''}{p'} \right] \ ,$$ (2.45)

where the prime indicates derivative with respect to u. This is a renormalized result that comes from a point-splitting calculation. In general it is not zero. It is also called the Schwarzian derivative of $p(u)$. While acceleration is responsible for particle creation, it is the change in acceleration (jerk) that is responsible for energy production. The Davies-Fulling stress tensor Eqn. (2.45) masks this fact because it is in terms of the ray tracing function, $p(u)$. This $p(u)$ is in turn a function of retarded time, $u = t - x$. The ray tracing function can be found from the trajectory of the mirror if one is able to perform the relevant function inversion. It is useful to have the stress tensor in terms of the trajectory, $z(t_u)$. One may determine flux without the need to do transcendental inversions, which are often not possible analytically, (i.e. if one has only $z(t_u)$ but not $p(u)$, one can still solve for flux). The solution is [5],

$$\langle T_{uu} \rangle = \left. \frac{\dddot{z}(\dot{z}^2 - 1) - 3\dot{z}\ddot{z}^2}{12\pi(\dot{z} - 1)^4(\dot{z} + 1)^2} \right|_{t=t_u} \ .$$ (2.46)

Here the dots refer to coordinate time derivatives and they are to be evaluated at t_u. We have defined $z \equiv z(t_u)$. Equation (2.46) is equivalent to (2.45) evaluated at the surface of the mirror. That is, using $p(u)$ where $u = t_u - z(t_u)$ in (2.45) yields the same flux evaluated where $x = z(t_u)$. Equation (2.46) is derived by utilizing the appropriate derivative function inversions of $p(u)$.

The time derivative of coordinate acceleration (the triple dot, $\dddot{z}$) suggests that energy production may be dependent on the relativistic jerk (the time derivative of the proper acceleration, $\alpha = \gamma^3 \ddot{z}$). Indeed, Eqn. (2.46) can be reformulated in terms of only the time derivative of proper acceleration (what is referred to as 'relativistic jerk') and the velocity of the trajectory.

$$\langle T_{uu} \rangle = -\frac{\dot{\alpha}}{12\pi\gamma(1-v)^2} \; , \tag{2.47}$$

where, $v = \dot{z}$, $\gamma = (1 - v^2)^{-1/2}$, and $\alpha = \gamma^3 \ddot{z}$. It looks as if, despite the creation of particles being dependent on acceleration, the creation of energy is dependent on the jerk. This expression (2.47) allows one to compute the flux without even knowing either the trajectory function or the ray tracing function. All that is required is to have a form for the velocity and the jerk. Notice the negative sign out front. A mirror that jerks away from you gives off energy, while a mirror that jerks towards you gives off negative energy. Schematically,

- Mirror Jerks Left $\rightarrow$ Positive Flux

- Mirror Jerks Right $\rightarrow$ Negative Flux

with respect to the right side of the mirror.

Total Energy from Energy Flux

To find the expectation value of the total energy produced, one can use Eqn. (2.45),

$$E = \int_{z(t)}^{\infty} \langle T^{00} \rangle \, dx = \int_{u_{min}}^{u_{max}} \langle T_{uu} \rangle \, du \, . \tag{2.48}$$

While using (2.46), we integrate over u using $du \to (1 - v) \, dt_u$ to get

$$E = \int_{-\infty}^{\infty} \frac{\dddot{z}(\dot{z}^2 - 1) - 3\dot{z}\ddot{z}^2}{12\pi(1 - \dot{z})^3(\dot{z} + 1)^2} \, dt_u \, , \tag{2.49}$$

and equivalently, using (2.47)

$$E = -\frac{1}{12\pi} \int_{-\infty}^{\infty} \frac{\dot{\alpha}}{\gamma(1 - v)} \, dt_u \, . \tag{2.50}$$

We may integrate (2.45) by parts to isolate the surface term,

$$E = -\frac{1}{24\pi} \frac{p''}{p'} \bigg|_{-\infty}^{\infty} + \frac{1}{48\pi} \int_{-\infty}^{\infty} du \left(\frac{p''}{p'} \right)^2 \, . \tag{2.51}$$

Rewriting the boundary term in (2.51) using, $z(t_u) = \frac{1}{2}(p(u) - u)$ gives

$$-\frac{\alpha}{12\pi} \sqrt{\frac{1 + \dot{z}}{1 - \dot{z}}} \Bigg|_{t_u = -\infty}^{t_u = +\infty} \, . \tag{2.52}$$

If this boundary term vanishes, as in the case of a mirror without a horizon (as pointed out by Walker [15]), whose $\alpha \to 0$ as $t_u \to \pm\infty$, then we may utilize integration by parts and write the total energy simply as

$$E = \frac{1}{48\pi} \int_{-\infty}^{\infty} \left(\frac{p''}{p'} \right)^2 \, du \, , \tag{2.53}$$

28

or, equivalently

$$E = \frac{1}{12\pi} \int_{-\infty}^{\infty} \frac{\dddot{z}^2}{(1+\dot{z})^2(1-\dot{z})^3} dt_u \ .$$

(2.54)

Notice that this form masks the jerk dependence.

2.1.4 Stress Tensor Components with a Moving Mirror

For background reference, we will need the various stress tensor components in $1+1$ dimensions with a moving mirror. For the original stress tensor result see Eqn. (2.7), Davies and Fulling [6],

$$\langle T_{uu} \rangle = (12\pi)^{-1}(p')^{1/2}[(p')^{-1/2}]'' \equiv F_{DF} \ ,$$

(2.55)

where $\langle T_{vv} \rangle = \langle T_{uv} \rangle = \langle T_{vu} \rangle = 0$. Here $p \equiv p(u)$ is the ray tracing formula of the mirror, which is related to the trajectory as previously addressed. The previous Davies and Fulling result [5], Eqn. (3.11) and Eqn. (3.7) are, using our definition above,

$$\langle T_{00} \rangle = -\langle T_{01} \rangle = F_{DF} \ , \quad \langle T_{00} \rangle = \langle T_{11} \rangle \ , \quad \langle T_{10} \rangle = \langle T_{01} \rangle \ .$$

(2.56)

In order to find the stress tensor in the $t - x$ basis, we use $\langle T_{uu} \rangle = \frac{1}{4}\langle T^{vv} \rangle$, $\langle T_{vv} \rangle = \frac{1}{4}\langle T^{uu} \rangle$, $\langle T_{uv} \rangle = \frac{1}{4}\langle T^{vu} \rangle$, and $\langle T_{vu} \rangle = \frac{1}{4}\langle T^{uv} \rangle$, which gives

$$\langle T^{vv} \rangle = 4F_{DF} \ ,$$

(2.57)

and $\langle T^{uu} \rangle = \langle T^{vu} \rangle = \langle T^{uv} \rangle = 0$. While, in addition, using

$$\langle T^{uu} \rangle = \langle T^{tt} \rangle - 2\langle T^{tx} \rangle + \langle T^{xx} \rangle \ , \qquad \langle T^{vv} \rangle = \langle T^{tt} \rangle + 2\langle T^{tx} \rangle + \langle T^{xx} \rangle \ ,$$

(2.58)

$$\langle T^{uv} \rangle = \langle T^{tt} \rangle - \langle T^{xx} \rangle = \langle T^{vu} \rangle \,, \tag{2.59}$$

which gives

$$\langle T^{tt} \rangle = \langle T^{xx} \rangle \,, \qquad \langle T^{tt} \rangle = \langle T^{tx} \rangle \,, \qquad \langle T^{tt} \rangle = F_{DF} \,. \tag{2.60}$$

So we have, in the $t - x$ basis

$$
\begin{bmatrix} \langle T^{00} \rangle & \langle T^{01} \rangle \\ \langle T^{10} \rangle & \langle T^{11} \rangle \end{bmatrix} = \begin{bmatrix} \langle T^{tt} \rangle & \langle T^{tx} \rangle \\ \langle T^{xt} \rangle & \langle T^{xx} \rangle \end{bmatrix} = \begin{bmatrix} F_{DF} & F_{DF} \\ F_{DF} & F_{DF} \end{bmatrix} \,. \tag{2.61}
$$

2.1.5 Correlation Functions for Energy Flux with a Moving Mirror

The mode functions for the moving mirror are all that is needed to compute the correlation functions for the stress-energy tensor. The stress-energy tensor correlation function is of interest because it reveals more about the flux than just what the stress tensor alone can. The energy fluxes emitted by a moving mirror can be positive and negative, but they are only average values. There are fluctuations around this average value. The quantum state is not an eigenstate of the stress tensor operator so fluctuations are expected.

The correlation function for the stress tensor is

$$C_{\mu\nu,\mu'\nu'} = \langle T_{\mu\nu}(y) T_{\mu'\nu'}(y') \rangle - \langle T_{\mu\nu}(y) \rangle \langle T_{\mu'\nu'}(y') \rangle \,, \tag{2.62}$$

where the spacetime points are indicated by $y = (u, v)$ and $y' = (u', v')$. The correlation functions between two right-moving rays, two left-moving rays, and right and

left moving rays are:

$$C_{RR}(u, u') = \langle T_{uu}(u)T_{uu}(u')\rangle - \langle T_{uu}(u)\rangle\langle T_{uu}(u')\rangle \ , \tag{2.63}$$

$$C_{LL}(v, v') = \langle T_{vv}(v)T_{vv}(v')\rangle - \langle T_{vv}(v)\rangle\langle T_{vv}(v')\rangle \ , \tag{2.64}$$

$$C_{RL}(v, u') = \langle T_{vv}(v)T_{uu}(u')\rangle - \langle T_{vv}(v)\rangle\langle T_{uu}(u')\rangle \ , \tag{2.65}$$

One can re-express these as: (See the use of Wick's Theorem in Ford and Roman 2004)

$$C_{RR}(u, u') = 2[\partial_u\partial_{u'}D(y, y')]^2 \tag{2.66}$$

$$C_{LL}(v, v') = 2[\partial_v\partial_{v'}D(y, y')]^2 \tag{2.67}$$

$$C_{RL}(v, u') = 2[\partial_{u'}\partial_v D(y, y')]^2 \tag{2.68}$$

where

$$D(y, y') = \langle\phi(y)\phi(y')\rangle \ , \tag{2.69}$$

is the scalar field two point function. Using the well-known Davies-Fulling two point function for the region to the right of the mirror in the 1+1 dimensional case (Birrell and Davies [19]), (dropping the $i\epsilon$ terms)

$$D(y, y') = -\frac{1}{4\pi}\ln\frac{[p(u) - p(u')][v - v']}{[v - p(u')][p(u) - v']} \ , \tag{2.70}$$

one can express the energy flux correlation functions as

$$C_{RR}(u, u') = \frac{[p'(u')p'(u)]^2}{8\pi^2[p(u') - p(u)]^4} \ , \tag{2.71}$$

$$C_{LL}(v, v') = \frac{1}{8\pi^2[v' - v]^4} \ , \tag{2.72}$$

31

$$C_{RL}(v, u') = \frac{[p'(u')]^2}{8\pi^2[p(u') - v]^4} \, , \tag{2.73}$$

where $p'(u) = dp(u)/du$ and $p'(u') = dp(u')/du'$. We will deal more with particular forms of $p(u)$ later. The above expressions deal only with correlations of distinct rays, so the $i\epsilon$ terms have been dropped from the Davies-Fulling two point function. These expressions simplify, as would be expected, in vacuum or with a static mirror present. For a static mirror we have the condition, $v = p(u) = u$, and the limits:

$$C_{RR}(u, u') = C_{vac\oplus static}(u, u') = \frac{1}{8\pi^2[u' - u]^4} \, , \tag{2.74}$$

$$C_{LL}(v, v') = C_{vac\oplus static}(v, v') = \frac{1}{8\pi^2[v' - v]^4} \, , \tag{2.75}$$

$$C_{RL}(v, u') = C_{static}(v, u') = \frac{1}{8\pi^2[u' - v]^4} \, . \tag{2.76}$$

In vacuum $C_{RL}(v, u') = 0$ because there can only be correlations with left and right moving fluxes with a mirror present. The correlation limits for C_{RR} and C_{LL} hold for either vacuum or a static mirror, hence the xor, $\oplus$, in the subscript. The ratios

$$R_1 = \frac{C_{RR}(u, u')}{C_{vac\oplus static}(u, u')} \, , \tag{2.77}$$

$$R_2 = \frac{C_{RL}(v, u')}{C_{static}(v, u')} \, , \tag{2.78}$$

can tell us about enhancement and suppression of correlations. For $R > 1$ one interprets enhancement, for $R < 1$ there is suppression.

2.2 The Scalar Product and Normalization

2.2.1 Torus Waves: Discrete Normalization

This section outlines discrete box normalization of the modes. Using right-moving waves, and the scalar product, normalization is straightforward in 2D Minkowski spacetime. The scalar field inner product for (1+1) dimensions is

$$(\phi_1, \phi_2) = -i \int_t (\phi_1 \partial_t \phi_2^* - [\partial_t \phi_1]\phi_2^*)dx \; , \tag{2.79}$$

where t signifies a spacelike hyperplane of simultaneity at instant t.

The u_k modes are restricted to the interior of a spacelike $(n-1)$-torus of side L. They will have periodic boundary conditions. We will show, that

$$(u_k, u_{k'}) = \delta_{kk'} \; . \tag{2.80}$$

The waves, without their normalization constants are $u_k \propto e^{ikx - i\omega t}$ and $u_{k'} \propto e^{ik'x - i\omega't}$. To normalize, one uses, $(u_k, u_{k'}) = -i \int_t dx \; (u_k \partial_t u_{k'}^* - [\partial_t u_k]u_{k'}^*)$. After taking the time partials, this becomes

$$(u_k, u_{k'}) = -i \int_t dx \; e^{ikx - i\omega t}[i\omega']e^{-ik'x - i\omega't} - [-i\omega]e^{ikx - i\omega t}e^{-ik'x + i\omega't} \; . \tag{2.81}$$

After simplifying, one gets

$$(u_k, u_{k'}) = [\omega' + \omega] \int_t dx \; e^{-i(k'-k)x}e^{-i(\omega - \omega')t}dx \; . \tag{2.82}$$

This is evaluated on the convenient hypersurface $t = 0$,

$$(u_k, u_{k'}) = [\omega' + \omega] \int_{-\infty}^{\infty} dx \; e^{-i(k'-k)x} \; . \tag{2.83}$$

For discretely integrable 'box' waves, the integral is defined as $V\delta_{kk'}$, i.e.

$$\int_{-\infty}^{\infty} dx \; e^{-i(k'-k)x} \equiv V\delta_{kk'} \; . \tag{2.84}$$

Since our space is one dimensional, the normalization gives

$$(u_k, u_{k'}) = [\omega' + \omega]L\delta_{kk'} \; . \tag{2.85}$$

It is now clear that the normalization factor must be $(2L\omega)^{-1/2}$. Therefore the modes are,

$$u_k = \frac{1}{\sqrt{2L\omega}}e^{ikx-i\omega t} \; , \quad u_{k'} = \frac{1}{\sqrt{2L\omega'}}e^{ik'x-i\omega' t} \; . \tag{2.86}$$

This gives the properly normalized result:

$$(u_k, u_{k'}) = \frac{\omega' + \omega}{2L\sqrt{\omega\omega'}}L\delta_{kk'} \; . \tag{2.87}$$

Recall $\omega \equiv \sqrt{k^2 + m^2}$ and that we are working with a massless field so that $\omega = |k|$). Therefore

$$(u_k, u_{k'}) = \delta_{kk'} \; , \tag{2.88}$$

If it were assumed that the modes Eqn. (2.86) were actually distinct solutions, then the Bogolubov transformation mechanism would give

$$\alpha_{kk'} = \delta_{kk'} \; . \tag{2.89}$$

These 'torus waves' satisfy the Bogolubov identities, which are $\alpha_{kk'} = (u_k, u_{k'})\delta_{kk'}$ and $\beta_{kk'} = -(u_k, u_{k'}^*) = 0$. To calculate $\beta_{kk'}$ it is the same procedure as above, but one must notice the double complex conjugate due to the scalar product.

2.2.2 Right Moving Waves: Continuous Normalization

This section will derive the Dirac delta function result for scalar product normalization of 2D Minkowski continuous right-moving plane waves. Using the scalar field inner product for (1+1) dimensions, $(\phi_1, \phi_2) = -i \int_t (\phi_1 \partial_t \phi_2^* - [\partial_t \phi_1]\phi_2^*)dx$ and choosing

$$u_k = (4\pi\omega)^{-1/2} e^{i\omega(x-t)} , \tag{2.90}$$

and allowing

$$N \equiv (4\pi\omega)^{-1/2} , \quad N' \equiv (4\pi\omega')^{-1/2} , \tag{2.91}$$

we then obtain

$$(u_\omega, u_{\omega'}) = -i \int_t N e^{i\omega(x-t)} \partial_t N' e^{-i\omega'(x-t)} - N' e^{-i\omega'(x-t)} \partial_t N e^{i\omega(x-t)} dx . \tag{2.92}$$

Pulling out the constants and take the partial time derivatives gives

$$(u_\omega, u_{\omega'}) = -iNN' \int_t e^{i\omega(x-t)}(i\omega')e^{-i\omega'(x-t)} - e^{-i\omega'(x-t)}(-i\omega)e^{i\omega(x-t)} dx . \tag{2.93}$$

After grouping terms, and simplifying, the result is

$$(u_\omega, u_{\omega'}) = NN' \int_t (\omega' + \omega) e^{-i(\omega'-\omega)(x-t)} dx \ . \tag{2.94}$$

The delta function result is found by evaluate the above expression on the convenient hypersurface $t = 0$, make the substitution $x = 2\pi s$ and plug back in N and N',

$$(u_\omega, u_{\omega'}) = (4\pi)^{-1}(\omega\omega')^{-1/2}(\omega' + \omega) \int_{-\infty}^{\infty} 2\pi e^{-i2\pi(\omega'-\omega)s} ds \ . \tag{2.95}$$

This yields the Dirac delta function

$$(u_\omega, u_{\omega'}) = \frac{1}{2}(\omega\omega')^{-1/2}(\omega' + \omega)\delta(\omega' - \omega) \ . \tag{2.96}$$

The delta function will be zero if $\omega \neq \omega'$, so the only nonzero answer is that when $\omega = \omega'$, in which case, the term out front is simply 1. Thus, the plane waves are properly normalized

$$(u_\omega, u_{\omega'}) = \delta(\omega' - \omega) \ . \tag{2.97}$$

The plane waves also satisfy the Bogolubov identities, since $\alpha_{\omega\omega'} = (u_\omega, u_{\omega'})$ and in our case $\alpha_{\omega\omega'} = \delta(\omega' - \omega)$. For the calculation of $\beta_{\omega\omega'}$, we recall that $\beta_{\omega\omega'} = -(u_\omega, u_{\omega'}^*)$. This is the same procedure as above, where attention is given to the double complex conjugate in the scalar product

$$-(u_\omega, u_{\omega'}^*) = (-)(-i)NN' \int_t e^{i\omega(x-t)}\partial_t e^{i\omega'(x-t)} - [\partial_t e^{i\omega(x-t)}]e^{i\omega'(x-t)} dx \ . \tag{2.98}$$

Taking the time partials gives

$$-(u_\omega, u_{\omega'}^*) = (-)(-i)NN'\int_t e^{i\omega(x-t)}(-i\omega')e^{i\omega'(x-t)} - (-i\omega)e^{i\omega(x-t)}e^{i\omega'(x-t)}dx \ . \quad (2.99)$$

Grouping terms and canceling i's, gives

$$-(u_\omega, u_{\omega'}) = NN'\int_t (\omega' - \omega)e^{i(\omega'+\omega)(x-t)}dx \ . \quad (2.100)$$

Evaluating on the convenient hypersurface $t = 0$, and noting that as $\omega, \omega' \geq 0$ then as,

$$-(u_\omega, u_{\omega'}) = \frac{1}{2}\frac{\omega' - \omega}{\sqrt{\omega\omega'}}\delta(\omega' + \omega) \ , \quad (2.101)$$

the result is $\beta_{\omega\omega'} = 0$. With β and α as derived, the Bogolubov identities will be satisfied. These waves have only the right moving pieces in them. They satisfy the null and unit identities. Therefore the Bogolubov condition holds for the continuously normalized right moving plane waves.

2.2.3   Right and Left Moving Waves Combined in Flat Space

Plane waves with right and left moving pieces may be normalized to the Dirac delta function. Note that the inner product is defined for all space. Starting with the scalar field inner product, $(\phi_1, \phi_2) = -i\int_t(\phi_1\partial_t\phi_2^* - [\partial_t\phi_1]\phi_2^*)dx$ and using the integral

$$\int_{-\infty}^{\infty} \sin\omega x \sin\omega' x dx = \pi\delta(\omega' - \omega) \ , \quad (2.102)$$

the positive frequency mode with right and left moving pieces is

$$u_\omega \propto \sin\omega x e^{-i\omega t} \ . \quad (2.103)$$

This form satisfies the field equation. Solving for α gives

$$\alpha = (u_\omega, u_{\omega'}) = -i \int_t dx \ u_\omega \partial_t u_{\omega'}^* - [\partial_t u_\omega] u_{\omega'}^* \ . \tag{2.104}$$

Plugging in the modes, one obtains

$$\alpha = -i \int_{-\infty}^{\infty} \sin \omega x \sin \omega' x [e^{-i\omega t}(i\omega')e^{i\omega' t} - [-i\omega e^{-i\omega t}]e^{i\omega' t}]dx \ . \tag{2.105}$$

Evaluating on $t = 0$ one finds

$$\alpha = -i \int_{-\infty}^{\infty} dx \ \sin \omega x \sin \omega' x [i\omega' + i\omega] \ . \tag{2.106}$$

Using the integral result above, we get

$$\alpha = [\omega' + \omega]\pi\delta(\omega - \omega') \ . \tag{2.107}$$

Therefore, the normalization factor needs to be

$$N \equiv \frac{1}{\sqrt{2\pi\omega}} \ . \tag{2.108}$$

Using this normalization, the α is $\alpha_{\omega\omega'} = \delta(\omega - \omega')$. For β the procedure follows

$$\begin{aligned}
\beta_{\omega\omega'} &= -i \int_t dx \ u_\omega \partial_t u_{\omega'} - [\partial_t u_\omega] u_{\omega'} &\tag{2.109}\\
&= -i \int_{-\infty}^{\infty} dx \ \sin \omega x \sin \omega' x [e^{-i\omega t}(-i\omega')e^{-i\omega' t} - (-i\omega)e^{-i\omega t}e^{-i\omega' t}] \\
&= -i \int_{-\infty}^{\infty} dx \ \sin \omega x \sin \omega' x [-i\omega' + i\omega] \\
&= [\omega - \omega']\pi\delta(\omega' - \omega) \ .
\end{aligned}$$

The result is $\beta_{\omega\omega'} = 0$. The Bogolubov identities hold trivially. The crucial aspect associated with this example is the integration over all space. When there is a boundary, such as a static mirror at $x = 0$, there will naturally be left and right moving pieces of the mode solutions but the normalization will be over only a limited spatial region, i.e. to the right of the mirror. This renders a different normalization coefficient while the procedure of fixing it remains the same.

2.2.4 Flat Spacetime Limit of the Curved Spacetime Scalar Product

With a general spacelike hypersurface σ with future-directed unit normal n^μ and hypersurface element $d\sigma$, the curved spacetime scalar product is, see Parker and Toms [20], Equation (2.49),

$$(f_1, f_2) = i \int_\sigma d\sigma |g|^{1/2} n^\nu f_1^* \overset{\leftrightarrow}{\partial_\nu} f_2 \ . \tag{2.110}$$

We look at the general surface,

$$t - \epsilon x = \text{constant} \ , \tag{2.111}$$

and we see

$$\left. \begin{array}{ll} \epsilon \to 0 & t = \text{constant} \\ \epsilon \to 1 & u = \text{constant} \\ \epsilon \to -1 & v = \text{constant} \end{array} \right\} \tag{2.112}$$

where

$$\left. \begin{array}{l} u = t - x \\ v = t + x \end{array} \right\} \ . \tag{2.113}$$

The two-dimensional Minkowski space metric, with signature consistent with Birrell and Davies[19], $ds^2 = dt^2 - dx^2$ is written

$$ds^2 = \left(\frac{dt^2}{dx^2} - 1 \right) dx^2 = (\epsilon^2 - 1) dx^2 , \tag{2.114}$$

so that $|g|^{1/2} = \sqrt{\epsilon^2 - 1}$ The unit normal will be a constant times the gradient of the surface

$$\hat{n} = \frac{\vec{n}}{||\vec{n}||} = \frac{1}{\sqrt{-g_{\mu\nu} n^\mu n^\nu}} \vec{\nabla} S(x, t) , \tag{2.115}$$

where $S(x, t) = t - \epsilon x$, is the surface. Further simplifying gives

$$\hat{n} = \frac{1}{\sqrt{-g_{00}(1)^2 - g_{11}\epsilon^2}} (1, -\epsilon) = \frac{1}{\sqrt{\epsilon^2 - 1}} (1, -\epsilon) . \tag{2.116}$$

It is easy to see that

$$\begin{aligned} n^\mu \partial_\mu &= g^{\mu\nu} n_\nu \partial_\mu \\ &= \frac{1}{\sqrt{\epsilon^2 - 1}} (\partial_t + \epsilon \partial_x) . \end{aligned} \tag{2.117}$$

Writing $\partial_t + \epsilon \partial_x = (1 - \epsilon)\partial_u + (1 + \epsilon)\partial_v$ because, using a test function, f,

$$\partial_x f = \frac{\partial f}{\partial u} \frac{\partial u}{\partial x} + \frac{\partial f}{\partial v} \frac{\partial v}{\partial x} = -\frac{\partial f}{\partial u} + \frac{\partial f}{\partial v} , \tag{2.118}$$

we obtain $\partial_x = \partial_v - \partial_u$. Similarly for the partial with respect to time,

$$\partial_t f = \frac{\partial f}{\partial u} \frac{\partial u}{\partial t} + \frac{\partial f}{\partial v} \frac{\partial v}{\partial t} = \frac{\partial f}{\partial u} + \frac{\partial f}{\partial v} , \tag{2.119}$$

one obtains $\partial_t = \partial_u + \partial_v$. Substituting into the scalar product

$$(f_1, f_2) = i \int_\sigma d\sigma \sqrt{\epsilon^2 - 1} \frac{1}{\sqrt{\epsilon^2 - 1}} f_1^* \left[(1 - \epsilon) \overset{\leftrightarrow}{\partial}_u + (1 + \epsilon) \overset{\leftrightarrow}{\partial}_v \right] f_2 . \tag{2.120}$$

Clearly,

$$(f_1, f_2) = i \int_\sigma d\sigma f_1^* \left[(1 - \epsilon) \overset{\leftrightarrow}{\partial_u} + (1 + \epsilon) \overset{\leftrightarrow}{\partial_v} \right] f_2 \ . \tag{2.121}$$

The spacelike hypersurface differential $d\sigma$ is expressed in terms of v or u by taking a limit for ϵ. As $t - \epsilon x = c$ and $v = t + x$, we have $v = c + (\epsilon + 1)x$. For u constant we take the limit $\epsilon \to 1$ and obtain

$$\frac{1}{2} dv = dx \ . \tag{2.122}$$

Thus, for the constant u surface, we may integrate over I_R^- or I_L^+, if we take the limit as $\epsilon \to 1$,

$$(f_1, f_2) = \lim_{\epsilon \to 1} i \int_\sigma d\sigma f_1^* \left((1 - \epsilon) \overset{\leftrightarrow}{\partial_u} + (1 + \epsilon) \overset{\leftrightarrow}{\partial_v} \right) f_2 \ . \tag{2.123}$$

This gives

$$(f_1, f_2)|_v = i \int_{-\infty}^\infty dv \ f_1^* \overset{\leftrightarrow}{\partial_v} f_2 \ . \tag{2.124}$$

For the constant v surface, we may integrate over I_L^- or I_R^+ if we take the limit as $\epsilon \to -1$, and as $u = t - x$ we have

$$u = c + (\epsilon - 1)x \ , \tag{2.125}$$

and for v constant we take the $\epsilon \to -1$ limit

$$-\frac{1}{2} du = dx \ , \tag{2.126}$$

and we get

$$(f_1, f_2) = \lim_{\epsilon \to -1} i \int_\sigma d\sigma f_1^* \left((1 - \epsilon) \overset{\leftrightarrow}{\partial_u} + (1 + \epsilon) \overset{\leftrightarrow}{\partial_v} \right) f_2 \ , \tag{2.127}$$

which is

$$(f_1, f_2)|_u = -i \int_{+\infty}^{-\infty} du \, f_1^* \overleftrightarrow{\partial_u} f_2 \, . \tag{2.128}$$

However, for full integration over either the future or past Cauchy surface, one must take into account both surfaces, the left and right pieces. That is for the past, $I_L^- \bigcup I_R^-$ or for the future, $I_L^+ \bigcup I_R^+$. Including the limits of integration for following either the past or future Cauchy surface, the result is

$$(f_1, f_2) = (f_1, f_2)|_u + (f_1, f_2)|_v = -i \int_{\infty}^{-\infty} du \, f_1^* \overleftrightarrow{\partial_u} f_2 + i \int_{-\infty}^{\infty} dv \, f_1^* \overleftrightarrow{\partial_v} f_2 \, , \tag{2.129}$$

which further simplified to its final form gives

$$(f_1, f_2) = i \int_{-\infty}^{\infty} du \, f_1^* \overleftrightarrow{\partial_u} f_2 + i \int_{-\infty}^{\infty} dv \, f_1^* \overleftrightarrow{\partial_v} f_2 \, . \tag{2.130}$$

Typically, however, when one is working with exclusively right-moving modes or left-moving modes, only one of the integrals of Eqn. (2.130) will show up. For instance, with left-moving plane wave modes one will have no contribution from the u integral.

2.3 Static Casimir Effect

The Casimir effect [1] is the result of a force between two boundaries not ascribed to the electromagnetic force, the gravitational force, or the exchange of any particles. It is a disturbed vacuum force, in a very real sense. It is called the zero-point energy force and is due to the resonance of the field which is present in the space between two boundaries. It is a force due to quantization, similar to the Pauli exclusion 'force' that keeps negative electrons from collapsing into the positive nucleus.

As fields contribute to the energy of the vacuum, whether they be scalar fields, the electromagnetic field or any other fields, a disturbance of the vacuum occurs by introducing boundary conditions. Experimental observation and prediction of the Casimir effect is possible by adding up the energies of the standing waves between the two objects and renormalizing. Measuring the finite energy shift confirms the effect.

2.3.1   (1+1) dimensional massless scalar field Casimir effect

In this calculation I derive the Casimir force as quickly as possible, in the simplest case possible. The standing waves are:

$$\psi_n(x,t) = e^{-i\omega_n t} \sin(k_n x) \ . \tag{2.131}$$

There is no need to worry about y or z as we only have one spatial dimension. The calculation will not involve the electromagnetic field so there is no need to worry about polarization. The wave vector k_n is $k_n = \frac{n\pi}{a}$ where a is the distance between the two objects. We have via $\omega = kc$, $\omega_n = \frac{n\pi c}{a}$. The vacuum energy of all the standing waves is the sum of the excitation modes:

$$E = \frac{\hbar}{2} \sum_{n=1}^{\infty} \omega_n \ . \tag{2.132}$$

This is divergent as there is no cut off value for the highest energy waves. There is now an infinity to deal with. In real life though, nothing can stop ultra high frequency waves from leaking out. So we need to account for this vital piece of physics. This is done by introducing a factor to remove the high energy waves that will leak

out. This is called regularizing. We make this sum finite by introducing a regulator, manipulate the sum, then follow it up by taking a limit that will remove the regulator.

$$E = \frac{\hbar}{2} \sum_n^\infty \frac{n\pi c}{a} = \frac{\hbar\pi c}{2a} \sum_n^\infty \frac{1}{n^{-1}} \tag{2.133}$$

Invoke the Riemann zeta function regulator of -1. This is called renormalization by zeta function regularization. Here

$$\xi(s) = \sum_{n=1}^\infty \frac{1}{n^s} \tag{2.134}$$

is the Riemann zeta function and in our case, $\xi(-1) = -\frac{1}{12}$. So our regularization is considered complete. Our sum is now

$$E = \frac{\hbar\pi c}{2a}\left(-\frac{1}{12}\right) = -\frac{\hbar\pi c}{24a} . \tag{2.135}$$

The force between the two objects is found by $F = -\partial_a E$, that is

$$F = -\partial_a\left(-\frac{\hbar\pi c}{24a}\right) = -\frac{\hbar\pi c}{24a^2} . \tag{2.136}$$

This is the Casimir effect. Note that the effect is attractive as indicated by the negative sign and that $\hbar$ reveals the quantum nature of this force.

2.3.2 (1+1) dimensional canonical Casimir effect

For the massless, scalar field Casimir effect in (1+1) dimensions (this example can be checked with the result in Zee [52]), the field will be forced to obey two boundary conditions:

$$\psi(0,t) = \psi(a,t) = 0 \ . \tag{2.137}$$

The general scalar field wave equation is, restated as $c \neq 1$,

$$\frac{1}{c^2}\partial_t^2\psi(x,t) - \partial_x^2\psi(x,t) = 0 \ , \tag{2.138}$$

where the field is massless, $m = 0$. The solutions are

$$\psi_n^\pm(x,t) = \left(\frac{c}{a\omega_n}\right)^{1/2} e^{\pm i\omega_n t}\sin k_n x \tag{2.139}$$

$$\omega_n = ck_n, \quad k_n = \frac{\pi n}{a}, \quad n = 1,2,... \tag{2.140}$$

To proceed with canonical quantization, one expands the field, applies the usual commutation relations and defines a vacuum state:

$$\psi(x,t) = \sum_n [\psi_n^{(-)}(x,t)a_n + \psi_n^{(+)}(x,t)a_n^+] \ , \tag{2.141}$$

$$[a_n, a_{n'}^+] = \delta_n^{n'}, \quad [a_n, a_{n'}] = [a_n^+, a_{n'}^+] = 0 \ , \tag{2.142}$$

$$a_n|0\rangle = 0 \ . \tag{2.143}$$

The operator of the energy density is

$$T_{00} = \frac{\hbar c}{2}\left(\frac{1}{c^2}[\partial_t\psi]^2 + [\partial_x\psi]^2\right) \ . \tag{2.144}$$

Using the above, one obtains

$$\langle 0|T_{00}|0\rangle = \frac{\hbar}{2a} \sum_{n=1}^{\infty} \omega_n \; . \tag{2.145}$$

The total vacuum energy will be

$$E_0(a) = \int_0^a \langle 0|T_{00}|0\rangle dx = \frac{\hbar}{2} \sum_{n=1}^{\infty} \omega_n \; . \tag{2.146}$$

Finally, we are at the standard starting point. Regularizing this infinite result is done by the damping term $e^{-\delta \omega_n}$. We will apply the limit $\delta \to 0$ to remove the regularization. This gives:

$$E_0(a, \delta) = \frac{\hbar c \pi}{2a} \sum_{n=1}^{\infty} n e^{-\delta c \pi n/a} \; . \tag{2.147}$$

You can solve this by

$$E_0(a, \delta) = -\frac{\hbar}{2} \frac{\partial}{\partial \delta} \sum_{n=1}^{\infty} e^{-\delta \pi n c/a} \; , \tag{2.148}$$

$$E_0(a, \delta) = -\frac{\hbar}{2} \frac{\partial}{\partial \delta} \frac{e^{-\delta \pi c/a}}{1 - e^{-\delta \pi c/a}} = \frac{\hbar \pi c}{2a} \frac{e^{\delta \pi c/a}}{(e^{\delta \pi c/a} - 1)^2} \; , \tag{2.149}$$

$$E_0(a, \delta) = \frac{\hbar \pi c}{2a} \frac{1}{(e^{\delta \pi c/2a} - e^{-\delta \pi c/2a})^2} = \frac{\hbar \pi c}{8a} \sinh^{-2} \frac{\delta \pi c}{2a} \; . \tag{2.150}$$

In limit of small δ, the following is true:

$$\sinh x = x + \frac{x^3}{3!} + \frac{x^5}{5!} + \dots \; , \tag{2.151}$$

$$\sinh^2 x = x^2 + \frac{x^4}{3} + \dots \; , \tag{2.152}$$

$$\sinh^{-2} x \approx \frac{x^{-2}}{1 + x^2/3} \approx x^{-2}(1 - x^2/3) \; , \tag{2.153}$$

46

$$E_0(a, \delta) = \frac{\hbar \pi c}{8a} \sinh^{-2} \frac{\delta \pi c}{2a} = \frac{\hbar a}{2\pi c \delta^2} - \frac{\hbar \pi c}{24a} + O(\delta^2) . \tag{2.154}$$

Compare the field and boundary set up with the unbounded interval:

$$\psi_k^\pm(x, t) = \left(\frac{c}{4\pi \omega} \right)^{1/2} e^{\pm i(\omega t - kx)} \quad \omega = ck \quad -\infty < k < \infty , \tag{2.155}$$

$$\psi(x, t) = \int_{-\infty}^{\infty} \frac{dk}{2\pi} [\psi_k^{(-)}(x, t) a_k + \psi_k^{(+)}(x, t) a_k^+] , \tag{2.156}$$

$$[a_k, a_{k'}^+] = \delta(k - k'), \quad [a_k, a_{k'}] = [a_k^+, a_{k'}^+] = 0 , \tag{2.157}$$

$$a_k |0_M\rangle = 0 \qquad \langle 0_M | T_{00} | 0_M \rangle = \frac{\hbar}{2\pi} \int_0^\infty \omega dk . \tag{2.158}$$

The total vacuum energy is $E_{0M}(-\infty, \infty) = \frac{\hbar}{2\pi} \int_0^\infty \omega dk L$ and the interval of interest is $E_{0M}(a) = E_{0M}(-\infty, \infty) \frac{a}{L} = \frac{\hbar a}{2\pi} \int_0^\infty \omega dk$. Regularizing gives

$$E_{0M}(a) = \frac{\hbar a}{2\pi} c \int_0^\infty k e^{-\delta ck} dk = \frac{\hbar a}{2\pi c \delta^2} , \tag{2.159}$$

The renormalized energy is therefore

$$E_0^{ren}(a) = \lim_{\delta \to 0} [E_0(a, \delta) - E_{0M}(a, \delta)] = -\frac{\hbar \pi c}{24a} , \tag{2.160}$$

$$F = -\frac{\partial E(a)}{\partial a} = -\frac{\hbar \pi c}{24a^2} . \tag{2.161}$$

This is the same result as given by the renormalization by zeta function regularization, but here we have been more rigorous by subtracting the energies to obtain the difference.

2.3.3 (3+1) dimensional massless scalar field Casimir effect

Consider the next step up in complexity, a massless neutral scalar field in four-dimensional Minkowski spacetime. Vanishing boundary conditions exist on plates located at $z = 0$ and $z = a$. The standing waves have the form

$$\phi_n(x, y, z, t) = e^{-i\omega_n t} e^{ik_x x + ik_y y} \sin(k_z z) \,, \tag{2.162}$$

$$k_z = \frac{n\pi}{a} \quad \omega_n = c\sqrt{k_x^2 + k_y^2 + \frac{n^2 \pi^2}{a^2}} \,. \tag{2.163}$$

The vacuum energy is the sum of the excitation modes:

$$\frac{E}{A} = \int_{-\infty}^{\infty} \frac{dk_x dk_y}{(2\pi)^2} \sum_{n=1}^{\infty} \frac{\hbar \omega_n}{2} \,, \tag{2.164}$$

The negative values of n are not included because they do not correspond to linearly independent mode functions. The renormalization proceeds along the route of introducing a regulator for this divergent sum. Apply $|\omega|^{-s}$, the zeta function regulator. The idea again is that we regulate, manipulate the sum, take the limit so the regulator will be removed. The summation

$$\frac{E}{A} = \frac{\hbar}{8\pi^2} \int_{-\infty}^{\infty} dk_x dk_y \sum_{n=1}^{\infty} \omega_n \,, \tag{2.165}$$

becomes

$$\frac{E}{A} = \frac{\hbar}{8\pi^2} \int_{-\infty}^{\infty} dk_x dk_y \sum_{n=1}^{\infty} \omega_n |\omega_n|^{-s} \,, \tag{2.166}$$

after applying the regulator. This application is justified in the end by applying the limit $s \to 0$ after we manipulate this infinite sum. Converting to polar coordinates will simplify the double integral, so introduce $q^2 = k_x^2 + k_y^2$:

$$\frac{E}{A} = \frac{\hbar c^{1-s}}{8\pi^2} \sum_{n=1}^{\infty} \int_0^{\infty} 2\pi q dq \left| q^2 + \frac{\pi^2 n^2}{a^2} \right|^{(1-s)/2} . \tag{2.167}$$

The 2π comes from integration over ϕ, and the q in front is the Jacobian. The c out front will not be affected by manipulation of the sum, so simplifying,

$$\frac{E}{A} = \frac{\hbar c}{4\pi} \sum_{n=1}^{\infty} \int_0^{\infty} q dq \left| q^2 + \frac{\pi^2 n^2}{a^2} \right|^{(1-s)/2} , \tag{2.168}$$

and using $u^2 = q^2 + \pi^2 n^2/a^2$, where $u du = q dq$ the integral becomes

$$\frac{E}{A} = \frac{\hbar c}{4\pi} \sum_{n=1}^{\infty} \int_{\pi n/a}^{\infty} u^{2-s} du . \tag{2.169}$$

Then finally we find

$$\frac{E}{A} = -\frac{\hbar c}{4\pi} \sum_{n=1}^{\infty} \frac{\pi^{3-s} n^{3-s}}{(3-s) a^{3-s}} . \tag{2.170}$$

The infinite vacuum energy of the quantized field in Minkowski space was subtracted. We did this because we are looking for the shift of the disturbed vacuum. Ignoring the s for the constants as they are unaffected:

$$\frac{E}{A} = -\frac{\hbar c \pi^2}{4(3-s) a^3} \sum_{n=1}^{\infty} \frac{1}{n^{s-3}} . \tag{2.171}$$

The sum may be taken to be the Riemann zeta function. Let us use the $\xi(-3)$. Taking the limit as $s \to 0$ and using $\xi(-3) = 1/120$,

$$\lim_{s \to 0} \frac{E}{A} = -\frac{\hbar c \pi^2}{12 a^3} \xi(-3) \quad \frac{E}{A} = -\frac{\hbar c \pi^2}{1440 a^3} . \tag{2.172}$$

The force per area between the plates is then $F/A = -\partial_a(E/A)$:

$$\frac{F}{A} = -\frac{\hbar c \pi^2}{480 a^4} \ .$$ (2.173)

This is the force per unit area in the z direction on the plate at $z = a$ for the massless scalar field with vanishing boundary conditions.

2.3.4 (3+1) dimensional electromagnetic field Casimir effect

This calculation is identical to the (3+1) dimensional scalar case above except for the inclusion of a polarization factor of 2. This example was first calculated by Casimir [1]. The standing waves are

$$\psi_n(x, y, z, t) = e^{-i\omega_n t} e^{ik_x x + ik_y y} \sin(k_z z) \ .$$ (2.174)

The plates are in the x-y plane. Polarization and magnetic components are ignored and $k_z = \frac{n\pi}{a}$ and $\omega_n = c\sqrt{k_x^2 + k_y^2 + \frac{n^2 \pi^2}{a^2}}$. Summing over all possible modes to get the vacuum energy per unit area yields

$$\frac{E}{A} = 2 \cdot \int_{-\infty}^{\infty} \frac{dk_x dk_y}{(2\pi)^2} \sum_{n=1}^{\infty} \frac{\hbar \omega_n}{2} \ ,$$ (2.175)

where the factor of 2 is for the two possible polarizations of the wave. It can be seen already that this integral will diverge. Introducing a regulator, particularly, the zeta function regulator $|\omega|^{-s}$ will make our result physically meaningful.[4] So therefore:

$$\frac{E}{A} = \frac{\hbar}{4\pi^2} \int_{-\infty}^{\infty} dk_x dk_y \sum_{n=1}^{\infty} \omega_n \ ,$$ (2.176)

---

[4]The zeta function regulator is not very useful in numerical calculations, but great for theoretical calculations. The Gaussian regulator $e^{-t^2 |\omega_n|^2}$ is better suited for numerical calculations because of its superior convergence properties but harder to use in theoretical calculations.

becomes

$$\frac{E}{A} = \frac{\hbar}{4\pi^2} \int_{-\infty}^{\infty} dk_x dk_y \sum_{n=1}^{\infty} \omega_n |\omega_n|^{-s} \,, \tag{2.177}$$

and we will take the limit and set the complex number $s = 0$ after we manipulate this infinite sum. Convert to polar coordinates to get rid of the double integral:

$$\frac{E}{A} = \frac{\hbar c^{1-s}}{4\pi^2} \sum_{n=1}^{\infty} \int_0^{\infty} 2\pi q dq \left| q^2 + \frac{\pi^2 n^2}{a^2} \right|^{(1-s)/2} . \tag{2.178}$$

Here $q^2 = k_x^2 + k_y^2$, the 2π comes from integration over ϕ, and the q in front is the Jacobian. Simplifying,

$$\frac{E}{A} = \frac{\hbar c^{1-s}}{2\pi} \sum_{n=1}^{\infty} \int_0^{\infty} q dq \left| q^2 + \frac{\pi^2 n^2}{a^2} \right|^{(1-s)/2} , \tag{2.179}$$

and making $u^2 = q^2 + \pi^2 n^2/a^2$, where $u du = q dq$ the integral is evaluated as

$$\frac{E}{A} = \frac{\hbar c^{1-s}}{2\pi} \sum_{n=1}^{\infty} \int_{\pi n/a}^{\infty} u^{2-s} du \,. \tag{2.180}$$

This is

$$\frac{E}{A} = -\frac{\hbar c^{1-s}}{2\pi} \sum_{n=1}^{\infty} \frac{\pi^{3-s} n^{3-s}}{(3-s)a^{3-s}} \,. \tag{2.181}$$

The infinite vacuum energy of the quantized electromagnetic field in free Minkowski space was subtracted (i.e. we are looking for the shift of the disturbed vacuum).

$$\frac{E}{A} = -\frac{\hbar c^{1-s} \pi^{2-s}}{2(3-s)a^{3-s}} \sum_{n=1}^{\infty} \frac{1}{n^{s-3}} \,. \tag{2.182}$$

The sum may be taken to be the Riemann zeta function. It can be shown that the use of the $\xi(-3)$ is equivalent to the renormalization of the vacuum energy of our

situation under consideration. For different and more complicated geometric configurations additional renormalization is generally needed. Taking the limit as $s \to 0$ and using $\xi(-3) = 1/120$,

$$\lim_{s \to 0} \frac{E}{A} = -\frac{\hbar c \pi^2}{6a^3} \xi(-3) \, , \tag{2.183}$$

$$\frac{E}{A} = -\frac{\hbar c \pi^2}{720 a^3} \, . \tag{2.184}$$

The force per area between the plates is then $F/A = -\partial_a(E/A)$:

$$\frac{F}{A} = -\frac{\hbar c \pi^2}{240 a^4} \, . \tag{2.185}$$

This is the well-known Casimir effect. This force, though small, has been measured and proves that the renormalized vacuum energy exists. It also shows that quantum field theory in curved spacetime gives physical predications and may be useful for extracting other fundamental results. It is one of a few macroscopic quantum effects, added to list of the more well-studied effects of superfluidity, superconductivity and the quantum Hall effect.

2.4 Acceleration in Special Relativity

Efforts to understand acceleration have led to a better understanding of gravitation. This has happened through equivalence principle in the formulation of general relativity. Since the creation of particles from quantum fluctuation amplification depends on acceleration, we dedicate a section to the fundamentals of acceleration in flat spacetime. This acceleration, and the surface gravity of a black hole are phenomena that are intimately tied together. A deep understanding of acceleration may

therefore be worthwhile to understanding more on quantum aspects of gravitation. We therefore embark on a study of the foundations of acceleration, restricting ourselves to flat-spacetime, where the dynamics take on the most simple mathematical framework. The moving mirror model is formulated in flat-spacetime as well. Acceleration is undertreated in basic texts on special relativity. There is even a common non-expert misconception that special relativity cannot adequately deal with acceleration. It developed during the construction of special relativity (SR), as SR indeed, was originally only applied to non-accelerated reference systems. In 1907, in 'On the relativity principle and the conclusions drawn from it' Einstein asked, "Is it conceivable that the principle of relativity applies to systems that are accelerated relative to each other?" But, after maturing, we now understand that special relativity is far more powerful and capable, and that the answer to Einstein's question is 'yes'. It is made clear in any reasonably advanced textbook that SR has been developed precisely to handle accelerated observers and accelerated motion. SR is routinely used to predict the physics of very large accelerations, such as bound neutrons in the nucleus or high-energy particle scattering events. SR is capable of handling more than just acceleration. For instance, if one uses the ideas of the equivalence principle and the local nature of physics, SR can be used to calculate the influences of any gravitational field. [53] (of course for all practical purposes you would be using general relativity at this point)

As stated above, these sections only consider flat spacetime, without mirrors, and there will be no quantum ideas presented here or gravitational complications. Important points of interest on how special relativity deals with acceleration are exemplified in order to remove any Galilean intuitive bias in our understanding of how acceleration works. For more depth look to Rindler[54]. This treatment draws

heavily from Rindler's pioneering work on acceleration in special relativity[55].

2.4.1 Four-Acceleration

The four-acceleration is

$$a^\mu = \frac{d^2 x^\mu}{d\tau^2} = \frac{du^\mu}{d\tau} \, , \tag{2.186}$$

where u^μ is the four-velocity

$$u^\mu = \frac{dx^\mu}{d\tau} \, , \tag{2.187}$$

and $d\tau$ is the element of proper time from the spacetime invariant

$$d\tau^2 = dt^2 - (dx^2 + dy^2 + dz^2) \, , \tag{2.188}$$

with $c = 1$. Four vectors must be used when working with spacetime. Four vectors have superior utility than three vectors and relativistically valid relationships are revealed by their employment. In particular, acceleration undergoes a drastic relativistic revamping when examined as a four vector. From this metric, writing u for the speed (with three-velocity, $\boldsymbol{u} = dx^i/dt$), we obtain

$$\frac{d\tau^2}{dt^2} = 1 - u^2 \, , \qquad \frac{dt}{d\tau} = \frac{1}{\sqrt{1 - u^2}} \equiv \gamma \, . \tag{2.189}$$

Examining the relationship between the four-velocity u^μ and the three-velocity $\boldsymbol{u} = dx^i/dt$,

$$u^\mu = \frac{dx^\mu}{d\tau} = \frac{dt}{d\tau} \frac{dx^\mu}{dt} = \gamma \frac{dx^\mu}{dt} = \gamma(1, \boldsymbol{u}) \, . \tag{2.190}$$

54

The prime result is the relationship between the four-acceleration a^μ and the three-acceleration, $\boldsymbol{a} = d^2 x^i / dt^2$.

$$a^\mu = \frac{du^\mu}{d\tau} = \gamma \frac{du^\mu}{dt} = \gamma \frac{d}{dt}(\gamma, \gamma\boldsymbol{u}) = \gamma(\dot{\gamma}, \dot{\gamma}\boldsymbol{u} + \gamma\boldsymbol{a}) \ , \tag{2.191}$$

where the dot refers to the derivative with respect to coordinate time, t. A world line $C(\tau)$ with coordinates $x^\mu(\tau)$ has a tangent spacetime velocity vector $u^\mu = dx^\mu / d\tau$ and so the coordinate basis components of the four acceleration are, using the chain rule

$$a^\mu = \frac{du^\mu}{d\tau} = \frac{\partial u^\mu}{\partial x^\nu}\frac{dx^\nu}{d\tau} = u^\nu \partial_\nu u^\mu \ . \tag{2.192}$$

2.4.2   Acceleration Measured in the Instantaneous Rest Frame

We come to understand the 'proper' or 'felt' acceleration by asking about the scalar invariants $u_\mu u^\mu$ and $a_\mu a^\mu$. The easiest way to evaluate these is to simply pick the instantaneous rest frame, $u = 0$. Using the helpful relation $\dot{\gamma} = \gamma^3 u\dot{u}$, we see that $a^\mu = (0, \boldsymbol{a})$, so we have for the scalars,

$$u_\mu u^\mu = (1, 0) \cdot (1, 0) = 1 \ , \tag{2.193}$$

$$a_\mu a^\mu = (0, \boldsymbol{a}) \cdot (0, -\boldsymbol{a}) = -\boldsymbol{a} \cdot \boldsymbol{a} \equiv -\alpha^2 \ , \tag{2.194}$$

where α is the acceleration measured in the instantaneous rest frame. We call this quantity, the proper acceleration[54], in keeping with the meaning of 'one's own', *property*. The acceleration as measured by an accelerometer carried along by the observer can be called the *felt-acceleration* or, *local-acceleration* as well. Some authors will address the four-velocity and the four-acceleration as the proper-velocity and proper-acceleration. However, in general, a 'proper' measure of a quantity is that

55

taken in the relevant instantaneous rest frame. There can be confusion with 'proper' terminology, as many authors address the 'spatial components of the four-velocity' (called *celerity*) as the proper-velocity as well. Note that in the instantaneous rest frame ($u = 0$), $a^\mu = 0$ only if the magnitude of the three-acceleration in the rest frame vanishes. The four-acceleration is not necessarily the acceleration which is measured in the instantaneous rest frame of the traveler. Notice that the scalar invariant

$$u^\mu \cdot a^\mu = (1,0) \cdot (0,-\boldsymbol{a}) = 0 \ , \tag{2.195}$$

shows the four-acceleration is always orthogonal to the four-velocity. The general case of the scalar invariant of the four-acceleration is:

$$a_\mu a^\mu = \gamma^2 \dot{\gamma}^2 - \gamma^2 (\dot{\gamma} \boldsymbol{u} + \gamma \boldsymbol{a})^2 \ , \tag{2.196}$$

where we are no longer necessarily in the instantaneous rest frame of the traveler. Using $\dot{\gamma} = \gamma^3 u \dot{u}$, as well as $\boldsymbol{u}^2 = u^2$ and $\boldsymbol{u} \cdot \dot{\boldsymbol{u}} = u \dot{u}$ we find

$$-a_\mu a^\mu = \gamma^2 (\dot{\gamma}^2 u^2 + 2\gamma \dot{\gamma} u \dot{u} + \gamma^2 a^2 - \dot{\gamma}^2) \ , \tag{2.197}$$

which gives our the general formula for proper acceleration, using the invariant $\alpha^2 = -a_\mu a^\mu$,

$$\alpha^2 = \gamma^6 u^2 \dot{u}^2 + \gamma^4 a^2 = \gamma^6 [a^2 - (\boldsymbol{u} \times \boldsymbol{a})^2] \ . \tag{2.198}$$

Notice that for motion in a straight line, the rectilinear condition holds $\dot{u}^2 = a^2$, (use $\gamma^2 = 1 + \gamma^2 u^2$) and therefore

$$\alpha = \gamma^3 a \ . \tag{2.199}$$

Notice that for motion with a constant speed u, i.e. $\dot{u} = 0$, we obtain

$$\alpha = \gamma^2 a \ . \tag{2.200}$$

That is, if that motion is in a circle of radius r, i.e. $a = u^2/r$ we'll have $\alpha = \gamma^2 u^2/r$. In a frame S we consider a particle moving in a straight line (rectilinearly) with velocity u, proper acceleration α and proper time τ of the particle. With the rapidity ϕ of a particle defined as a parametrized velocity, $\phi = \tanh^{-1} u$ we ask, what is the proper time derivative of this parametrized velocity? (i.e. $d\phi/d\tau$?) The answer is

$$\frac{d\phi}{d\tau} = \frac{d}{d\tau} \tanh^{-1} u = \frac{dt}{d\tau} \frac{d}{dt} \tanh^{-1} u = \gamma \frac{1}{1 - u^2} \frac{du}{dt} = \gamma^3 a \ , \tag{2.201}$$

where we have used $\frac{d}{dx} \tanh^{-1} x = (1 - x^2)^{-1}$ and $dt/d\tau = \gamma$. Therefore we have another way of arriving at the proper acceleration: $\alpha = \frac{d\phi}{d\tau}$.

Transforming Acceleration in One Dimension

To better understand the felt-acceleration, consider only one-dimensional motion of a particle P and the velocity addition formula, along with the differentials of the Lorentz transformation

$$dt' = \gamma(dt - vdx) \ , \qquad u = \frac{u' + v}{1 + u'v} \ . \tag{2.202}$$

We are interested in the acceleration that is measured in P's instantaneous rest frame, called α, the proper acceleration. The particle moves along the x-axis of an inertial frame S with a varying velocity u. So, the particle is accelerating measured with respect to the inertial frame S with an acceleration du/dt. If we let S' be the instantaneous rest frame of P at some moment in time $t = t_0$, then we are looking for du'/dt'.

57

At this moment of time, t_0, $u = v$ and $u' = 0$. The idea is that u and u' vary but v remains constant. Since we want the acceleration measured in P's instantaneous rest frame, $\alpha = du'/dt'$, we can differentiate the velocity addition formula

$$\frac{du}{dt} = \frac{du'}{dt} - u^2 \frac{du'}{dt} \ . \tag{2.203}$$

Here I have set $v = u$ and $u' = 0$ after differentiation. Using the Lorentz transformation, $\frac{dt'}{dt} = \gamma(1 - uv)$ we have $\frac{du}{dt} = \frac{du'}{dt'}(1 - u^2)^{3/2}$ therefore

$$\alpha = \frac{du'}{dt'} = \gamma^3 \frac{du}{dt} = \gamma^3 a = \frac{d}{dt}(\gamma u) \ . \tag{2.204}$$

In a more general case, where S' is not just P's rest frame, but S' is any frame in one dimensional motion relative to S, then the following relationship may be proven in general (see Rindler[54] Equation 14.2 where he assumes standard configuration for instance)

$$(1 - u'^2)^{-3/2} \frac{du'}{dt'} = (1 - u^2)^{-3/2} \frac{du}{dt} \ . \tag{2.205}$$

The interesting aspect of this is that this relationship, $\gamma(u')^3 du'/dt = \gamma(u)du/dt$, is the analogue of invariant general acceleration in Galilean relativity: $du/dt = du'/dt'$. The felt-acceleration, $\alpha = \gamma^3 a$ with $a = du/dt$, and $\gamma = \gamma(u)$ will therefore be a quantity of interest. In particular, this quantity will reappear in moving mirror calculations.

General Transformations of Acceleration

For reference, we state the general transformation equations for acceleration. Using the instantaneous rest system, we have the simple expressions for the relations

of accelerations: $\alpha_x = \gamma^3 a_x$, $\alpha_y = \gamma^2 a_y$ and $\alpha_z = \gamma^2 a_z$. These are clear from Equation's (2.200) and (2.199). However, the more general expressions, not involving the instantaneous rest frame are derived starting from the general Lorentz transformations equations (see Einstein 1905).

$$a'_x = \frac{a_x}{\gamma^3(1 - u_x v)^3} \, , \tag{2.206}$$

$$a'_y = \frac{a_y}{\gamma^2(1 - u_x v)^2} + \frac{u_y a_x v}{\gamma^2(1 - u_x v)^3} \, , \tag{2.207}$$

$$a'_z = \frac{a_z}{\gamma^2(1 - u_x v)^2} + \frac{u_z a_x v}{\gamma^2(1 - u_x v)^3} \, . \tag{2.208}$$

2.4.3 Prototypical Example: Hyperbolic Trajectory

Looking briefly at the most common example used to understand proper acceleration in special relativity, consider (1+1) spacetime, and suppose α_0 is a constant (the symbol is fortuitously chosen ahead of time). Let a particle undergo motion according to, $x^2 = \alpha_0^{-2} + t^2$ so that we take only the positive piece of

$$x = \pm\sqrt{\alpha_0^{-2} + t^2} \, . \tag{2.209}$$

The acceleration 'felt' by the particle is the proper acceleration. The four-acceleration has time dependent components in both space and time. Using the one dimensional definition, Eqn. (2.199), $\alpha = \gamma^3 a = \frac{a}{(1-v^2)^{3/2}}$ we obtain

$$v = \pm\frac{t}{\sqrt{\alpha_0^{-2} + t^2}} \, , \tag{2.210}$$
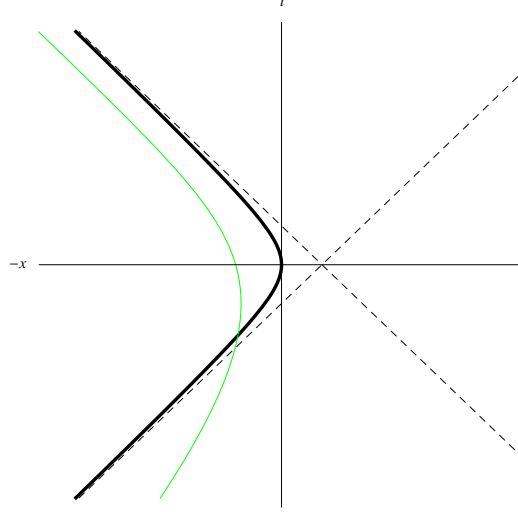
Figure 2.2: Hyperbolic Trajectory.

$$a = \pm \frac{\alpha_0^{-2}}{(\alpha_0^{-2} + t^2)^{3/2}} \ , \tag{2.211}$$

and

$$\gamma^3 = \alpha_0^3 (\alpha_0^{-2} + t^2)^{3/2} \ , \tag{2.212}$$

gives

$$\alpha = \pm \alpha_0 \ . \tag{2.213}$$

Therefore the proper acceleration is constant for hyperbolic motion. Uniform acceleration motion corresponds to the absolute magnitude of the four-acceleration or 'proper-acceleration'.

2.4.4 Special Example: Carlitz-Willey Trajectory

Now consider a trajectory that has an intimate relationship to black hole collapse.

$$x = -t - \kappa^{-1} W(e^{-2\kappa t}) , \qquad (2.214)$$

where W is the product log or Lambert W function and κ is a positive constant. The product log is defined through $z = W(z)e^{W(z)}$ where z is any complex number. The first and second derivatives are

$$\frac{dW}{dz} = \frac{W(z)}{z(1 + W(z))} , \qquad (2.215)$$

$$\frac{d^2W}{dz^2} = -\frac{W(z)^2(2 + W(z))}{z^2(1 + W(z))^3} . \qquad (2.216)$$

Note that it looks somewhat similar to the hyperbolic trajectory:
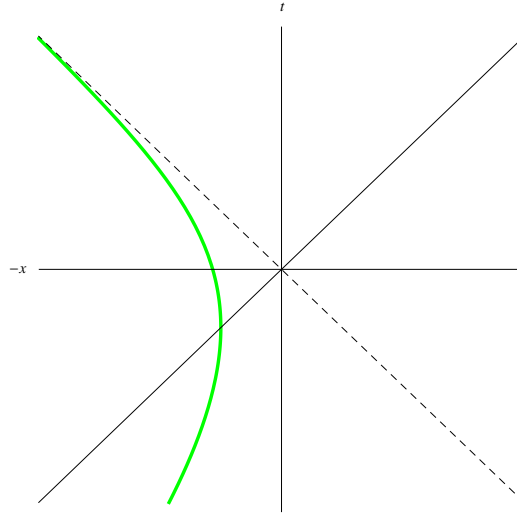
Figure 2.3: Carlitz-Willey Trajectory

What is the acceleration felt by the particle in this case? Using

$$v = \dot{x} = -1 + \frac{2W(e^{-2\kappa t})}{1 + W(e^{-2\kappa t})} , \qquad (2.217)$$

61

$$a = \ddot{x} = -\frac{4\kappa W(e^{-2\kappa t})}{(1 + W(e^{-2\kappa t}))^3} \; , \tag{2.218}$$

one finds

$$\alpha = \gamma^3 \ddot{x}(t) = \frac{-\kappa}{2\sqrt{W(e^{-2\kappa t})}} \; . \tag{2.219}$$

Notice the dichotomy,

$$\lim_{t \to \infty} a = 0 \qquad \lim_{t \to \infty} \alpha = -\infty \tag{2.220}$$

$$\lim_{t \to -\infty} a = 0 \qquad \lim_{t \to -\infty} \alpha = 0 \tag{2.221}$$

For a moving mirror emitting constant energy flux, Carlitz and Willey have shown that thermal radiation occurs for all times.[11] I have done the transcendental inversion necessary to uncover the trajectory for this radiation and encountered $\alpha = \frac{-\kappa}{2\sqrt{W(e^{-2\kappa t})}}$ as the proper acceleration necessary for Planckian character. This is treated in detail in Chapter 3.

Chapter 3

Moving Mirror Trajectories

3.1 Basic Categories

This chapter is concerned with moving mirror trajectories and associated physical quantities. We will treat each mirror trajectory separately, generally categorized by their common motions. The beta Bogolubov coefficient, Eqn. (2.40) is computed. Not all mirror trajectories treated here have had their beta transformation coefficients found, and not all mirror trajectories are capable of having their beta transformation coefficients found analytically. Those few mirror trajectories whose betas have not been found are relegated to the heterogeneous solutions section. It is often much easier to solve for the energy flux than beta transformation coefficients, so computation of the energy flux is attempted for all the mirror trajectories. When possible, the trajectories, $z(t)$ are presented, along with their ray tracing functions, $p(u)$.

The sections are organized mostly by the type of moving mirror motion, starting off with trivial mirrors in Section 3.2 which undergo no acceleration, and produce no particles. These mirror trajectories serve as a useful introduction to the calculational techniques. They are easy to solve for and useful to understand the non-trivial cases.

Section 3.3 involves the previously, well-studied, and well-known canonical moving mirror trajectories. These have widely varying properties.

Section 3.4 includes those mirror trajectories which emit negative energy flux during a phase of their motion. In each case, motion is asymptotically inertial in the past and future, see Figure 3.1[23]. These asymptotically inertial mirror trajectories can be 'time-evolved', i.e. their particle production can be localized to any point in time during their motion. These trajectories do not have horizons or pathological properties. For these trajectories the total energy emitted is finite. Trajectories in this section are the COnstant-velocity ASymptotic Trajectories (COAST mirrors), subsections 3.4.2 and 3.4.3. They have not been studied before. Special emphasis should be placed on the COAST mirrors, because these final coasting motion trajectories have a spectra which can be time-evolved with an appropriate localization procedure, determining particle production at any point in time. This is due to the lack of an acceleration singularity. COAST mirrors are unitary by construction and emit negative energy flux.
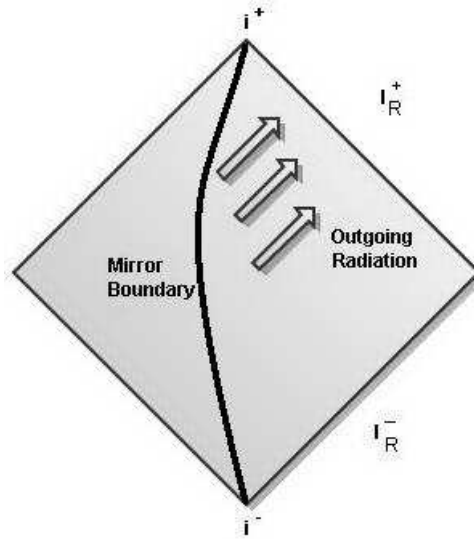

Figure 3.1: Penrose diagram describing a moving mirror trajectory which is inertial in the asymptotic past and future.

Trajectories that have never been studied before, which have horizons and start statically, are introduced in Section 3.5. These avoid splicing, and have exactly known beta transformation coefficients. They emit positive energy flux throughout their motion, asymptotically approach an infinite proper acceleration and have thermal character (Planck spectrum) in the high frequency limit. Each one has a unique motion with strikingly different and interesting properties.

Heterogeneous trajectories are introduced in Section 3.6 that incorporates those mirror trajectories whose betas cannot be obtained analytically. Section 3.6 also includes trajectories whose ray tracing functions may be transcendentally inverted, but whose betas have not been computed. As well, I have included an arguably physically irrelevant but mathematically important trajectory, in subsection 3.6.1, which has tractable beta solutions and which inspired the technique and pursuit of all of the other exactly solvable boundaries.

In Section 3.7, there are four tables that summarize the main results. Trajectories, ray tracing functions, energy flux, accelerations, total energy and beta coefficients are displayed in Tables 3.1, 3.2, 3.3, and 3.4.

3.2   Trivial Mirror Trajectories

The nonaccelerated trivial mirror trajectories presented in this chapter are treated with detail in order to clarify the calculational procedures used in the later sections. These mirror are not physically interesting with regards to the particle transformation calculation. These mirrors all have $\beta_{\omega'\omega} = 0$ transformation coefficients and therefore none create particles. The 'constant velocity' mirror is treated efficiently using null coordinates and together with the static mirror acts as a demonstration of the superior utility of null coordinates when calculating in the moving mirror

model. The 'light speed' boundary and the 'constant velocity' mirror are included only for academic reference and completeness. For pedagogical analogy the static, drifting, and light speed boundaries coincide respectfully to the final motions of the asymptotically inertial mirrors of Walker-Davies (static), Darcx (drifting) and Proex (light speed).
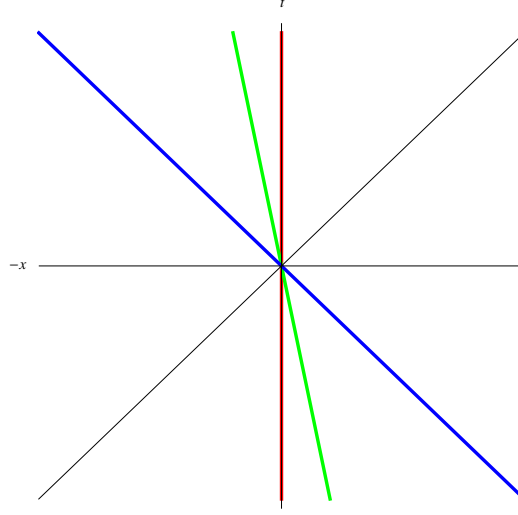
Figure 3.2: Static, drift ($v_0 = \frac{1}{5}$), and light speed mirrors.

3.2.1 Static Mirror Trajectory

The $\beta_{\omega'\omega} = 0$ result for the static mirror is arrived quickly by using null coordinates. Although coupled to a massless scalar field in 1+1 dimensional flat spacetime, the mirror trajectory analyzed with the Bogulobov mechanism provides no interesting radiation. Null coordinates are used for both the mode functions and Bogolubov transformations coefficients. Recall, $v = t + x$, and $u = t - x$. The normalization can be computed via

$$(u_\omega, u_{\omega'}) = i \int_{-\infty}^{\infty} dv \; u_{\omega'}^* \partial_v u_\omega - u_\omega \partial_v u_{\omega'}^* \,. \tag{3.1}$$

This integral is done over the past hypersurface, I_R^-. The right moving modes do not extend behind the mirror and therefore there is only a contribution from the left moving modes at the past surface. Using, $u_\omega = \frac{1}{\sqrt{4\pi\omega}}(e^{-i\omega v} - e^{-i\omega u})$ and $u_{\omega'}^* = \frac{1}{\sqrt{4\pi\omega'}}(e^{i\omega' v} - e^{i\omega' u})$, the inner product definition, $(u_\omega, u_{\omega'}) = \delta(\omega - \omega')$ is satisfied. Solving for $\beta_{\omega,\omega'}$, using Equation (2.40) yields,

$$\beta_{\omega,\omega'} = \frac{\omega' - \omega}{4\pi\sqrt{\omega\omega'}} \int_{-\infty}^{\infty} dv \, e^{-i(\omega'+\omega)v} = \frac{2\pi(\omega' - \omega)}{4\pi\sqrt{\omega\omega'}}\delta(\omega' + \omega) = 0 \ . \tag{3.2}$$

As this confirms, the null coordinate approach is efficient for normalization and transformation calculations.

3.2.2 Drifting Mirror Trajectory

This trivial case has a correspondence to the Darcx trajectory, which approaches constant velocity. The beta transformation calculation for a constant speed mirror trajectory gives zero particle production. An important aspect of the drifting mirror calculations resides in the fact that null coordinates are overwhelmingly more efficient than the usual spacetime coordinate approach. To derive the correct form for the modes, the relativistic Doppler shift formula is needed. An observer will notice a new frequency of light, ω_o, when moving away from an emitter,

$$\omega_o = \sqrt{\frac{1 - v_0}{1 + v_0}}\omega \ . \tag{3.3}$$

It is obvious that ω_o has the smaller magnitude frequency, with less energy, longer redshifted wavelength. Consider the observer holding a mirror and reflecting that redshifted light back to the emitting source. The emitter will now observe a second redshift, with a frequency ω'.

$$\omega' = \sqrt{\frac{1 - v_0}{1 + v_0}} \omega_0 = \sqrt{\frac{1 - v_0}{1 + v_0}} \sqrt{\frac{1 - v_0}{1 + v_0}} \omega \ . \tag{3.4}$$

This relation is $\omega' = \omega D$,

$$\omega' = \frac{1 - v_0}{1 + v_0} \omega \ , \tag{3.5}$$

with $D \equiv \frac{1 - v_0}{1 + v_0}$.

Consider a massless quantized scalar field in the moving mirror model. The mirror will have a non-accelerated trajectory, to the left, $z(t) = x_0 - v_0 t \rightarrow z(t_u) = -v_0 t_u$, where $x_0 = 0$, v_0 is the constant speed of the mirror relative to our frame. This gives $z(t_u) = -v_0 t_u$. Using Equation (2.35) one can derive $p(u) = Du$, and the IN modes will have the properly normalized form;

$$u_\omega^{in} = (4\pi\omega)^{-1/2}\left(e^{-i\omega v} - e^{-i\omega u D}\right) \ . \tag{3.6}$$

The OUT modes have the form,

$$u_{\omega'}^{out} = (4\pi\omega')^{-1/2}\left(e^{-i\omega' v D^{-1}} - e^{-i\omega' u}\right) \ . \tag{3.7}$$

Computing $\beta_{\omega,\omega'}$ gives four terms, two of which are identically zero, yielding

$$\beta_{\omega,\omega'} = \int_{-\infty}^{\infty} dv \ (-\omega + \omega' D^{-1})e^{-i(\omega + \omega' D^{-1})v} \ , \tag{3.8}$$

$$= 2\pi(\omega' D^{-1} - \omega)\delta(\omega + \omega' D^{-1}) = 0 \ . \tag{3.9}$$

Thus there is no particle creation. It is worth noting that obtaining this result using the spacetime coordinate approach is a much longer and more tedious calculation.

3.2.3 Light Speed Boundary

This boundary has a correspondence to the asymptotic future speed of the Proex trajectory. A light speed boundary is included, only to demonstrate the extreme situation. The transformation mechanism continues to give consistent results. Choosing $p(u) = 0$ gives a trajectory of $z(t_u) = -t_u$. Thus the boundary where the scalar field vanishes is at a null surface. A solution to the wave equation is

$$u_\omega = N(e^{-i\omega v} - 1) \,, \tag{3.10}$$

where N is a normalization factor to be determined. Using the scalar product,

$$(u_\omega, u_{\omega'}) = i \int_{-\infty}^{\infty} dv \, u_\omega^* \partial_v u_{\omega'} - u_{\omega'} \partial_v u_\omega \tag{3.11}$$

$$= NN'(\omega + \omega') \int_{-\infty}^{\infty} dv \, e^{i(\omega - \omega')v} \tag{3.12}$$

$$= |N|^2 4\pi\omega\delta(\omega - \omega') \,. \tag{3.13}$$

The correct mode normalization is therefore $N = 1/\sqrt{4\pi\omega}$. One can show that there is zero particle production for this boundary, as in the inertial static and drifting cases.

3.3 Canonical Accelerated Mirrors

3.3.1 Carlitz-Willey Trajectory

This trajectory gives a thermal spectrum for all times and has a constant flux of energy. By dealing with the past hypersurface using null coordinate integration and through the introduction of left and right 'split' mode convention, Carlitz-Willey[11] were able to exactly solve for the beta coefficients of this mirror. The convention

utilizes different modes defined on both I_R^+ and I_L^+. The left and right coefficient formulation lies at the crux of their calculation and despite the call for more attention [35], the construction has been little utilized. We have confirmed their solution on the past surface and here we present a confirmation via the future surface which must be the same.
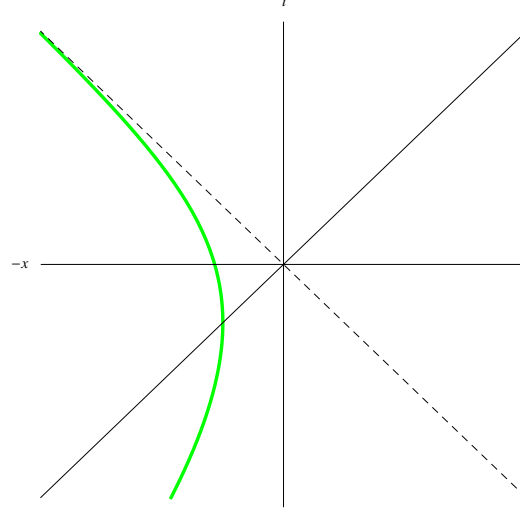
Figure 3.3: Carlitz-Willey Trajectory

Although the original paper[11] does not give the trajectory in the form of $z(t)$, I find that the defining trajectory is

$$z(t) = -t - \frac{1}{\kappa} W(e^{-2\kappa t}) \, . \tag{3.14}$$

This trajectory utilizes the Lambert W function (the product log), as introduced in Equation 2.214. The product log underlies the thermal radiation and constant energy flux for the Carlitz-Willey mirror, as will be shown.

The proper acceleration, i.e. the acceleration in the instantaneous rest frame of

the mirror, Equation 2.199, is

$$\alpha(t) = -\frac{\kappa}{2\sqrt{W(e^{-2\kappa t})}} \ .$$

(3.15)

It is important to emphasize that the proper acceleration is not constant. It is a common mistake to assume that accelerated mirrors that emit thermal radiation possess a constant proper acceleration. This is likely due to the related prediction (the Unruh effect) that a uniformly accelerating observer will observe black-body radiation where an inertial observer would observe none, in flat spacetime (or even curved spacetime). This acceleration radiation as described by Unruh [10] is so closely related, that it is sometimes called the Fulling-Davies-Unruh effect. At constant uniform acceleration, Unruh radiation is thermal. To be clear, the moving mirror model as a particular manifestation of the dynamical Casimir effect, is different. It is hard to overstate that only the uniformly accelerated mirror has constant proper acceleration and for thermal radiation at all times, the moving mirror accelerates with the time-dependent function indicated in Equation (3.15). Consider the features of this trajectory. It initially approaches at the speed of light, $\lim_{t\to-\infty} v = 1$ and does not intersect the origin. Its final limiting velocity is the speed of light to the left, $\lim_{t\to\infty} v = -1$. The initial limiting proper acceleration is 0 yet the final limiting proper acceleration is $-\infty$. The asymptotic celerity, γv, is infinite. Notice the unusual features of the trajectory: It initially moves at the speed of light (asymptotically null) with a zero proper acceleration! It does not intersect the origin. The ray tracing functions are

$$p(u) = -\tfrac{1}{\kappa}e^{-\kappa u}$$
$$f(v) = -\tfrac{1}{\kappa}\ln(-\kappa v) \qquad v < 0 \ .$$

(3.16)

Integration, using Equation (2.40) gives the result for the beta transformation coefficient in Table 3.4.

The beta in Table 3.4 is the 'Right' bogolubov coefficient, in the Carlitz-Willey construction, [11] as discussed in more detail when the coefficient is computed on the future hypersurface. The 'Right' and 'Left' mode construction is more complex than the conventional approach. The appendix in the original Carlitz and Willey paper [11] is recommended for further elucidation of the process with the CW 'split' mode technique. Squaring the modulus yields

$$|\beta_{\omega'\omega}|^2 = \frac{1}{2\pi\kappa\omega'}\frac{1}{e^{2\pi\omega/\kappa}-1} \ . \tag{3.17}$$

The mirror has a constant flux for all times.

$$\langle T_{uu} \rangle = \frac{\kappa^2}{48\pi} \ , \tag{3.18}$$

which is calculated from Equation (2.45) using the ray tracing function for $p(u)$. The occupation number per mode ω, $\langle N_\omega \rangle$, the occupation number per mode ω', $\langle N'_\omega \rangle$, the total particle number $\langle N_\rangle$ and the total energy, E are all divergent. This is because the flux is constant for all times and this is due to the mirror traveling with an ever increasing acceleration. The CW mirror produces one-dimensional thermal radiation at all times. Incidentally, a resistor is another example of a system which has a one-dimensional thermal power density spectrum [56].

Particle Creation via Future Cauchy Surface

The computation of beta coefficients using the future surface is done by using the Carlitz-Willey 'split-mode' convention. This is done by using the general mode forms:

$$\phi_{\omega'} = e^{-i\omega'v} - e^{-i\omega'p(u)} \qquad \begin{cases} \phi_\omega^R = e^{-i\omega V(v)}\Theta(-v) - e^{-i\omega u} \\ \phi_\omega^L = e^{-i\omega W(v)}\Theta(v) \ . \end{cases} \tag{3.19}$$

Here

$$p(u) = -\kappa^{-1} e^{-\kappa u} \qquad \begin{cases} V(v) = -\kappa^{-1} \ln(-\kappa v) & v < 0 \\ W(v) = +\kappa^{-1} \ln(+\kappa v) & v > 0 \ . \end{cases} \qquad (3.20)$$

Consider the calculation involving the only the right future surface. The I_R^+ surface is typically not used for calculating particle creation, particularly in the case of a mirror. This is because, technically, I_R^+ is not a proper Cauchy surface, the full surface is actually $I_L^+ \bigcup I_R^+$. The Carlitz-Willey 'split' mode construction allows us to deal with this complication. The division of the future surface is broken into two distinct horizons, the left and right ones, where *two* distinct Bogolubov coefficients are calculated. Here I present a new $\beta_{\omega'\omega}^R$ calculation as done on the future hypersurface.

$$\beta_{\omega'\omega}^R = i \int_{-\infty}^{\infty} du \ \phi_{\omega'}^* \ \overleftrightarrow{\partial_u} \ \phi_\omega^{R*} \ , \qquad (3.21)$$

where the integral is done on I_R^+. Here the modes assume the CW convention[11],

$$\phi_{\omega'} = e^{-i\omega' p(u)} \ , \qquad \phi_\omega^R = e^{-i\omega u} \ , \qquad (3.22)$$

for the CW trajectory, $p(u) = -\kappa^{-1} e^{-\kappa u}$, so we obtain $\phi_{\omega'} = e^{i\frac{\omega'}{\kappa} e^{-\kappa u}}$, $\phi_\omega^R = e^{-i\omega u}$, $\phi_{\omega'}^* = e^{-i\frac{\omega'}{\kappa} e^{-\kappa u}}$, $\phi_\omega^{R*} = e^{i\omega u}$. Using these modes,

$$\beta_{\omega'\omega}^R = i \int_{-\infty}^{\infty} du \ e^{-i\frac{\omega'}{\kappa} e^{-\kappa u}} \ \overleftrightarrow{\partial_u} \ e^{i\omega u} \ . \qquad (3.23)$$

Partial integration can be done because the modes vanish at infinite distances.

One finds

$$\beta_{\omega'\omega}^R = -2\omega \int_{-\infty}^{\infty} du \ e^{i\omega u - i\frac{\omega'}{\kappa} e^{-\kappa u}} \ , \qquad (3.24)$$

using the substitution $e^t = i\frac{\omega'}{\kappa}e^{-\kappa u}$, where $dt = -\kappa du$ gives

$$\beta^R_{\omega'\omega} = -\frac{2\omega}{\kappa}\int_{-\infty}^{\infty}dt e^{-i\frac{\omega}{\kappa}(t-\ln i\frac{\omega'}{\kappa})-e^t} = -\frac{2\omega}{\kappa}e^{i\frac{\omega}{\kappa}\ln i\frac{\omega'}{\kappa}}\int_{-\infty}^{\infty}dt\ e^{-i\frac{\omega}{\kappa}t-e^t}\ . \tag{3.25}$$

where we now use

$$\Gamma(z) = \int_{-\infty}^{\infty}dt e^{zt-e^t} \qquad Re[z] > 0\ , \tag{3.26}$$

to obtain for all times, (not just late times)

$$\beta^R_{\omega'\omega} = -\frac{2\omega}{\kappa}e^{-\frac{\pi\omega}{2\kappa}}\big(\frac{\omega'}{\kappa}\big)^{i\frac{\omega}{\kappa}}\Gamma\big(-i\frac{\omega}{\kappa}\big)\ . \tag{3.27}$$

3.3.2 Uniformly Accelerated Mirror Trajectory

A mirror accelerating uniformly emits quanta, but there is no radiation of energy. Davis and Fulling first discovered this seemingly paradoxical effect, see [5]. A hyperbolic trajectory is:

$$z(t) = B - \sqrt{B^2 - t^2}\ , \tag{3.28}$$

where a plot is given in Figure 3.4.

Using a splice between the static mirror and hyperbolic mirror, Davies and Fulling [5] found

$$\beta_{\omega\omega'} = \frac{B}{\pi}e^{i(\omega'-\omega)B}K_1(2B\sqrt{\omega\omega'})\ , \tag{3.29}$$

(see the Hyperbolic plus Static mirror in Section 3.6), where K_1 is the modified Bessel function. This result was used with questionable assumptions, involving a static mirror spliced to a hyperbolic mirror. We present the results for the hyperbolic trajectory throughout all times.

Substituting $p(u)$ into Eqn. (2.45) gives $\langle T_{uu}\rangle = 0$. No paradox exists, despite a
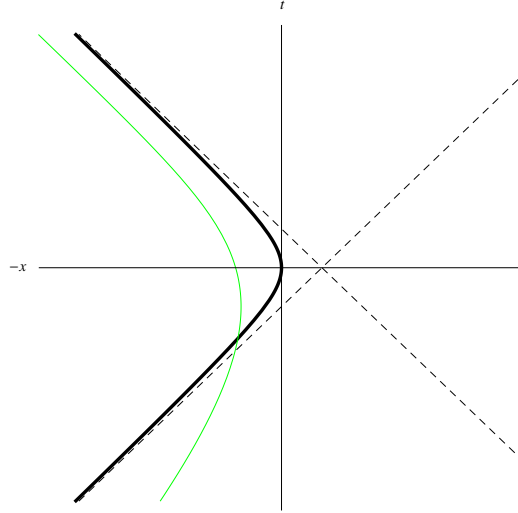
Figure 3.4: Hyperbolic, $B = \frac{1}{2}$.

detector absorbing quanta and making a transition to an excited state in the absence of all field energy. A detector, as described by Walker[15] emits negative energy into the field to compensate. This strange result is not without precedent in quantum field theory. Similar situations are explored by Epstein, Glaser and Jaffe (1965)[57], who construct many-particle states with negative or zero fluxes even in the absence of mirrors or detectors.

Hyperbolic and Mobius Trajectories on Null Surfaces

Constant acceleration mirror trajectories have beta coefficients which can be solved straightforwardly using null hypersurfaces for the Cauchy surface in the scalar product. For two hyperbolic mirrors (Mobius trajectory), an arguably more natural manifestation of hyperbolic motion, there is no appearance of particles or energy. This is to be contrasted with the single hyperbolic mirror which has particle production, yet $\langle T_{uu} \rangle = 0$. The Mobius expression is more simple and both $\pm$ branches are included. In addition there is no transformation shift to intersect zero.

Hyperbolic Mirror on Null Surface: Particles without Energy

The hyperbolic trajectory is $z_h(t) = B - \sqrt{B^2 + t^2}$. The modes solutions used that satisfy the boundary condition and wave equation are, using the CW normalization convention:

$$\phi_{\omega'} = e^{-i\omega'v} - e^{-i\omega'p(u)}\Theta(B+u) \ , \qquad \phi_\omega = e^{-i\omega f(v)}\Theta(B-v) - e^{-i\omega u} \ , \qquad (3.30)$$

while the beta coefficient is $\beta_{\omega'\omega} = -i\frac{B}{\pi}e^{i(\omega-\omega')}K_1(2B\sqrt{\omega\omega'})$. To solve for this beta coefficient, the conversions (using $u = t - z$, $v = t + z$) begin via

$$
\begin{aligned}
u(t) &= -B + t + \sqrt{B^2 + t^2} \\
v(t) &= \ B + t + \sqrt{B^2 + t^2} \ .
\end{aligned}
\qquad (3.31)
$$

Inversion gives

$$
\begin{aligned}
t(u) &= \tfrac{u(2B+u)}{2(B+u)} \ , \\
t(v) &= \tfrac{v(2B-v)}{2(B-v)} \ .
\end{aligned}
\qquad (3.32)
$$

In null coordinates, Eqn. (2.35), and the inverse, Eqn. (2.36), are

$$
\begin{aligned}
p(u) &= \tfrac{Bu}{B+u} \qquad u > -B \ , \\
f(v) &= \tfrac{Bv}{B-v} \qquad v < B \ .
\end{aligned}
\qquad (3.33)
$$

For solving for the beta coefficient on the past hypersurface, the mode solutions are therefore, $\phi_{\omega'}^* = e^{i\omega'v}$, $\phi_\omega^* = e^{i\omega \frac{Bv}{B-v}}$ and the integral

$$\beta_{\omega'\omega} = \frac{1}{4\pi\sqrt{\omega\omega'}} \int_{-\infty}^{\infty} dv \ e^{i\omega'v}e^{i\omega\frac{Bv}{B-v}}(\omega' - \omega\frac{B^2}{(B-v)^2})\Theta(B-v) \ , \qquad (3.34)$$

is obtained. This is solved to give,

$$\beta_{\omega'\omega} = \frac{1}{4\pi\sqrt{\omega\omega'}}\left(-4i\sqrt{\omega\omega'}Be^{i(\omega-\omega')B}K_1(2B\sqrt{\omega\omega'})\right) , \qquad (3.35)$$

$$\beta_{\omega'\omega} = -i\frac{B}{\pi}e^{i(\omega-\omega')B}K_1(2B\sqrt{\omega\omega'}) . \qquad (3.36)$$

Solving for the beta by using the future surface results in the integral

$$\beta_{\omega'\omega} = \frac{1}{4\pi\sqrt{\omega\omega'}}e^{i(\omega-\omega')B}\int_{-\infty}^{\infty} da\ e^{i\omega a}e^{-i\omega'\frac{B^2}{a}}(\omega'\frac{B^2}{a^2} - \omega)\Theta(a) , \qquad (3.37)$$

which also gives Eqn. (3.36).

The energy flux is found by the expectation value of the stress-energy tensor, Eqn. (2.45) where the total energy is found by Equ (2.48), $E = \int_{u_{min}}^{u_{max}} \langle T_{uu} \rangle\ du$. Here $p(u) = \frac{Bu}{B+u}$. Using Eqn. (2.45), one finds zero flux, $\langle T_{uu} \rangle = 0$. Therefore, incorporating Eqn. (3.36), the well known 'particles without energy' or 'radiation without energy' result is confirmed. Obadia and Parentani study how to switch off the interaction of the mirror-field coupling at large times. [58] They found that if the coupling is constant they were able to obtain $\langle T_{uu} \rangle = 0$.

Two Hyperbolic Mirrors: Acceleration without Particles

Two hyperbolic mirrors (Mobius mirror) produce no energy or particles[23]. This double mirror trajectory is included in this constant acceleration section as the only demonstration of a radiationless, yet accelerated trajectory. It is a trivial example of preserving purity during the mode 'evolution' from I_R^- to I_R^+. Asymptotically inertial mirrors in Section 3.4 are unitary like the Mobius mirror. There is no particle production because the two constant acceleration mirrors cancel each other's particle creation effect. Using the CW normalization, the modes solutions that satisfy the boundary condition and wave equation are, Equ. (3.19). The Mobius trajectory has

been studied before[59] from a conformal field theory point of view in an attempt to illustrate the close relationship between the production of particles and energy. The only new aspect presented here is the use of the past and future hypersurfaces to derive the same results and confirm our technique. The trajectory is,

$$z_{mobius}(t) = \pm\sqrt{B^2 + t^2} \ . \tag{3.38}$$
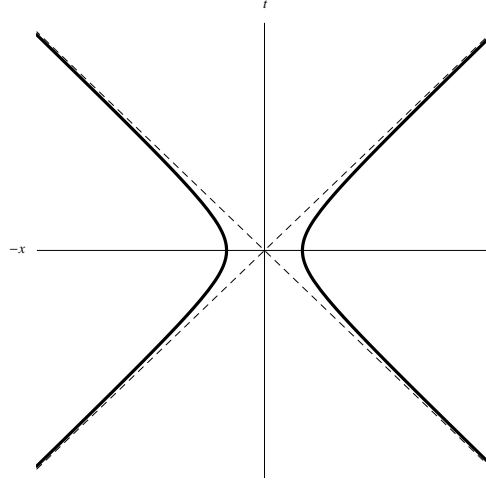
Figure 3.5: Mobius Trajectory: two hyperbolic mirrors, $B = \frac{1}{2}$.

The ray tracing formulae are solved by inverting $u(t)$ and $v(t)$:

$$
\begin{aligned}
u(t) &= t \pm \sqrt{B^2 + t^2} \ , \\
v(t) &= t \pm \sqrt{B^2 + t^2} \ ,
\end{aligned}
\tag{3.39}
$$

with the result,

$$
\begin{aligned}
t(u) &= \frac{u}{2} - \frac{B^2}{2u} \ , \\
t(v) &= \frac{v}{2} - \frac{B^2}{2v} \ .
\end{aligned}
\tag{3.40}
$$

In null coordinates,

$$p(u) = -\frac{B^2}{u} \qquad u \neq 0 \,,$$
$$f(v) = -\frac{B^2}{v} \qquad v \neq 0 \,. \tag{3.41}$$

The beta transformation coefficient integral is done using the past hypersurface by $\beta_{\omega'\omega} = i \int_{-\infty}^{\infty} dv \; \phi_{\omega'}^* \overset{\leftrightarrow}{\partial_v} \phi_{\omega}^*$ such that the modes are, $\phi_{\omega'}^* = e^{i\omega'v}$ and $\phi_{\omega}^* = e^{i\omega\frac{-B^2}{v}}$. The resulting integral is

$$\beta_{\omega'\omega} = \int_{-\infty}^{\infty} dv \; e^{i\omega'v} e^{i\omega\frac{-B^2}{v}} (\omega' - \omega\frac{B^2}{v^2}) \equiv \int_{-\infty}^{\infty} dv \; I(B, v, \omega, \omega') \,, \tag{3.42}$$

which must be done avoiding the pole at $v = 0$. Split into two, we obtain

$$\begin{aligned}
\beta_{\omega'\omega} &= \int_{-\infty}^{0} dv \; I(B, v, \omega, \omega')\Theta(-v) + \int_{0}^{\infty} dv \; I(B, v, \omega, \omega')\Theta(v) \\
&= 0 \,.
\end{aligned} \tag{3.43}$$

For integration using the future hypersurface, this result is obtained by a similar method which also gives zero. The energy flux, Eqn. (2.45) is found as was done for the hyperbolic mirror, however in this case, $p(u) = -\frac{B^2}{u}$ and the result is zero: $\langle T_{uu} \rangle = 0$.

3.3.3 Davies-Fulling Mirror Trajectories

The most famous moving mirror trajectory is that of Davies and Fulling[5]. This mirror accelerates with a time-dependent acceleration and becomes asymptotically null. The original calculation utilizes obscure approximations and Fulling has recently concluded [29] that although the end results still hold, the calculational approach used may have an error. The Davies-Fulling(DF) result was the first trajectory used to provide an understanding of the appearance of a thermal spectrum. Here

I present a 'late time Davies-Fulling' calculation which is done without obscure approximations. The defining characteristic of this DF mirror is the 'broken' and 'glued together' static and accelerating pieces:

$$z(t) = -t - Ae^{-2\kappa t} + B \qquad t \to \infty ,$$
$$z(t) = 0 \qquad\qquad\qquad t < 0 .$$

(3.44)

Without approximations, like high frequency or ignoring boundary terms from integration by parts, we compute the $\beta_{\omega'\omega}$'s for this mirror using the future surface, and the form originally [5] given for $p(u)$,

$$p(u) = B - Ae^{-\kappa(u+B)} .$$

(3.45)

I will use the specific values $A = \frac{2}{\kappa}$ and $B = \frac{\ln 2}{\kappa}$ so that $A = \frac{e^{\kappa B}}{\kappa}$.
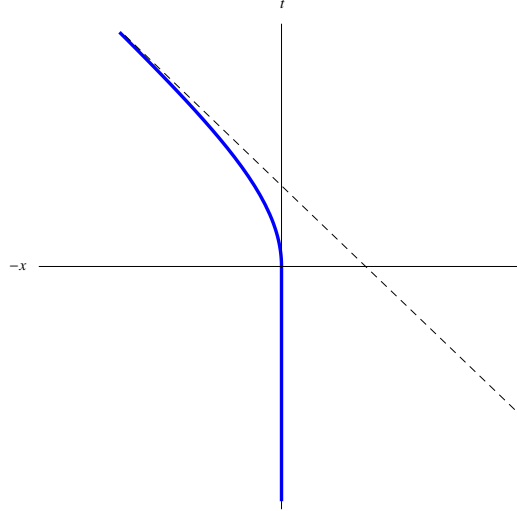

Figure 3.6: Davies-Fulling Trajectory

Notice the static 'glued' piece affect on the initial character of the mirror. The velocity is initially 0 while as $t \to \infty$ the velocity goes to -1. The proper acceleration as $t \to \infty$ is $-\infty$. The original ray tracing functions become

80

$$p(u) = \frac{\ln 2}{\kappa} - \frac{1}{\kappa} e^{-\kappa u} \qquad\qquad u \to \infty \ ,$$

$$f(v) = -\frac{1}{\kappa} \ln\left(\frac{\ln 2}{2} - \frac{\kappa v}{2}\right) - \frac{\ln 2}{\kappa} \qquad v < \frac{\ln 2}{\kappa} \ . \tag{3.46}$$

Solving for the beta coefficient using the same null surfaces as for the Carlitz-Willey mirror yields,

$$\beta_{\omega'\omega} = -\frac{2\omega}{\kappa} 2^{\frac{i\omega'}{\kappa}} \left(\frac{\omega'}{\kappa}\right)^{\frac{i\omega}{\kappa}} e^{-\frac{\pi\omega}{2\kappa}} \Gamma\left(-i\frac{\omega}{\kappa}\right) + Q \ , \tag{3.47}$$

where

$$Q \equiv 2^{\frac{i\omega'}{\kappa}} \left(\frac{\omega'}{\kappa}\right)^{\frac{i\omega}{\kappa}} e^{-\frac{\pi\omega}{2\kappa}} \left(\frac{\omega}{\kappa} \Gamma\left[-i\frac{\omega}{\kappa}, i\frac{\omega'}{\kappa}\right] + i\Gamma\left[1 - i\frac{\omega}{\kappa}, i\frac{\omega'}{\kappa}\right]\right) \ . \tag{3.48}$$

The thermal character appears in the high frequency limit, $\omega' >> \omega$. The incomplete gamma functions become negligible, and $Q \to 0$. Thus,

$$|\beta_{\omega'\omega}|^2 \approx \frac{1}{2\pi\kappa\omega'} \frac{1}{e^{2\pi\omega/\kappa} - 1} \quad \text{for } \omega' >> \omega \ . \tag{3.49}$$

Consider another new calculation for the Davies-Fulling trajectory. This one is for all times and it utilizes what we call the Hyperlog trajectory as shown in subsection 3.6.1. This new all-time DF solution is also a spliced trajectory. It contains the usual static piece for $t < 0$ and an accelerating piece of the form $\ln(\cosh(t))$ (Hyperlog form) for $t > 0$. This precise trajectory was originally suggested by Davies-Fulling [5]. I use it to do a new calculation of $\beta_{\omega'\omega}$.

$$z(t) = -\frac{1}{\kappa} \ln \cosh \kappa t \qquad t > 0 \ ,$$

$$z(t) = 0 \qquad\qquad t < 0 \ . \tag{3.50}$$

The $t > 0$, $\ln \cosh t$ form, is only the positive time part of what we call the 'Hyperlog' trajectory, which is solvable in and of itself and extends over all times. We solve this 'all-time', spliced Davies-Fulling mirror using the future surface, and the form

for $p(u)$, $p(u) = \frac{1}{\kappa}\ln(2 - e^{-\kappa u})$. Solving for the beta coefficient yields,

$$\beta_{\omega'\omega} = i - 2i({}_2F_1\{1, -\frac{i\omega'}{\kappa}, 1 - \frac{i\omega}{\kappa}, -1\}) ,\qquad(3.51)$$

where ${}_2F_1$ is a hypergeometric function.

3.4 Asymptotically Inertial Mirrors

3.4.1 Walker-Davies Mirror Trajectory

Figure 3.7: Walker-Davies Trajectory
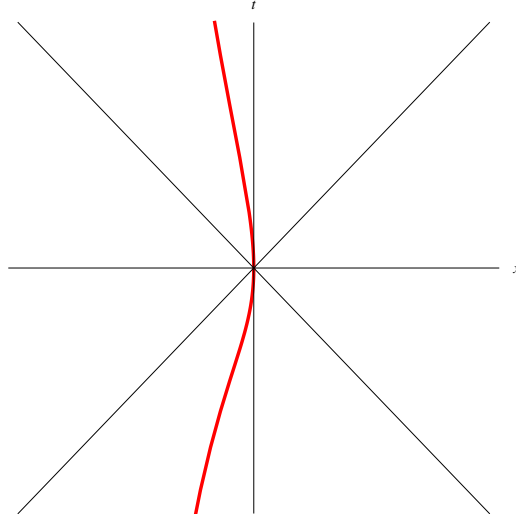
The Walker-Davies (WD) trajectory [34] is expressed in time as a function of z:

$$t = -z \pm A\sqrt{e^{-2z/B} - 1} .\qquad(3.52)$$

The WD trajectory is plotted in Figure 3.7. It has transformation coefficients which are exactly solvable This is a non-spliced, no approximation trajectory that has received little attention. Walker and Davies determined the particle creation due

to this asymptotically inertial (static in fact) trajectory in both the far past and far future. The main results are a finite, exactly-known total energy, and finite particle creation count (which is not exactly known but whose finiteness is inferred from the asymptotic behavior of the integrand). They found that the total energy produced is:

$$E_1 = \frac{B^2}{48(A^2 - B^2)^{3/2}} \, .$$

(3.53)

We numerically confirm that this total energy can be is equal to the energy found by adding quanta,

$$E_2 = \int_0^\infty \omega \langle N_\omega \rangle d\omega = \int_0^\infty dw \, w \int_0^\infty d\omega' |\beta_{\omega'\omega}|^2 \, .$$

(3.54)

By summing energy associated with each particle (summing quanta) we have confirmed the modulus squared Bogolubov coefficient for $A = 2$, $B = 1$ as presented in Eqn. (3.55). The total energy is $E_2 = 0.004009$ or $E_2 = E_1(A = 2, B = 1) = \frac{1}{144\sqrt{3}}$ to within 10^{-6} relative error. This is the first and only (so-far-existing) trajectory that is asymptotically **static** in both the far past and far future that has computed Bogolubov coefficients. It is very difficult to find asymptotically inertial trajectories, much less a transcendentally invertible asymptotically static trajectory.

We have used

$$|\beta_{\omega'\omega}|^2 = \frac{2AB}{\pi^2} \left(\frac{\omega'}{\omega' + \omega} \right) \sinh(\pi\omega B)|K_q(r)|^2 \, ,$$

(3.55)

where $q \equiv -\frac{1}{2} + i\omega B$ and $r \equiv A(\omega' + \omega)$. For the totality of the trajectory, the total energy, E, the total number of particles, $\langle N \rangle$, and both the occupation numbers per modes ω and ω', $\langle N_\omega \rangle$ and $\langle N_{\omega'} \rangle$, are all finite.

This trajectory is also the first finite energy result from a non-spliced mirror trajectory. As you can see it avoids late time approximations and problems with completeness of the field modes on the future null surface. This trajectory acts like a

model for total evaporation of a black hole [35]. The drawbacks of this trajectory involve the transcendentally irreversible form for the trajectory, the complexity of the ray tracing formulas and the inability to so far exactly integrate the modulus of the beta transformation coefficient to reveal the particle production count.

3.4.2 Darcx Mirror Trajectory

I have found a mirror trajectory that is asymptotically inertial in the past and future, but not necessarily static in the future. One would still expect this trajectory to produce a finite amount of particles and a finite total energy. This trajectory has no u or v asymptote as can be seen in Figure 3.8.

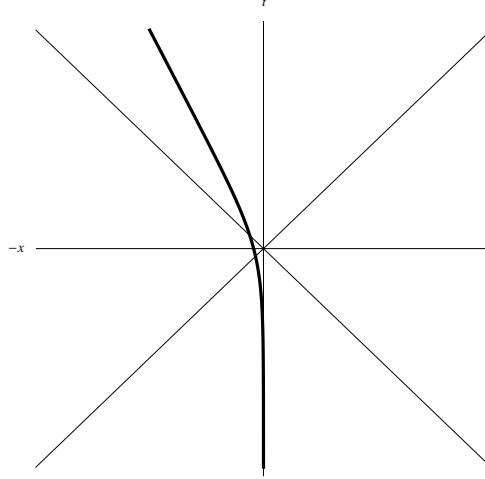Figure 3.8: An asymptotically drifting mirror, $v(t \to \infty) = |v_0| < 1$.

The defining trajectory is,

$$z(t) = -\frac{\xi}{\kappa} \sinh^{-1}(e^{\kappa t}) \,, \tag{3.56}$$

where ξ is the limiting final speed with $0 < \xi < 1$, and $\kappa > \xi$. This will be called Darcx ('D' for drifting, 'arc' for archyperbolic sine, and 'x' for exponent). We exactly

solve for the Bogolubov coefficients and the total energy.

The proper acceleration is

$$\alpha(t) = -\frac{\kappa \xi e^{\kappa t}}{\left(1 - \eta e^{2\kappa t}\right)^{3/2}} \ , \tag{3.57}$$

where $\eta \equiv \xi^2 - 1$. Notice the trajectory characteristics, where in the far past, $t \to -\infty$ both $v \to 0$ and $\alpha \to 0$. In the far future, as $t \to \infty$, $v \to -\xi$ and $\alpha \to 0$. The limiting celerity, γv is $-\frac{\xi}{\sqrt{1-\xi^2}}$. Using $p(u) = t_u + z(t_u)$, we may rewrite $\beta_{\omega'\omega}$ in terms of the general z trajectory,

$$\beta_{\omega'\omega} = \frac{1}{4\pi\sqrt{\omega\omega'}} \int_{-\infty}^{\infty} dt_u \ e^{i(\omega+\omega')t_u} e^{i(\omega'-\omega)z} \left((\omega' - \omega) + (\omega' + \omega)\dot{z}\right) \ . \tag{3.58}$$

With $b_+ \equiv b\omega + a\omega'$, $a_+ \equiv a\omega + b\omega'$ and $\omega_+ \equiv \frac{1}{\kappa}(\omega + \omega')$, where $a \equiv \frac{1}{2\kappa}(1 + \xi)$ and $b \equiv \frac{1}{2\kappa}(1 - \xi)$, we find

$$\beta_{\omega'\omega} = \frac{-i}{2^{i\omega_+}} \frac{1}{4\pi\sqrt{\omega\omega'}} \frac{\xi}{\kappa^2} \frac{2\omega'\omega}{b_+} \frac{\Gamma[i\omega_+]\Gamma[ia_+]}{\Gamma[ib_+]} \ . \tag{3.59}$$

Squaring the modulus, we get

$$|\beta_{\omega'\omega}|^2 = \frac{\xi^2}{4\pi\kappa^4} \frac{\omega'\omega}{\omega_+ a_+ b_+} \frac{\mathrm{csch}[\pi\omega_+]\mathrm{csch}[\pi a_+]}{\mathrm{csch}[\pi b_+]} \ . \tag{3.60}$$

This is easy to numerically integrate, over ω' to obtain the occupation number for a mode with frequency ω. We have not been able to find a closed form expression for N_ω. We have found a closed form solution for the total energy. The flux from Eqn. (2.47) is

$$\langle T_{uu} \rangle = \frac{\kappa^2}{12\pi} \frac{\xi\chi e^{\kappa t_u}(2\eta e^{2\kappa t_u} + 1)}{(\chi + \xi e^{\kappa t_u})^2(\eta e^{2\kappa t_u} - 1)^2} \ , \tag{3.61}$$

where, $\chi \equiv \sqrt{e^{2\kappa t} + 1}$. Again, $\eta \equiv \xi^2 - 1$ and ξ is the final drifting speed obtained by

the mirror, $0 < \xi < 1$. After lengthy algebraic simplification, one finds that the total energy created is obtained by using the integral of Equation (2.49), (2.50) or (2.54).

$$E = \frac{\kappa}{96\pi} \left(\frac{3 + \xi^2}{2\xi^2} \ln \frac{1 + \xi}{1 - \xi} - \frac{3 + \xi(3 + 2\xi)}{\xi(1 + \xi)} \right).$$

(3.62)

As a simple check consider the trajectory where the final speed is half that of light, $\xi = \frac{1}{2}$. The solution for the expectation value for total energy production is

$$E = \frac{39 \ln 3 - 40}{576\pi} \kappa = 1.57269 \times 10^{-3} \kappa .$$

(3.63)

We can confirm this by computing the energy using the beta Bogolubov coefficient to sum up the energy of each particle, associating to each, a quanta of energy:

$$\int_0^\infty dw \, w \int_0^\infty d\omega' |\beta_{\omega'\omega}|^2 = 1.57269 \times 10^{-3} \kappa .$$

(3.64)

This shows consistency between the description in terms of particles and that in terms of the energy flux. A plot of the energy flux for $\xi = 1/2$ is in Figure 3.10. Note the interesting feature of negative energy flux in the vacuum. Negative energy flux is a characteristic feature of QFT under external conditions. For the totality of the Darcx mirror trajectory, E, $\langle N_\omega \rangle$, $\langle N_{\omega'} \rangle$ and $\langle N \rangle$ are all finite.

3.4.3 Proex Mirror Trajectory

I have found a new mirror trajectory, with some very unusual features, called the Proex trajectory ('Pro' for Product Log, 'ex' for exponent). Particle creation is calculated on the past and future null surfaces. This trajectory results in a finite occupation number for particles per mode ω and produces a finite, non-zero energy. Using the CW normalization convention, the transformation coefficient is obtained. The

Proex trajectory is

$$z_{PX}(t) = -\frac{1}{\kappa}W(e^{\kappa t}) \ . \tag{3.65}$$
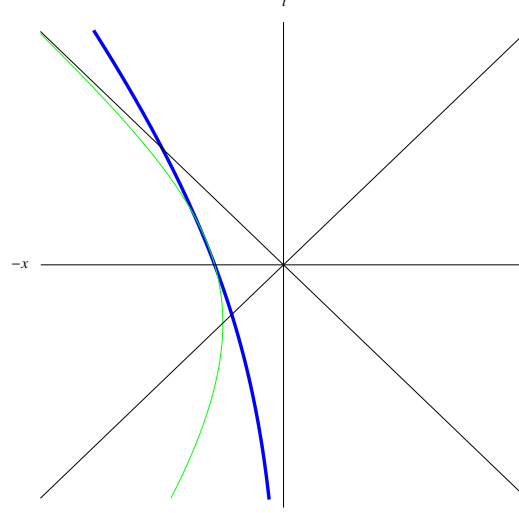
Figure 3.9: Proex Trajectory.

The beta coefficient is

$$\beta_{\omega'\omega} = 2\frac{\omega'}{\kappa}2^{-i\frac{\omega+\omega'}{\kappa}}\left(\frac{\omega}{\kappa}\right)^{-i\frac{\omega+\omega'}{\kappa}}e^{-\frac{\pi}{2}\frac{\omega+\omega'}{\kappa}}\Gamma\left(i\frac{\omega+\omega'}{\kappa}\right) \ . \tag{3.66}$$

The Proex trajectory has no asymptote, yet, it approaches the speed of light. Both its proper acceleration and acceleration go to zero in the far past and far future. It's proper velocity goes to $-\infty$, while the velocity goes to -1. The ability to express Eqn. (3.65) in different ways

$$z_{PX}(t) = -\frac{1}{\kappa}W(e^{\kappa t}) = -t + \frac{1}{\kappa}\ln W(e^{\kappa t}) = \frac{1}{\kappa}\ln(e^{-\kappa t}W(e^{\kappa t})) \ , \tag{3.67}$$

is crucial for calculating the beta transformation coefficient. We now proceed to solve for the relevant details to obtain the beta coefficient, Eqn. (3.66). To find the

ray-tracing function conversions, we start by noting that

$$u_{PX}(t) = t + \tfrac{1}{\kappa} W(e^{\kappa t}) \ ,$$

$$v_{PX}(t) = \tfrac{1}{\kappa} \ln W(e^{\kappa t}) \ .$$

(3.68)

Inverted, this gives

$$t_{PX}(u) = u - \tfrac{1}{2\kappa} W(2 e^{\kappa u}) \qquad \forall u \ ,$$

$$t_{PX}(v) = \tfrac{1}{\kappa} e^{\kappa v} + v \qquad\qquad \forall v \ .$$

(3.69)

In null coordinates, using $p(u) = 2t_u - u$, and the inverse, $f(v) = 2t_v - v$,

$$p(u) = u - \tfrac{1}{\kappa} W(2 e^{\kappa u}) \qquad \forall u \ ,$$

$$f(v) = \tfrac{2}{\kappa} e^{\kappa v} + v \qquad\qquad \forall v \ .$$

(3.70)

With $\kappa = 1$, $\phi_{\omega'}^{*} = e^{i\omega' v}$ and $\phi_{\omega}^{*} = e^{i\omega(2e^v + v)}$ one finds by integrating over I^-

$$
\begin{aligned}
\beta_{\omega'\omega} &= \int_{-\infty}^{\infty} dv \ e^{i\omega' v} e^{i\omega(2e^v + v)} (\omega' - \omega(2e^v + 1)) \\
&= 2\omega' 2^{-i(\omega+\omega')} \omega^{-i(\omega+\omega')} e^{-\frac{\pi}{2}(\omega+\omega')} \Gamma(i\omega + i\omega') \ .
\end{aligned}
$$

(3.71)

Integration along I^+ gives Eqn. (3.66) as well. Normalizing and squaring the answer, one obtains

$$|\beta_{\omega'\omega}|^2 = \frac{\omega'}{2\pi\omega\kappa(\omega + \omega')} \frac{1}{e^{\frac{2\pi}{\kappa}(\omega+\omega')} - 1} \ .$$

(3.72)

Note that for $\omega' >> \omega$ one obtains

$$|\beta_{\omega'\omega}|^2 \sim \frac{1}{2\pi\omega\kappa} \frac{1}{e^{2\pi\omega'/\kappa} - 1} \ .$$

(3.73)

This is unusual because ω and ω' have exchanged their normal places. Since the acceleration is asymptotically zero and there is no horizon, we would not expect a thermal result. I have not been able to exactly integrate Eqn. (3.72) with respect to ω'. Integrating Eqn. (3.72) exactly, over ω' would seemingly give results very close to Polygamma functions. However, one may wish to use the following result as an approximation:

$$\langle N_\omega \rangle \approx -\frac{1}{4\pi^2\omega} \ln(1 - e^{\frac{-2\pi\omega}{\kappa}}) \, . \tag{3.74}$$

This appromixation graphically coincides fairly well with the numerical computation. Use of a correction factor (multiplying by $\frac{1}{2}$), has been useful for comparisons with a numerically calculated answer, obtained by using a specific value for ω and numerically integrating over ω'. Integrating numerically, we find this is easily accomplished over ω' for the occupation number for a specific mode ω. That is, $\langle N_\omega \rangle = \text{finite}$.

The expectation value of the total number of created particles,

$$\langle N \rangle = \int_0^\infty d\omega \int_0^\infty d\omega' |\beta_{\omega'\omega}|^2 \, , \tag{3.75}$$

diverges. Solving for the flux via (2.45) yields

$$\langle T_{uu} \rangle = \frac{\kappa^2}{48\pi} \frac{(2 - W[2e^{\kappa u}])W[2e^{\kappa u}]}{(1 + W[2e^{\kappa u}])^4} \, . \tag{3.76}$$

This is integrated to obtain

$$E = \frac{\kappa}{96\pi} \, . \tag{3.77}$$

We may also express the energy flux using (2.46) as

$$\langle T_{uu} \rangle = \frac{\kappa^2}{12\pi} \frac{\left(1 - W\left[e^{\kappa t_u}\right]\right) W\left[e^{\kappa t_u}\right]}{\left(1 + 2W\left[e^{\kappa t_u}\right]\right)^4} \; . \tag{3.78}$$

Which appropriately integrated yields total energy $E = \kappa/96\pi$, as must be the case. As a warning, integration with or without the required Jacobian will still yield $E = \kappa/96\pi$ (see the use of the Jacobian in Eqn. (2.49)). In contrast to the total particle divergence, the total energy is numerically computed by adding the energy of each quantum,

$$\int_0^\infty \omega \langle N_\omega \rangle d\omega = \int_0^\infty dw \; w \int_0^\infty d\omega' |\beta_{\omega'\omega}|^2 = 0.00331573\kappa \sim \frac{\kappa}{96\pi} \; , \tag{3.79}$$

which confirms the stress tensor result (3.77) to 10^{-8} relative error. For the totality of the trajectory, E and $\langle N_\omega \rangle$ are finite, while $\langle N_{\omega'} \rangle$ and $\langle N \rangle$ diverge. A physical understanding of the difference in behavior of $\langle N_{\omega'} \rangle$ and $\langle N_\omega \rangle$ is needed.
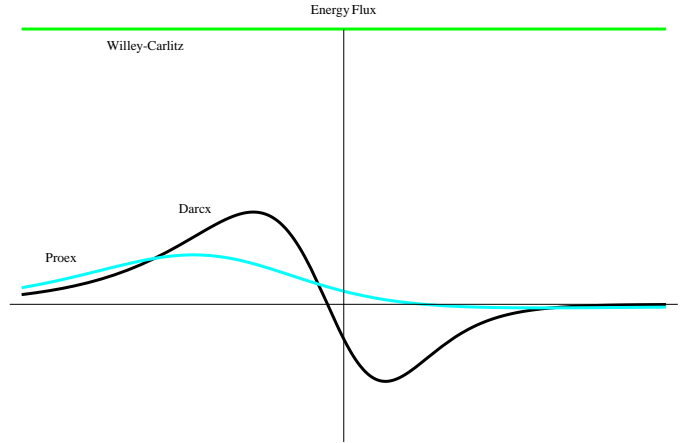
Figure 3.10: Darcx and Proex Energy Flux. The final drifting speed of Darcx, in this case, is half of light. ($\xi = 1/2$, $\kappa = 1$). The constant Willey-Carlitz flux is included for a relative comparison.

3.5 Static-Start Future-Horizon Mirrors

3.5.1 Arcx Mirror Trajectory

I have found a novel, exactly solvable mirror trajectory, called the Arcx trajectory ('Arc' for inverse hyperbolic sine, and 'x' for exponent). Particle creation is confirmed by integrating over the past and future hypersurfaces to solve for $\beta_{\omega\omega'}$. This trajectory is motivated by its static start and non-spliced nature. Unlike the Davies-Fulling trajectory, this trajectory in exactly solvable. It too has thermal late time emission and infinite acceleration, but does so without resorting to splicing the motion. This allows for a solution that is valid globally. There are numerous ways of solving for the transformation coefficients. We present one method where verification is done twice over, using the past and future surface. The Arcx trajectory is

$$z_{AX}(t) = -\tfrac{1}{\kappa}\sinh^{-1} e^{\kappa t} \ . \tag{3.80}$$

This trajectory is at rest when $t \to -\infty$. To express the ray-tracing functions, the

Figure 3.11: Arcx Trajectory.

conversions (using $u = t - z$, $v = t + z$) of

$$u_{AX}(t) = t + \frac{1}{\kappa} \sinh^{-1} e^{\kappa t}$$

$$v_{AX}(t) = t - \frac{1}{\kappa} \sinh^{-1} e^{\kappa t} \ . \tag{3.81}$$

are inverted[1]

$$t_{AX}(u) = \frac{1}{\kappa} \ln \sqrt{\frac{e^{2\kappa u}}{1 + 2e^{\kappa u}}} \qquad \forall \ u$$

$$t_{AX}(v) = \frac{1}{\kappa} \ln \sqrt{\frac{e^{2\kappa v}}{1 - 2e^{\kappa v}}} \qquad v < -\frac{\ln 2}{\kappa} \ . \tag{3.82}$$
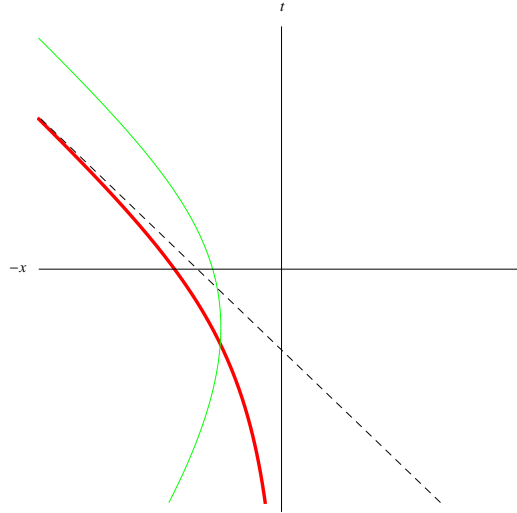
In null coordinates, using $p(u) = 2t_u - u$, and the inverse, $f(v) = 2t_v - v$,

$$p(u) = -\frac{1}{\kappa} \ln(e^{-\kappa u} + 2) \qquad \forall \ u$$

$$f(v) = -\frac{1}{\kappa} \ln \left(e^{-\kappa v} - 2 \right) \qquad v < -\frac{\ln 2}{\kappa} \ . \tag{3.83}$$

The modes used are $\phi_{\omega'}^* = e^{i\omega' v}$ and $\phi_\omega^* = e^{i\frac{\omega}{\kappa} \ln (e^{\kappa v} - 2)} \Theta(-\frac{\ln 2}{\kappa} - v)$. The integral over the past null hypersurface is

$$\beta_{\omega'\omega} = \int_{-\infty}^{\infty} dv \ e^{i\omega' v} (e^{-\kappa v} - 2)^{-i\omega/\kappa} \left(\omega' - \frac{\omega}{1 - 2e^{\kappa v}} \right) \Theta(-\frac{\ln 2}{\kappa} - v) \ . \tag{3.84}$$

With a substitution, $c = -\frac{\ln 2}{\kappa} - v$ we obtain

$$\beta_{\omega'\omega} = 2^{-\frac{i}{\kappa}(\omega'+\omega)} \int_{-\infty}^{\infty} dc \ e^{-i\omega' c} (e^{\kappa c} - 1)^{-\frac{i\omega}{\kappa}} \left(\omega' - \frac{\omega}{1 - e^{-\kappa c}} \right) \Theta(c)$$

$$= -\frac{2\omega}{\kappa} 2^{-\frac{i}{\kappa}(\omega+\omega')} \frac{\Gamma(-i\frac{\omega}{\kappa})\Gamma(\frac{i}{\kappa}(\omega + \omega'))}{\Gamma(i\frac{\omega'}{\kappa})} \ . \tag{3.85}$$

The future surface calculation gives the same result. Normalizing and squaring the answer gives

$$|\beta_{\omega'\omega}|^2 = \frac{4\omega^2}{\kappa^2} \left| \frac{\Gamma(-\frac{i\omega}{\kappa})\Gamma(\frac{i}{\kappa}(\omega + \omega'))}{\Gamma(\frac{i\omega}{\kappa})} \right|^2 \ . \tag{3.86}$$

---

[1]Caveat: This form for $t_{AX}(v)$ is only true for $v < -\frac{\ln 2}{\kappa}$

This diverges when integrated over ω' as expected for acceleration that continues for all time. Note that for $\omega' >> \omega$ for the bracketed portion we obtain

$$|\beta_{\omega'\omega}|^2 \sim \frac{1}{2\pi\kappa\omega'}\frac{1}{e^{2\pi\omega/\kappa}-1} \; . \tag{3.87}$$

The Arcx trajectory provided the inspiration for the Darcx trajectory. Notice how drastically different the solutions are and the approaches for solving them become, simply because Darcx contains a drifting factor. It is hoped that one can obtain time dependent spectra through the use of wavepackets for the Arcx mirror or solutions similar to it, which closely mimics gravitational collapse, (as it starts static and proceeds to a horizon). So far this has been challenging because of the acceleration singularity.

3.5.2   Logex Mirror Trajectory

I have found an exactly solvable mirror trajectory that emits a pulse of energy flux. The trajectory, called the Logex trajectory ('Log'- for natural log, 'ex' for exponent), has computable beta coefficients. A characteristic trait that distinguishes it from the Arcx trajectory is that the horizon is at $v = 0$. An extended pulse of positive energy is emitted which is unusual. This behavior is unique among all known mirror trajectories. The Logex trajectory is

$$z_{LG}(t) = -\tfrac{1}{2\kappa}\ln\!\left(e^{2\kappa t}+1\right) . \tag{3.88}$$

To express the Logex trajectory ray tracing functions, we use ($u = t - z$, $v = t + z$)

$$u_{LG}(t) = \tfrac{1}{2\kappa}\ln(e^{4\kappa t}+e^{2\kappa t}) \; ,$$
$$v_{LG}(t) = -\tfrac{1}{2\kappa}\ln(e^{-2\kappa t}+1) \; , \tag{3.89}$$

93
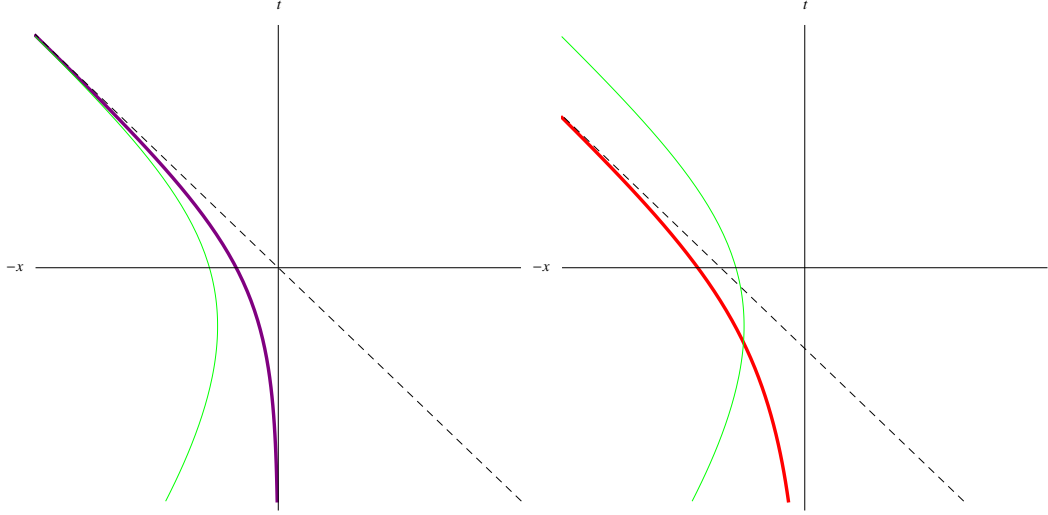
Figure 3.12: Logex and Arcx, respectively.

which yield[2]

$$t_{LG}(u) = \tfrac{1}{2\kappa} \ln(\tfrac{1}{2}(\sqrt{4e^{2\kappa u} + 1} - 1)) \ ,$$
$$t_{LG}(v) = -\tfrac{1}{2\kappa} \ln(e^{-2\kappa v} - 1) \qquad v < 0 \ . \tag{3.90}$$

In null coordinates, using $p(u) = 2t_u - u$, and the inverse, $f(v) = 2t_v - v$,

$$p(u) = -\tfrac{1}{\kappa}\operatorname{csch}^{-1}(2e^{\frac{2\kappa u}{2}}) \ ,$$
$$f(v) = -\tfrac{1}{\kappa} \ln(-2\sinh\tfrac{2\kappa v}{2}) \qquad v < 0 \ . \tag{3.91}$$

Using the derivatives for use in the integration $p'(u) = \frac{1}{\sqrt{4e^{2\kappa t}+1}}$, and $f'(v) = -\coth(\kappa v)$ and the past surface modes

$$\phi^*_{\omega'} = e^{i\omega' v} \qquad \phi^*_\omega = e^{i\omega(-\frac{1}{\kappa}\ln(-2\sinh(\kappa v)))}\Theta(-v) \ , \tag{3.92}$$

---

[2]Caveat: This form for $t_{LG}(v)$ is only true for $v < 0$

and the future surface modes

$$\phi^*_{\omega'} = e^{i\omega'(-\frac{1}{\kappa}\text{csch}^{-1}(2e^{\kappa u}))} \qquad \phi^*_{\omega} = e^{i\omega u} \; , \tag{3.93}$$

along with the integrals

$$\beta_{\omega'\omega} = -\int_{-\infty}^{\infty} dv \; e^{i\omega' v} e^{i\omega f(v)} \left(\omega f'(v) - \omega'\right) \; , \tag{3.94}$$

$$\beta_{\omega'\omega} = \int_{-\infty}^{\infty} du \; e^{i\omega u} e^{i\omega' p(u)} \left(\omega' p'(u) - \omega\right) \; , \tag{3.95}$$

One finds

$$\beta_{\omega'\omega} = -\frac{2\omega\omega'}{\kappa(\omega' - \omega)} B\left[-\frac{i\omega}{\kappa}, \frac{i(\omega + \omega')}{2\kappa}\right] \; . \tag{3.96}$$

After normalization and complex conjugation,

$$|\beta_{\omega'\omega}|^2 = \frac{\omega\omega'}{4\pi^2\kappa^2(\omega' - \omega)^2} \left| B\left(-\frac{i\omega}{\kappa}, \frac{i(\omega + \omega')}{2\kappa}\right)\right|^2 \; . \tag{3.97}$$

A thermal character is displayed for high frequency,

$$|\beta_{\omega'\omega}|^2 \approx \frac{1}{2\pi\kappa\omega'} \frac{1}{e^{2\pi\omega/\kappa} - 1} \quad \text{for } \omega' >> \omega \; . \tag{3.98}$$

Even though the Logex trajectory starts off asymptotically static, this mirror has a $v = 0$ asymptote horizon, with never ending acceleration. A mirror following the Logex trajectory produces an infinite total amount of particles and an infinite total energy. The proper acceleration is,

$$\alpha(t) = -\kappa \frac{2e^{2\kappa t}(1 + e^{2\kappa t})}{(1 + 2e^{2\kappa t})^{3/2}} \; . \tag{3.99}$$

The Logex trajectory results in a horizon and an infinite redshift. The flux is similar to Arcx,

$$\langle T_{uu} \rangle = \frac{\kappa^2}{3\pi} \frac{(1 + e^{2\kappa u})e^{2\kappa u}}{(1 + 4e^{2\kappa u})^2} \; .$$

(3.100)

It diverges when integrated over u, i.e. $E = \infty$. The flux expressed in t_u from the surface of the mirror takes the form

$$\langle T_{uu} \rangle = \frac{\kappa^2}{3\pi} \frac{2e^{5\kappa t_u}[1 + 2\cosh(2\kappa t_u)]\cosh(\kappa t_u)}{(1 + 2e^{2\kappa t_u})^4} \; .$$

(3.101)

There is some indication that this 'pulse' of energy as seen in Figure 3.13, from the energy flux expressions, manifests itself in time-dependent particle production evolution. Recalling that quanta summing fails for Logex because of the singularity and ultimately the infinite energy production, a localization procedure that could associate the pulse of energy with a pulse of particle production would be of interest for studying the spectral evolution in the presence of a horizon. The characteristic extended energy pulse of Logex is shown in comparison to several other trajectories in Figure 3.13.

3.5.3 Omex Mirror Trajectory

Like the other trajectories in this section, and in contrast to the Carlitz-Willey trajectory which starts off asymptotically inertial, this trajectory starts off asymptotically static. This exactly solvable trajectory which I have found is titled the Omex mirror ('Om' for the Omega Constant, and 'ex' for the exponent inside the product log). Like the Carlitz-Willey and Proex trajectories, it intersects $t = 0$ not at $x = 0$. The $t = 0$ intersection is located at $x = -\frac{\Omega}{2\kappa}$, where the Omega constant satisfies $\Omega e^{\Omega} = 1$, that is, $\Omega \approx 0.567...$.
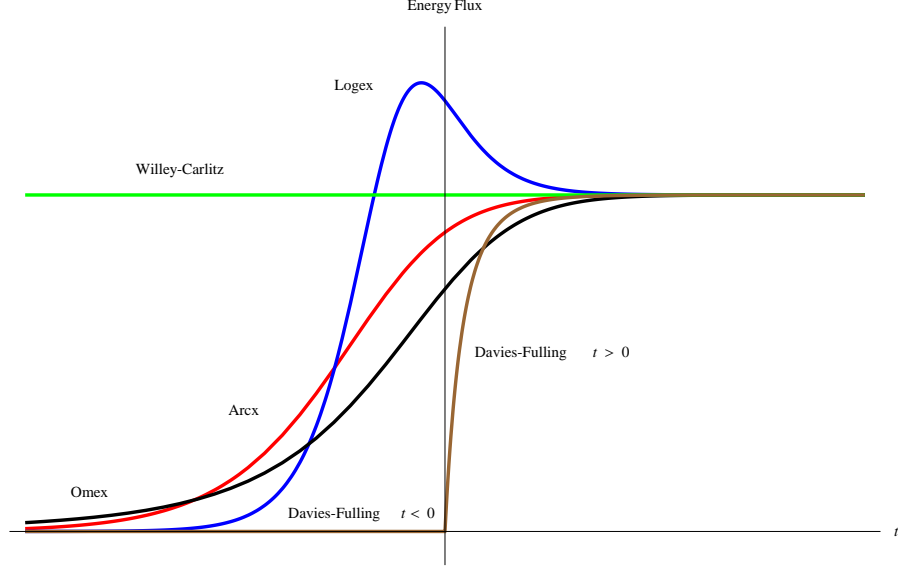
Figure 3.13: Energy flux of the three 'static-start / horizon-finish' mirrors along with Davies-Fulling and Willey-Carlitz flux.

$$z(t) = -t - \frac{W(e^{-2\kappa t})}{2\kappa} \; . \tag{3.102}$$

with proper acceleration given by

$$\alpha(t) = -\kappa \frac{2}{\sqrt{W(e^{-2\kappa t})(2 + W(e^{-2\kappa t}))}} \; . \tag{3.103}$$

Note the static start and that the initial position is at $x = \infty$. The Carlitz-Willey trajectory, in contrast, begins at $x = -\infty$. To express the trajectory in terms of ray-tracing functions, one can use

$$\begin{aligned} u_{OM}(t) &= 2t + \tfrac{1}{2\kappa}W(e^{-2\kappa t}) \; , \\ v_{OM}(t) &= -\tfrac{1}{2\kappa}W(e^{-2\kappa t}) \; . \end{aligned} \tag{3.104}$$

After making the transcendental inversions, one finds:
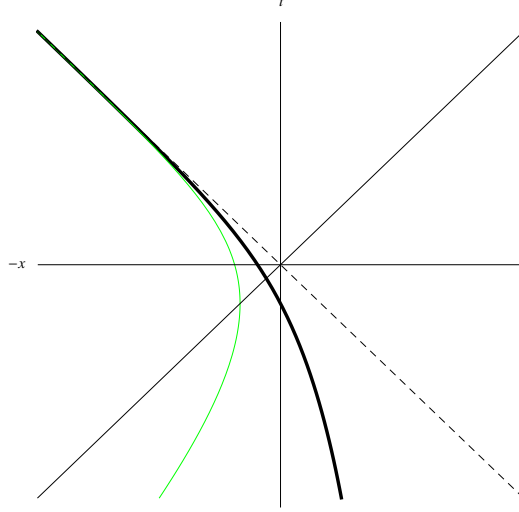
Figure 3.14: Omex Mirror Trajectory.

$$t_{OM}(u) = \frac{u}{2} - \frac{1}{2\kappa}W\left(\frac{e^{-\kappa u}}{2}\right) \qquad \forall\, u \ ,$$
$$t_{OM}(v) = -\frac{1}{2\kappa}\ln(-2\kappa v e^{-2kv}) \qquad \text{valid for } v < 0 \ . \tag{3.105}$$

In null coordinates,

$$p(u) = -\frac{1}{\kappa}W\left(\frac{e^{-\kappa u}}{2}\right) \ ,$$
$$f(v) = -v - \frac{1}{\kappa}\ln(-e^{-2\kappa v}2\kappa v) \qquad v < 0 \ . \tag{3.106}$$

The flux from (2.45),

$$\langle T_{uu}\rangle = \frac{\kappa^2}{48\pi}\frac{(1 + 4W[\frac{e^{-\kappa u}}{2}])}{(1 + W[\frac{e^{-\kappa u}}{2}])^4} \ , \tag{3.107}$$

diverges if integrated over all u. The flux in the frame of the mirror from (2.46) is

$$\langle T_{uu}\rangle = \frac{\kappa^2}{3\pi}\frac{(1 + 2W[e^{-2\kappa t_u}])}{(2 + W[e^{-2\kappa t_u}])^4} \ . \tag{3.108}$$

It also diverges when integrated over the entire trajectory, as must be the case. The solution using the past surface is obtained from the integral

98

$$\beta_{\omega'\omega} = \int_{-\infty}^{0} dv \ e^{i\omega'v} e^{i\omega f(v)} (\omega' - \omega f'(v)) \,, \tag{3.109}$$

which is solved exactly. Using the more natural form of $f(v)$, that is, $f(v) = -v - \frac{1}{\kappa}\ln(-2\kappa v)$ gives

$$\beta_{\omega'\omega} = \int_{-\infty}^{0} dv \ e^{i\omega'v} e^{i\omega(-v-\frac{1}{\kappa}\ln(-2\kappa v))} (\omega' - \omega(1 - \frac{1}{\kappa v})) \,. \tag{3.110}$$

The solution is found to be:

$$\beta_{\omega'\omega} = \frac{2\omega'\omega}{\kappa(\omega + \omega')} (\frac{\omega + \omega'}{2\kappa})^{i\omega/\kappa} e^{-\pi\omega/2\kappa} \Gamma[-\frac{i\omega}{\kappa}] \,. \tag{3.111}$$

After squaring with its complex conjugate

$$|\beta_{\omega'\omega}|^2 = \frac{\omega'}{2\pi\kappa(\omega + \omega')^2} \frac{1}{e^{2\pi\omega/\kappa} - 1} \,, \tag{3.112}$$

which demonstrates thermal character in the large ω' limit

$$|\beta_{\omega'\omega}|^2 \sim \frac{1}{2\pi\kappa\omega'} \frac{1}{e^{2\pi\omega/\kappa} - 1} \quad \text{for } \omega' >> \omega \,. \tag{3.113}$$

One finds that $\langle N_\omega \rangle = \infty$ and $E = \infty$.

3.6 Heterogeneous Solutions

The mirror trajectories presented so far have not exhausted all the possibilities. There are many interesting trajectories which have not yet been studied which could provide insight into quantum effects in moving mirror spacetimes. For instance, one important trajectory for which the beta Bogolubov coefficients have not been computed is the static-start, future-asymptotically-uniformly-accelerated trajectory which is

not asymptotically inertial yet whose acceleration does not diverge. This section serves as a springboard for those trajectories which may be interesting for further study. I have also included the Hyperlog mirror trajectory which has two horizons. There are three simple examples of spliced mirrors in subsection 3.6.2 which illustrate purely positive energy emission, purely negative energy emission and a hybrid negative energy emission trajectory using only uniformly accelerated pieces. In subsection 3.6.3 I have given two examples of transcendentally invertible forms. One class generalizes the initial static start property of the Proex trajectory to incorporate motions that could start at at any speed, up to the starting speed of light. The other class generalizes the Carlitz-Willey and Omex mirrors. Both class examples and the three spliced mirrors have not had their beta Bogolubov coefficients computed. In Subsection 3.6.4 I have made remarks on specific trajectories that one may wish to explore and the effectiveness of the techniques developed so far. A treatment of the hyperbolic tangent function as $z(t)$, $v(t)$ and $\alpha(t)$ is given.

3.6.1 Hyperlog Mirror Trajectory

In this section, I present the beta coefficient for a new trajectory, called the Hyperlog trajectory, which is unspliced. The Hyperlog trajectory is exactly solvable, and like the uniformly accelerated mirror, it has two horizons. Inspired by the suggestion of Davies [5] that this trajectory would smoothly map to a static mirror for $t < 0$, it seemed worthwhile to try to solve for the beta Bogolubov coefficients for this trajectory exactly, without splicing, to see if it could be done. After recognizing that this was possible, it was clear that more trajectories could have their coefficients solved for, without pathological problems. The mode functions are:
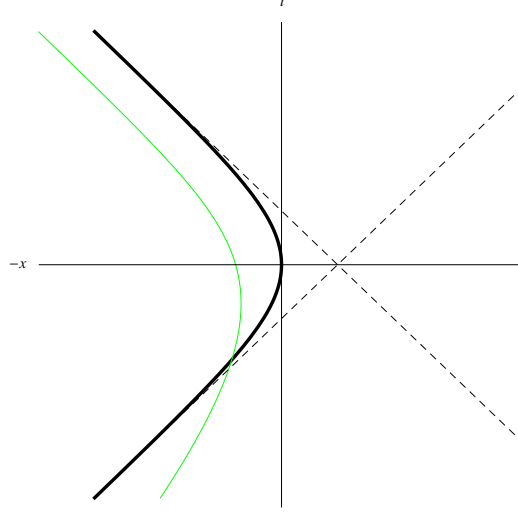
Figure 3.15: Hyperlog Trajectory.

$$\phi_{\omega'} = e^{-i\omega'v} - e^{-i\omega'p(u)}\Theta\left(\frac{\ln 2}{\kappa} + u\right) \qquad \phi_{\omega} = e^{-i\omega V(v)}\Theta\left(\frac{\ln 2}{\kappa} - v\right) - e^{-i\omega u} \ , \qquad (3.114)$$

and the trajectory is

$$z_{HL}(t) = -\frac{1}{\kappa}\ln\cosh\kappa t \quad . \qquad (3.115)$$

The beta Bogolubov coefficient is

$$\beta_{\omega'\omega} = \frac{2\omega'\omega}{\kappa(\omega'-\omega)}2^{i\frac{(\omega'-\omega)}{\kappa}}\frac{\Gamma(-i\frac{\omega}{\kappa})\Gamma(i\frac{\omega'}{\kappa})}{\Gamma(i\frac{\omega'}{\kappa} - i\frac{\omega}{\kappa})} \quad . \qquad (3.116)$$

To express the trajectory in terms of the ray-tracing functions, one uses

$$\begin{aligned} u_{HL}(t) &= t + \frac{1}{\kappa}\ln\cosh\kappa t \\ v_{HL}(t) &= t - \frac{1}{\kappa}\ln\cosh\kappa t \end{aligned} \ , \qquad (3.117)$$

and inverts to get[3]

$$t_{HL}(u) = \frac{1}{\kappa} \ln \sqrt{2e^{\kappa u} - 1} \qquad u > -\frac{\ln 2}{\kappa} \; ,$$
$$t_{HL}(v) = -\frac{1}{\kappa} \ln \sqrt{2e^{-\kappa v} - 1} \qquad v < \frac{\ln 2}{\kappa} \; . \tag{3.118}$$

In null coordinates, using $p(u) = 2t_u - u$, and the inverse, $f(v) = 2t_v - v$,

$$p(u) = \frac{1}{\kappa} \ln(2 - e^{-\kappa u}) \qquad u > -\frac{\ln 2}{\kappa} \; ,$$
$$f(v) = -\frac{1}{\kappa} \ln\left(2 - e^{\kappa v}\right) \qquad v < \frac{\ln 2}{\kappa} \; . \tag{3.119}$$

Normalizing beta in Eqn. (3.116) and squaring gives

$$|\beta_{\omega'\omega}|^2 = \frac{\omega\omega'}{4\pi^2\kappa^2(\omega'-\omega)^2} \left| \frac{\Gamma(-i\frac{\omega}{\kappa})\Gamma(i\frac{\omega'}{\kappa})}{\Gamma(i\frac{\omega'}{\kappa} - i\frac{\omega}{\kappa})} \right|^2 . \tag{3.120}$$

This diverges when integrated over ω' as expected for acceleration that continues for all time. Note that for $\omega' >> \omega$ we obtain

$$|\beta_{\omega'\omega}|^2 \sim \frac{1}{2\pi\kappa\omega'} \frac{1}{e^{2\pi\omega/\kappa} - 1} . \tag{3.121}$$

The main difference between the proposal by Davies-Fulling for $t > 0$, and this trajectory is that Eqn. (3.115) for $z(t)$ is used for *all* time. It now has both a u and a v asymptote, with an initially advancing infinite acceleration. Intersecting the origin, it turns around and travels away, eventually obtaining infinite receding acceleration. It produces an infinite number of particles and an infinite total energy. The proper acceleration is

$$\alpha(t) = -\kappa \frac{e^{\kappa t} + e^{-\kappa t}}{2} \; , \tag{3.122}$$

---

[3]Caveat: This form for $t_{HL}(u)$ is only true for $u > -\frac{\ln 2}{\kappa}$, $(t_{HL} \to -\infty)$, with a similar argument for $t_{HL}(v)$

with limiting behavior such that the proper acceleration, α and celerity, γv, diverges in the far past and future. The speed approaches the speed of light in the far past and far future. The flux is

$$\langle T_{uu} \rangle = \frac{\kappa^2}{12\pi} \frac{(-1 + e^{\kappa u})e^{\kappa u}}{(1 - 2e^{\kappa u})^2} \; . \tag{3.123}$$

Note the double horizon behavior in Figure 3.16. It is particularly useful to compare the different time-dependent accelerations for different trajectories as is done in Figure 3.16.
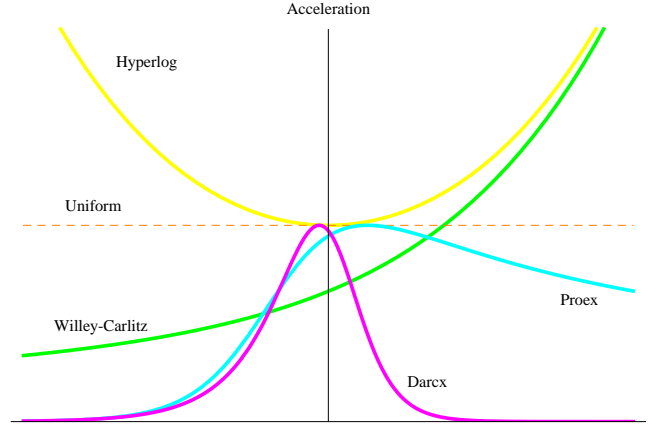
Figure 3.16: Magnitudes of proper accelerations where $\kappa = 1$ except for Proex($\kappa = 3\sqrt{3}$) and for Darcx ($\kappa = 9/2$) for visual clarity.

Even though the Hyperlog and the uniformly accelerated trajectories have double horizons, Hyperlog's strongly time-dependent acceleration results in a non-zero energy flux.

3.6.2 Variform Spliced Mirrors

Two of these spliced mirrors trajectories have been studied by Walker [15] and all three have probably been studied by others. They are included for completeness and

to demonstrate some interesting effects, e.g., infinite particle production with finite energy, and even pure negative energy production. These mirror trajectories have a serious drawback: it is much more difficult to explicitly calculate the Bogolubov transformation coefficients. We do not attempt this here. However, I have confirmed that the beta transformation coefficients are non-zero in each case.

Hyperbolic plus Static
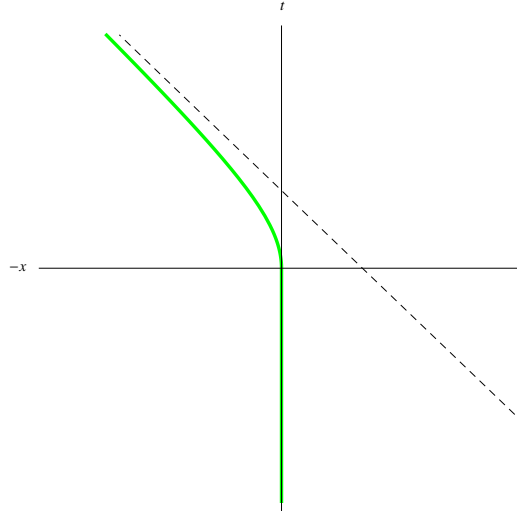
Figure 3.17: Hyperbolic plus static trajectories.

The two distinct static and hyperbolic trajectories may be joined together in such a way as to form

$$
\begin{aligned}
z(t) &= \kappa^{-1} - \sqrt{\kappa^{-2} + t^2} \qquad & t > 0 \ , \\
z(t) &= 0 & t < 0
\end{aligned}
\qquad .
\tag{3.124}
$$

The ray-tracing formula is

$$
p(u) = \Theta(u)\frac{u}{1+\kappa u} + u\Theta(-u) \quad .
\tag{3.125}
$$

The transformation coefficient, $\beta_{\omega\omega'}$ is non-zero. Integrating $\langle T_{uu} \rangle$ gives the total

energy production: $E = \frac{\kappa}{12\pi}$.

Purely Negative Energy Mirror
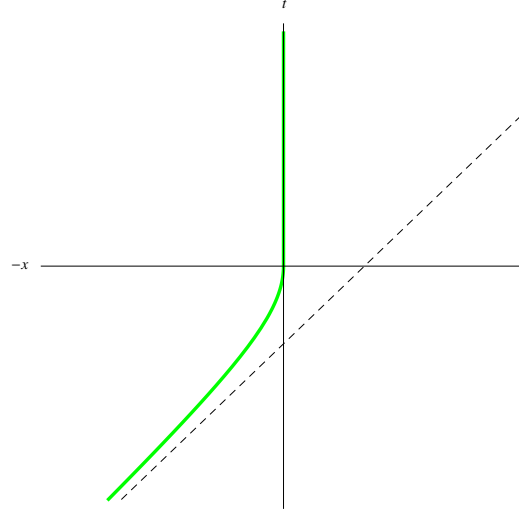
Figure 3.18: Purely Negative Energy Production.

It is a simple matter to splice together two distinct trajectories to obtain

$$
\begin{aligned}
z(t) &= 0 & t &> 0 \\
z(t) &= \kappa^{-1} - \sqrt{\kappa^{-2} + t^2} & t &< 0
\end{aligned}
\quad , \tag{3.126}
$$

with a ray tracing formula

$$
p(u) = \Theta(-u)\frac{u}{1+\kappa u} + u\Theta(u) \quad . \tag{3.127}
$$

Total energy production is negative: $E = -\frac{\kappa}{12\pi}$. This mirror has a brief jerk to the right at $t = 0$ which is responsible for the negative flux pulse at the origin and total negative energy.
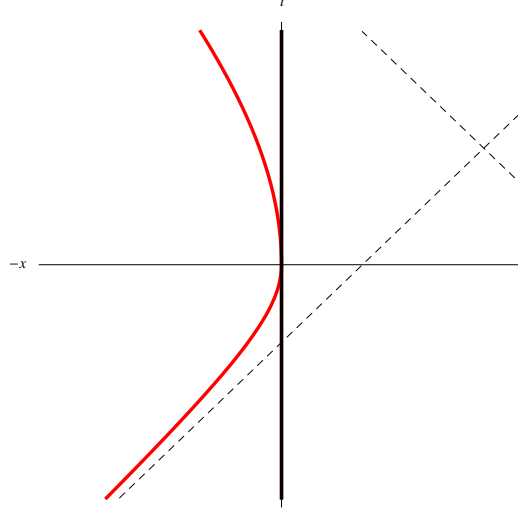
Figure 3.19: Negative energy mirror: $\kappa_2 = \frac{1}{4}$, $\kappa_1 = 1$.

Negative Energy Mirror

A generalization of the two examples above is possible by adding two distinct hyperbolic trajectories, where

$$
\begin{aligned}
z(t) &= \kappa_2^{-1} - \sqrt{\kappa_2^{-2} + t^2} \quad t > 0 \\
z(t) &= \kappa_1^{-1} - \sqrt{\kappa_1^{-2} + t^2} \quad t < 0
\end{aligned}
. \tag{3.128}
$$

The ray tracing functions are:

$$
p(u) = \Theta(u) \frac{u}{1 + \kappa_2 u} + \Theta(-u) \frac{u}{1 + \kappa_1 u} \quad u > -\frac{1}{\kappa_1} , \tag{3.129}
$$

$$
f(v) = \Theta(v) \frac{v}{1 - \kappa_2 v} + \Theta(-v) \frac{v}{1 - \kappa_1 v} \quad v < \frac{1}{\kappa_2} . \tag{3.130}
$$

The energy production is, of course, $E = \frac{\kappa_2 - \kappa_1}{12\pi}$ and only when $\kappa_1 > \kappa_2$, does the characteristic feature of this mirror become evident, i.e. the total energy emission is actually negative. The Walker-Davies, Darcx and Proex trajectories emit negative energy but in contrast their total energy emission is positive.

3.6.3 Generalized Transcendental Prototypes

Proex to Light Speed Generalization

As a generalization of the Proex trajectory, this mirror is asymptotically inertial in the past and future, but may have an initial velocity. It produces particles and a finite total energy. It has no u or v asymptote despite the fact that the mirror approaches the speed of light. The defining trajectory is,

$$z(t) = (\frac{1}{A} - 1)t - \frac{1}{\kappa}W(\frac{1}{A}e^{\kappa t/A}) \; . \tag{3.131}$$

Note that as $A \to \infty$ the trajectory approaches the light speed mirror trajectory, $z(t) = -t$. We expect and obtain zero particles and energy production in this case. On the other hand, as $A \to 1$, this mirror approaches the Proex form. It is possible to
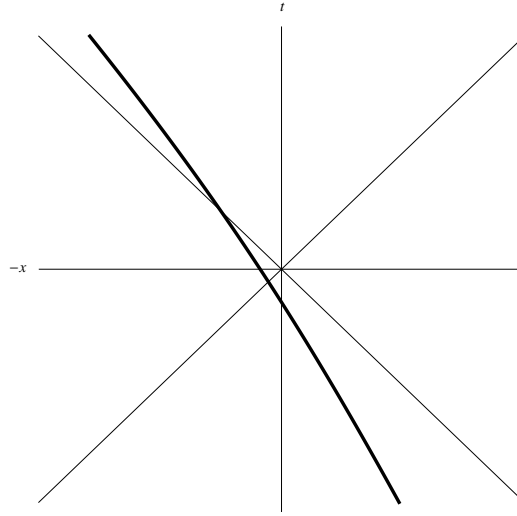
Figure 3.20: Proex Generalization, $A = 2$.

solve for the ray-tracing formulas and they are:

$$p(u) = \frac{u}{B} - \frac{1}{\kappa}W(\frac{2}{B}e^{\frac{\kappa u}{B}}) \; ,$$
$$f(v) = \frac{2}{\kappa}e^{\kappa v} + Bv \; . \tag{3.132}$$

The flux is

$$\langle T_{uu} \rangle = \frac{\kappa^2}{48\pi B^2} \frac{(2 - W(\frac{2}{B}e^{\frac{\kappa u}{B}}))W(\frac{2}{B}e^{\frac{\kappa u}{B}})}{(1 + W(\frac{2}{B}e^{\frac{\kappa u}{B}}))^4} \ . \tag{3.133}$$

Integration of $\langle T_{uu} \rangle$ yields

$$E = \frac{\kappa}{96\pi B} \ , \tag{3.134}$$

where $B = 2A - 1$ with $A > 1/2$.

Omex to Carlitz-Willey Generalization
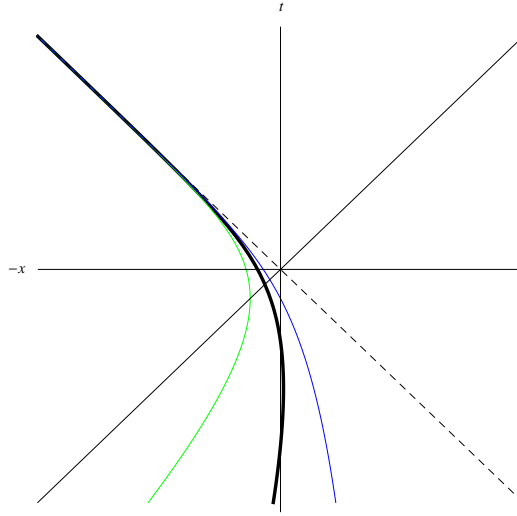
Figure 3.21: Carlitz-Willey, a generalization with $A = 3/2$ and Omex.

As a generalization of Carlitz-Willey and Omex mirrors, this class of mirrors has trajectories of the form,

$$z(t) = -t - \frac{1}{A\kappa}W(e^{\kappa t}) \ , \tag{3.135}$$

Note that as $A \to 2$ the trajectory approaches the Omex trajectory form, while as $A \to 1$ the Carlitz-Willey trajectory is approached. The ray-tracing functions are

$$p(u) = -\frac{1}{\kappa(A-1)} W\left(\frac{(A-1)}{A} e^{-\kappa u}\right),$$
$$f(v) = -\frac{1}{\kappa} \ln(-A e^{-A\kappa v} \kappa v) - v,$$

(3.136)

with $A > 1$. The energy flux is

$$\langle T_{uu} \rangle = \frac{\kappa^2}{48\pi} \frac{\left(1 + 4W\left(\frac{A-1}{A} e^{-\kappa u}\right)\right)}{\left(1 + 4W\left(\frac{A-1}{A} e^{-\kappa u}\right)\right)^4}.$$

(3.137)

3.6.4 Hyperbolic Tangent Archetypes

An Asymptotically Static Mirror

Even in a situation that has nonzero particle production and whose beta coefficients cannot be easily computed analytically, we may still compute the energy production. As an illustration of the ease and utility of Equation (2.49) and (2.54) , consider the specific trajectory

$$z(t) = -\frac{1}{2}(\tanh(t) + 1),$$

(3.138)

plotted in Figure 3.22. This starts off at $z = 0$ and ends at a new position, $z = z_0 = -1$. Using lengthy but straightforward expressions for the energy flux and the jerk, integration is possible and one finds that the total energy emitted is

$$E = \frac{1}{864\pi} \left(9\pi - 60 + \sqrt{3} \ln\left[\frac{\left(7 - 4\sqrt{3}\right)^{23}}{\left(2 - \sqrt{3}\right)^{68}}\right]\right).$$

(3.139)

An Asymptotically Drifting Mirror

Consider the case where we might not have an analytical expression for the trajectory $z(t)$, but the velocity is known analytically. We would like to know the energy production from such a trajectory that moves with an analytically known $v(t)$. For
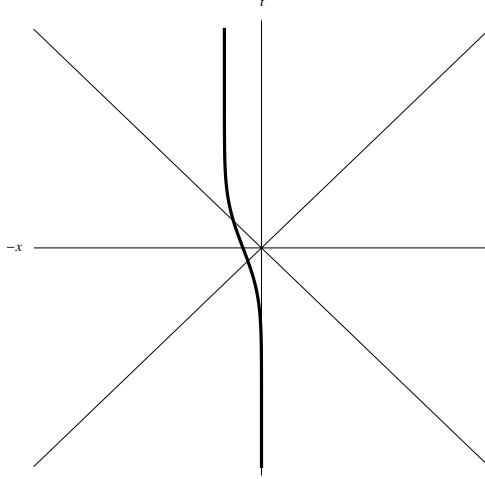
Figure 3.22: An asymptotically static mirror or 'shifted mirror'. As $t \to \infty$, the position, $z(t) \to z_0$.

consistency (and for the sake of the argument), consider the same form for the formula used for $z(t)$ for the Asymptotically Static Mirror, now used for the velocity

$$v(t) = -\frac{\xi}{2}(\tanh(t) + 1) .$$

(3.140)

The trajectory shape is similar to Darcx's asymptotic motion in the far future. As an example of the utility of Equation (2.47), $\langle T_{uu} \rangle = -\frac{\dot{\alpha}}{12\pi\gamma(1-v)^2}$ which does not require the form of the trajectory, we note that this mirror starts off at, $t = -\infty$ with $v = 0$ and ends as $t \to \infty$ with the final velocity, $|v| = \xi < 1$. Rather lengthy expressions for the energy flux and the jerk still allow analytical integration of the total emitted energy with the result

$$E = \frac{(1 + \xi)^2 \tanh^{-1}(\xi) - (1 + 2\xi)\xi}{48\pi\xi(1 + \xi)} .$$

(3.141)
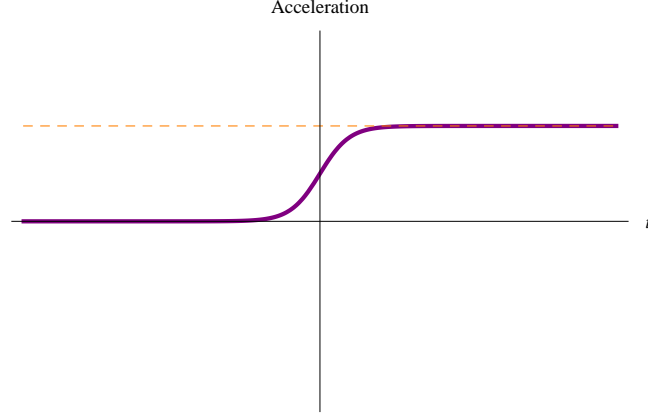
Figure 3.23: An asymptotically uniform mirror with unknown, $z(t)$ but known $\alpha(t)$ permitting solutions for jerk and flux.

An Asymptotically Uniform Mirror

Consider an analytically unknown trajectory that has a proper acceleration function,

$$\alpha(t) = -\frac{\kappa}{2}(\tanh(\kappa t) + 1) \, , \tag{3.142}$$

which starts inertial ($\alpha = 0$), but as $t \to \infty$, approaches a constant proper acceleration, $|\alpha| = \kappa$. This is not the same trajectory as the Davies-Fulling mirror because this analytically unknown mirror trajectory reduces to a constant acceleration in the far future. This trajectory constitutes a particularly difficult situation and elusive solution. Not only are the beta Bogolubov transformation coefficients difficult to solve for, but the energy is difficult to compute as well. Intuition tells us that the total energy produced may be gleaned from looking at simply the jerk. The 'Negative Energy Mirror' hints at the answer because the total energy in that case is simply the total change in acceleration divided by 12π. The total energy produced is proportional to the total jerk. For the above trajectory, we also have a total time integrated jerk of κ. The trajectory gets its acceleration jerked all the way from 0 to κ and by analogy, we would expect the total energy produced to be nearly equal to this

111

change divided by 12π if the jerk happens over a brief enough interval. The answer being positive because the jerk is away from us. Left jerking creates positive energy, right jerking creates negative energy. The numerical analysis involves lengthy expressions and integration over the energy flux is not straightforward. The answer, to approximately 5% relative error is

$$E = \frac{\kappa}{12\pi} \; .$$

(3.143)

Of course, the asymptotic proper acceleration must be κ. Be reminded that the flux does not depend on only the change of acceleration, it also depends on the velocity. The answer for the energy is not expected to be Eqn. (3.143), but the intuitive choice of (3.143) becomes more accurate the more similar one can make an future-uniformly-accelerating trajectory approach the case of 'Hyperbolic plus Static'.

3.7 Trajectory Tables

This short summary section is concerned with non-comprehensive tables of several mirrors solutions discussed in the previous subsections. The ray tracing functions are included, $p(u) \equiv 2\tau_u - u$, where τ_u is found through $\tau_u - z(\tau_u) = u$, and $z(t)$ is the trajectory of the mirror. Some of the mirror trajectories listed here have been studied by other authors. The two asymptotically inertial mirrors Proex and Darcx, and the three static-start horizon-finish mirrors: Arcx, Logex, Omex, were found by the present author. The three most well known trajectories of the moving mirror model are those by Davies-Fulling[6], Carlitz-Willey[11] and the uniformly accelerated mirror[58]. All three accelerate until asymptotically null, forming a horizon and modes which do not intersect the mirror. Special trajectory cases like the Mobius or

Hyperlog are referred to in the text and are not entirely novel, as they have been discussed or suggested by others [23], [31]. The exploratory generalized transcendental solutions and the hyperbolic tangent archetypes are new. The trivial 'constant velocity' mirror has probably been analyzed before somewhere, however I have not seen its treatment. The 'light speed' boundary is my invention. The constant velocity mirror trajectory and light speed trajectory are included only for academic reference and completeness. For pedagogical purposes the static, drifting, and light speed mirrors coincide analogously to the future motional states of the asymptotically inertial mirrors: Walker-Davies, Darcx and Proex.

Table 3.1: Ray tracing functions and trajectories.

Mirror	Ray Tracing Function	Mirror Trajectory
Static	$p(u) = u$	$z(t) = 0$
Constant Velocity	$p(u) = \frac{1-v_0}{1+v_0}u \equiv Du$	$z(t) = -v_0 t$
Light Speed	$p(u) = 0$	$z(t) = -ct$
Uniform Acc.	$p(u) = \frac{u}{1+\kappa u}$	$z(t) = \kappa^{-1} - \sqrt{\kappa^{-2} + t^2}$
Carlitz-Willey	$p(u) = -\frac{1}{\kappa}e^{-\kappa u}$	$z(t) = -t - \kappa^{-1}W(e^{-2\kappa t})$
Walker-Davies	N/A.[4]	$t = -z(t) \pm A\sqrt{e^{-2z(t)/B} - 1}$
Darcx	Unknown.	$z(t) = -\frac{\xi}{\kappa}\sinh^{-1}(e^{\kappa t})$
Continued on Next Page...		

---

[4]Eqs (10) and (11) of Walker and Davies 1982 [34] are not in the invertable form for $p(u)$.

Table 3.1 – Continued

Mirror	Ray Tracing Function	Mirror Trajectory
Proex	$p(u) = u - \frac{1}{\kappa}W(2e^{\kappa u})$	$z(t) = -\frac{1}{\kappa}W(e^{\kappa t})$
Arcx	$p(u) = -\frac{1}{\kappa}\ln(e^{-\kappa u} + 2)$	$z(t) = -\frac{1}{\kappa}\sinh^{-1} e^{\kappa t}$
Logex	$p(u) = -\frac{1}{\kappa}\mathrm{csch}^{-1}(2e^{\kappa u})$	$z(t) = -\frac{1}{2\kappa}\ln(e^{2\kappa t} + 1)$
Omex	$p(u) = -\frac{1}{\kappa}W(\frac{e^{-\kappa u}}{2})$	$z(t) = -t - \frac{W(e^{-2\kappa t})}{2\kappa}$
Mobius	$p(u) = -\kappa^{-2}u^{-1}$	$z(t) = \pm\sqrt{\kappa^{-2} + t^2}$
Hyperlog	$p(u) = \frac{1}{\kappa}\ln(2 - e^{-\kappa u})$	$z(t) = -\frac{1}{\kappa}\ln\cosh\kappa t$
DF Late Times[5]	$p(u) = B - Ae^{-\kappa(u+B)}$	$z(t \to \infty) = -t - Ae^{-2\kappa t} + B$ $z(t < 0) = 0$
DF All Times	$p(u) = \frac{1}{\kappa}\ln(2 - e^{-\kappa u})$	$z(t > 0) = -\frac{1}{\kappa}\ln\cosh\kappa t$ $z(t < 0) = 0$

In Table 3.1 we have organized the trajectories as they are sectioned in this chapter. We have decided to keep the constant acceleration mirror listed as the first trajectory after the the non-accelerated trajectories for logical simplicity.

---

[5]See Section 3.3.3 or Davies and Fulling [5]

Table 3.2: Proper Accelerations and Energy Flux

Mirror	Proper Acceleration	Energy Flux as function of t_u
Static	$\alpha = 0$	$\langle T_{uu} \rangle = 0$
Constant Velocity	$\alpha = 0$	$\langle T_{uu} \rangle = 0$
Light Speed	$\alpha = 0$	$\langle T_{uu} \rangle = 0$
Uniform Acc.	$\alpha = -\kappa$	$\langle T_{uu} \rangle = 0$
Carlitz-Willey	$\alpha = -\kappa \frac{1}{2\sqrt{W(e^{2\kappa t})}}$	$\langle T_{uu} \rangle = \frac{\kappa^2}{48\pi}$
Darcx	$\alpha = -\kappa \frac{\xi e^{\kappa t}}{(1-\eta e^{2\kappa t})^{3/2}}$	$\langle T_{uu} \rangle = \frac{\kappa^2}{12\pi} \frac{\xi \chi e^{\kappa t_u}(2\eta e^{2\kappa t_u}+1)}{(\chi+\xi e^{\kappa t_u})^2(\eta e^{2\kappa t_u}-1)^2}$
Proex	$\alpha = -\kappa \frac{W[e^{\kappa t}]}{(1+2W[e^{\kappa t}])^{3/2}}$	$\langle T_{uu} \rangle = \frac{\kappa^2}{12\pi} \frac{(1-W[e^{\kappa t_u}])W[e^{\kappa t_u}]}{(1+2W[e^{\kappa t_u}])^4}$
Arcx	$\alpha = -\kappa e^{\kappa t}$	$\langle T_{uu} \rangle = \frac{\kappa^2}{12\pi} \frac{e^{\kappa t_u}\sqrt{1+e^{2\kappa t_u}}}{\left(1+2e^{\kappa t_u}\left(e^{\kappa t_u}+\sqrt{1+e^{2\kappa t_u}}\right)\right)}$
Logex	$\alpha = -\kappa \frac{2e^{2\kappa t}(1+e^{2\kappa t})}{(1+2e^{2\kappa t})^{3/2}}$	$\langle T_{uu} \rangle = \frac{\kappa^2}{3\pi} \frac{2e^{5\kappa t_u}[1+2\cosh(2\kappa t_u)]\cosh(\kappa t_u)}{(1+2e^{2\kappa t_u})^4}$
Omex	$\alpha = -\kappa \frac{2}{\sqrt{W[e^{-2\kappa t}](2+W[e^{-2\kappa t}])}}$	$\langle T_{uu} \rangle = \frac{\kappa^2}{3\pi} \frac{(1+2W[e^{-2\kappa t_u}])}{(2+W[e^{-2\kappa t_u}])^4}$

In Table 3.2 we have left out the Walker-Davies[34] mirror as the trajectory form is not transcendentally invertible for uncovering the proper acceleration and we have

not yet verified their flux, despite verifying their total energy with quanta summing. The Davies-Fulling late-time mirror has also been left out as its form is not appropriate for early-time proper acceleration. The Davies-Fulling all-time mirror, the Mobius and Hyperlog mirrors have also been left out as we deem their solutions no more physically relevant than the uniform accelerated mirror due to either splicing or double horizons.

Table 3.3: Energy Flux in u and Total Energy.

Mirror	Energy Flux of u	Total Energy
Static	$\langle T_{uu} \rangle = 0$	$E = 0$
Constant Velocity	$\langle T_{uu} \rangle = 0$	$E = 0$
Light Speed	$\langle T_{uu} \rangle = 0$	$E = 0$
Uniform Acc.	$\langle T_{uu} \rangle = 0$	$E = 0$
Willey-Carlitz	$\langle T_{uu} \rangle = \frac{\kappa^2}{48\pi}$	$E = \infty$
Walker-Davies	N/A.[6]	$E = \frac{B^2}{48(A^2-B^2)^{3/2}}$
Darcx	Unknown.	$E = \frac{\kappa}{96\pi} \left(\frac{3+\xi^2}{2\xi^2} \ln \frac{1+\xi}{1-\xi} - \frac{3+\xi(3+2\xi)}{\xi(1+\xi)} \right)$
Proex	$\langle T_{uu} \rangle = \frac{\kappa^2}{48\pi} \frac{(2-W[2e^{\kappa u}])W[2e^{\kappa u}]}{(1+W[2e^{\kappa u}])^4}$	$E = \frac{\kappa}{96\pi}$
Arcx	$\langle T_{uu} \rangle = \frac{\kappa^2}{12\pi} \frac{(1+e^{\kappa u})e^{\kappa u}}{(1+2e^{\kappa u})^2}$	$E = \infty$

Continued on Next Page...

---

[6]Eqs (10) and (11) of Walker and Davies 1982 [34] are not in the invertable form for $\langle T_{uu}(u) \rangle$

Table 3.3 – Continued

Mirror	Energy Flux of u	Total Energy
Logex	$\langle T_{uu} \rangle = \frac{\kappa^2}{3\pi} \frac{(1+e^{2\kappa u})e^{2\kappa u}}{(1+4e^{2\kappa u})^2}$	$E = \infty$
Omex	$\langle T_{uu} \rangle = \frac{\kappa^2}{48\pi} \frac{(1+4W[\frac{e^{-\kappa u}}{2}])}{(1+W[\frac{e^{-\kappa u}}{2}])^4}$	$E = \infty$
Hyperlog	$\langle T_{uu} \rangle = \frac{\kappa^2}{12\pi} \frac{(-1+e^{\kappa u})e^{\kappa u}}{(1-2e^{\kappa u})^2}$	$E = \infty$

In Table 3.3 I have shown the standard mirror trajectories like Table 3.2, however I have included Hyperlog to point out the similarity in form to Arcx, despite having two horizons. A salient point from Table 3.3 is the general intractability of the energy flux for asymptotically inertial mirrors. We have been unable to find a form for the energy flux as a function of u from the Darcx trajectory because we do not have a transcendental inversion for $p(u)$. The relative simplicity of the Proex trajectory's total energy is notable.

Table 3.4: Beta Coefficients and Counts.

Mirror	Beta: $\beta_{\omega'\omega}$	Unintegrated Count: $\lvert\beta_{\omega'\omega}\rvert^2$
Static	$\beta_{\omega'\omega} = 0$	$\lvert\beta_{\omega'\omega}\rvert^2 = 0$

Continued on Next Page...

Table 3.4 – Continued

Mirror	Beta: $\beta_{\omega'\omega}$	Unintegrated Count: $|\beta_{\omega'\omega}|^2$
Drifting	$\beta_{\omega'\omega} = 0$	$|\beta_{\omega'\omega}|^2 = 0$
Light	$\beta_{\omega'\omega} = 0$	$|\beta_{\omega'\omega}|^2 = 0$
Uniform	$-\frac{i}{\pi\kappa}e^{i\frac{\omega'-\omega}{\kappa}}K_1\big(2\frac{\sqrt{\omega\omega'}}{\kappa}\big)$	$\big|\frac{1}{\pi\kappa}K_1\big(2\frac{\sqrt{\omega\omega'}}{\kappa}\big)\big|^2$
CW	$\frac{1}{4\pi\sqrt{\omega\omega'}}\Big[-\frac{2\omega}{\kappa}e^{-\pi\omega/2\kappa}\big(\frac{\omega'}{\kappa}\big)^{i\omega/\kappa}\Gamma\big(-\frac{i\omega}{\kappa}\big)\Big]$	$\frac{1}{2\pi\kappa\omega'}\frac{1}{e^{2\pi\omega/\kappa}-1}$
WD	Lengthy Expression[7]	$\frac{2AB}{\pi^2}\frac{\omega'}{\omega'+\omega}\sinh(\pi\omega B)|K_q(r)|^2$
Darcx	$\frac{1}{4\pi\sqrt{\omega\omega'}}\frac{-i}{2^{i\omega_+}}\frac{\xi}{\kappa^2}\frac{2\omega'\omega}{b_+}\frac{\Gamma[i\omega_+]\Gamma[ia_+]}{\Gamma[ib_+]}$	$\frac{\xi^2}{4\pi\kappa^4}\frac{\omega'\omega}{\omega_+ a_+ b_+}\frac{\mathrm{csch}[\pi\omega_+]\mathrm{csch}[\pi a_+]}{\mathrm{csch}[\pi b_+]}$
Proex	$\frac{1}{4\pi\sqrt{\omega\omega'}}2\frac{\omega'}{\kappa}\big(\frac{2\omega}{\kappa}\big)^{-i\frac{\omega+\omega'}{\kappa}}e^{-\frac{\pi}{2}\frac{\omega+\omega'}{\kappa}}\Gamma\big(i\frac{\omega+\omega'}{\kappa}\big)$	$\frac{\omega'}{2\pi\omega\kappa(\omega+\omega')}\frac{1}{e^{\frac{2\pi}{\kappa}(\omega+\omega')}-1}$
Arcx	$\frac{1}{4\pi\sqrt{\omega\omega'}}\Big[-\frac{2\omega}{\kappa}2^{-\frac{i}{\kappa}(\omega+\omega')}B\big[-\frac{i\omega}{\kappa},\frac{i(\omega+\omega')}{\kappa}\big]\Big]$	$\frac{\omega}{4\pi^2\kappa^2\omega'}\Big|B\big(-\frac{i\omega}{\kappa},\frac{i(\omega+\omega')}{\kappa}\big)\Big|^2$
Logex	$\frac{1}{4\pi\sqrt{\omega\omega'}}\Big[-\frac{2\omega\omega'}{\kappa(\omega'-\omega)}B\big[-\frac{i\omega}{\kappa},\frac{i(\omega+\omega')}{2\kappa}\big]\Big]$	$\frac{\omega\omega'}{4\pi^2\kappa^2(\omega'-\omega)^2}\Big|B\big(-\frac{i\omega}{\kappa},\frac{i(\omega+\omega')}{2\kappa}\big)\Big|^2$
Omex	$\frac{1}{4\pi\sqrt{\omega\omega'}}\Big[-\frac{2\omega'\omega}{\kappa(\omega+\omega')}\big(\frac{\omega+\omega'}{2\kappa}\big)^{i\omega/\kappa}e^{-\pi\omega/2\kappa}\Gamma\big[-\frac{i\omega}{\kappa}\big]\Big]$	$\frac{\omega'}{2\pi\kappa(\omega+\omega')^2}\frac{1}{e^{2\pi\omega/\kappa}-1}$
Hyperlog	$\frac{1}{4\pi\sqrt{\omega\omega'}}\Big[-\frac{2\omega'\omega}{\kappa(\omega'-\omega)}2^{i\frac{(\omega'-\omega)}{\kappa}}B\big[-i\frac{\omega}{\kappa},i\frac{\omega'}{\kappa}\big]\Big]$	$\frac{\omega'\omega}{4\pi^2\kappa^2(\omega'-\omega)^2}\Big|B\big[-i\frac{\omega}{\kappa},i\frac{\omega'}{\kappa}\big]\Big|^2$

---

[7]See Subsection 3.4.1 or Walker and Davies [34]

In Table 3.4 I have shown the standard mirror trajectories as in Table 3.2, however, I have included the Hyperlog trajectory as it has some similarities in form to Arcx and to the other COnstant-velocity ASymptotic Trajectories- COAST mirrors. Table 3.4 displays the common appearance of the Beta function $B(a, b)$ (not to be confused with the beta coefficient transformation function $\beta_{\omega'\omega}$).

Chapter 4

Dynamics of Spectra

4.1 Wavepackets

The average number of particles of a given frequency received at I^+ is the expectation value

$$\langle in|N_\omega^{out}|in\rangle = \int_0^\infty d\omega'|\beta_{\omega\omega'}|^2 \tag{4.1}$$

where the quantum state of the matter field is in the natural vacuum, $|in\rangle$, at I^-. For mirrors which accelerate forever this quantity is infinite. The mean number of particles detected at I^+ using Eqn. (4.1) is the mean number of particles in the definite frequency mode ω. The uncertainty principle dictates that full certainty in frequency means total uncertainty in time. Therefore, $\langle in|N_\omega^{out}|in\rangle$ represents the number of particles emitted with a frequency ω *at anytime*. A localization procedure, incorporating wavepackets, will allow partial time and frequency resolution. Divergent artifacts may be rendered finite with packetization, particularly, for the asymptotic inertial trajectories and the CW mirror.

To utilize wavepackets as Hawking[3] and others [23][36] have done, the plane

wave, $\psi(v, \omega) = e^{i\omega v}$ is 'packetized' by

$$\psi_{jn}(v) = \frac{1}{\sqrt{\epsilon}} \int_{j\epsilon}^{(j+1)\epsilon} d\omega e^{2\pi i \omega n/\epsilon} \psi(v, \omega) \; , \qquad (4.2)$$

where $j \geq 0$ and n are both integer quantities. The wavepackets peak at the time $2\pi n/\epsilon$ with a temporal width $2\pi/\epsilon$. Taking ϵ small makes the modes narrowly centered in frequency around $\omega \approx \omega_j = (j + 1/2)\epsilon$.
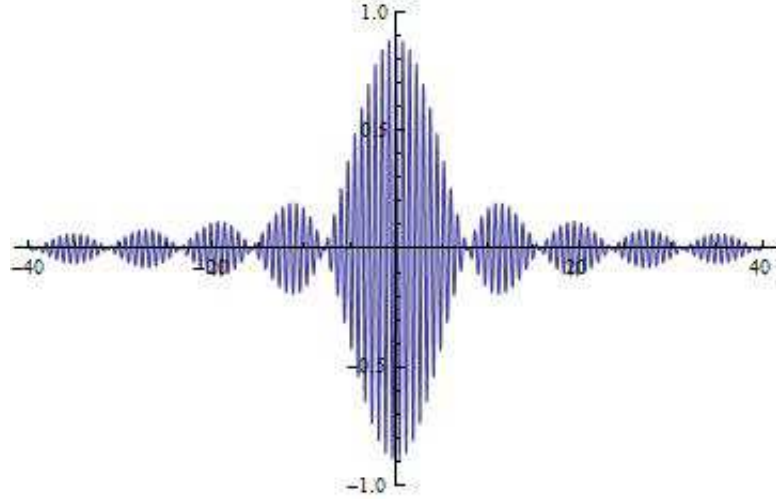
Figure 4.1: A packetized plane wave, where the x-axis is v.

Figure 4.1 shows the real part of the wavepacket construction of ψ with $n = 0$, $j = 10$, and $\epsilon = 0.8$. Raising j increases the density of oscillations, while using n other than $n = 0$ shifts the central peak to the left or right in v. Choosing ϵ smaller broadens out the packets in time. Using wavepackets one can calculate

$$\langle N_{jn} \rangle \equiv \int_0^\infty |\beta_{jn,\omega'}|^2 d\omega' \; , \qquad (4.3)$$

with either packetized modes or packetized Bogolubov coefficients in order to obtain a localized particle count. Equation (4.3) discretely samples the particles in frequency and time. A wavepacket labeled by j and n represents an excitation with

121

frequencies between $\pm\epsilon/2$ of ω_j and confined to a pulse in time of width $2\pi/\epsilon$ centered at $2\pi n/\epsilon$.

4.1.1 Equivalence of Packetization

Packetization of the Bogolubov coefficient with a negative sign on the exponent yields the same result as first performing 'positive' packetization on the mode solution and then solving for the now packetized Bogolubov coefficient. It does not matter whether you use the negative sign or the positive sign for, say, the Bogolubov coefficient as long as you use the other sign for the modes. Using $\beta_{jn,\omega'} \equiv \widehat{P_{jn}}^{+} \beta_{\omega\omega'}$ where

$$\widehat{P_{jn}}^{+} \equiv \frac{1}{\sqrt{\epsilon}} \int_{j\epsilon}^{(j+1)\epsilon} d\omega e^{+2\pi i \omega n/\epsilon} , \tag{4.4}$$

and

$$\beta_{\omega\omega'} \equiv 2i \int du \, \frac{e^{i\omega' p(u)}}{\sqrt{4\pi\omega'}} \partial_u \phi_\omega^* , \tag{4.5}$$

where integration by parts has been done to get Eqn. (4.5), and limits are left off the integration because this is a general expression for no specific mirror trajectory, only those trajectories where integration by parts is applicable. One obtains

$$\beta_{jn,\omega'} = \widehat{P_{jn}}^{+} \left(2i \int du \, \frac{e^{i\omega' p(u)}}{\sqrt{4\pi\omega'}} \partial_u \phi_\omega^* \right) = 2i \int du \, \frac{e^{i\omega' p(u)}}{\sqrt{4\pi\omega'}} \partial_u \widehat{P_{jn}}^{+} \phi_\omega^* . \tag{4.6}$$

This is because $[\partial_u, \widehat{P_{jn}}^{+}] = 0$. Therefore $\widehat{P_{jn}}^{+} \phi_\omega^* = (\widehat{P_{jn}}^{+*} \phi_\omega)^* = (\widehat{P_{jn}}^{-} \phi_\omega)^*$. If instead we packetize the mode first $\widehat{P_{jn}}^{-} \phi_\omega = \frac{1}{\sqrt{\epsilon}} \int_{j\epsilon}^{(j+1)\epsilon} d\omega e^{-2\pi i \omega n/\epsilon} \phi_\omega$, we get

$$\beta_{jn,\omega'} = 2i \int du \, \frac{e^{i\omega' p(u)}}{\sqrt{4\pi\omega'}} \partial_u (\widehat{P_{jn}}^{-} \phi_\omega)^* = \widehat{P_{jn}}^{+} 2i \int du \, \frac{e^{i\omega' p(u)}}{\sqrt{4\pi\omega'}} \partial_u \phi_\omega^* = \widehat{P_{jn}}^{+} \beta_{\omega\omega'} . \tag{4.7}$$

So therefore, first packetizing the mode will yield the packetized beta, $\widehat{P_{jn}}^{-}\phi_\omega \longrightarrow \beta_{jn,\omega'}$ or one can wait and packetize beta instead, $\widehat{P_{jn}}^{+}\beta_{\omega\omega'} \longrightarrow \beta_{jn,\omega'}$. The equivalence, $\widehat{P_{jn}}^{-}\phi_\omega \Leftrightarrow \widehat{P_{jn}}^{+}\beta_{\omega\omega'}$ holds. Negative packetization on the mode yields the same result as positive packetization on the beta. Packetization may be performed on either the mode or the beta Bogolubov coefficient one must watch the sign convention.

4.1.2 Carlitz-Willey Mirror Packets

In this section we summarize the packetization approach for a mirror following the Carlitz-Willey trajectory. The Planck spectrum character is found for the Carlitz-Willey mirror by wavepacket localization. This Planck distribution of thermal radiation for bosons is shown by first calculating the integral

$$\langle N_{\omega_1\omega_2}\rangle = \int_0^\infty d\omega' \beta_{\omega_1\omega'}\beta^*_{\omega_2\omega'} \ . \tag{4.8}$$

Inserting the properly normalized $\beta_{\omega\omega'}$ from the Carlitz-Willey calculation, as in Table 3.4 gives

$$\langle N_{\omega_1\omega_2}\rangle = \frac{\omega_1}{4\pi^2\kappa^2}e^{-\pi\omega_1/\kappa}\left|\Gamma\left(\frac{i\omega_1}{\kappa}\right)\right|^2 2\pi\kappa\delta(\omega_1-\omega_2) = \frac{1}{e^{2\pi\omega_1/\kappa}-1}\delta(\omega_1-\omega_2) \ , \tag{4.9}$$

where a change of variables has been utilized for integration. Introducing wavepackets for the Bogolubov coefficients

$$\beta_{jn,\omega'} = \frac{1}{\sqrt{\epsilon}}\int_{j\epsilon}^{(j+1)\epsilon} d\omega e^{2\pi i\omega n/\epsilon}\beta_{\omega\omega'} \ , \tag{4.10}$$

one finds that the Planckian character carries over to the discrete spectrum,

$$\langle N_{jn} \rangle = \int_0^\infty d\omega' |\beta_{jn,\omega'}|^2$$

$$= \frac{\kappa}{2\pi\epsilon} \ln \left(\frac{e^{\frac{2\pi(j+1)\epsilon}{\kappa}} - 1}{e^{\frac{2\pi j\epsilon}{\kappa}} - 1} \right) - 1 . \tag{4.11}$$

It is important to note that there is no time dependence in this particle count (the n-dependence drops out). To obtain Eqn. (4.11) from the integration, the mathematical conditions $e^{2\pi j\epsilon/\kappa} \leq 1$, $e^{2\pi(j+1)\epsilon/\kappa} \leq 1$ must hold. Equation (4.11) is relevant for early times (and all times) where the n variable has canceled out, independent of how small or large the frequency bins (size of ϵ) are. In the limit that the wavepackets are sharply peaked around frequencies $\omega_j = j\epsilon$, ϵ is small and one finds

$$\langle N_{jn} \rangle = \frac{1}{e^{2\pi\omega_j/\kappa} - 1} . \tag{4.12}$$
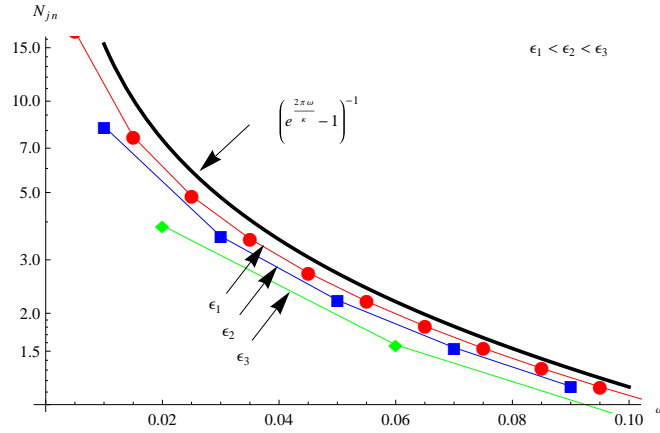
Figure 4.2: **CARLITZ-WILLEY**. Several spectra $\langle N_{jn} \rangle$ with differing ϵ of (4.11), with data points plotted at the center of the frequency bin, $\omega_c = (j + 1/2)\epsilon$. The thick black line is the Planckian approximation (4.12). $\kappa = 1$ throughout. A smaller ϵ value results in a spectrum more closely aligned with the Planck's spectrum. $\epsilon_3 = 25^{-1}$, $\epsilon_2 = 50^{-1}$, $\epsilon_1 = 100^{-1}$.

4.1.3 Dependence on 'n'

As we seek to develop an evolution of $\langle N_{jn} \rangle$, it is useful to look closely at the time dependence for packet localization. The CW mirror has no dependence on n as it radiates thermally for all time. We remind the reader that the expression for the CW mirror is

$$\langle N_{jn} \rangle = \frac{1}{\epsilon} \int_{j\epsilon}^{(j+1)\epsilon} d\omega \frac{1}{e^{\frac{2\pi\omega}{\kappa}} - 1} . \tag{4.13}$$

The exact answer, as derived in Equation (4.11), is

$$\langle N_{jn} \rangle = \frac{\kappa}{2\pi\epsilon} \ln \left(\frac{e^{\frac{2\pi(j+1)\epsilon}{\kappa}} - 1}{e^{\frac{2\pi j\epsilon}{\kappa}} - 1} \right) - 1 . \tag{4.14}$$

The above expression is clearly not dependent on n. How does this come about analytically? How did the n dependence vanish? The dependence on n is canceled out due to the calculation of

$$\langle N_\omega \rangle = \int_0^\infty d\omega' \beta_{\omega_1 \omega'} \beta_{\omega_2 \omega'}^* . \tag{4.15}$$

For the CW mirror specifically, the above expression gives,

$$\int_0^\infty d\omega' \beta_{\omega_1 \omega'} \beta_{\omega_2 \omega'}^* = \frac{1}{e^{2\pi\omega_1/\kappa} - 1} \delta(\omega_1 - \omega_2) . \tag{4.16}$$

Only with this delta function do the packetization $e^{2\pi\omega i n/\epsilon}$ terms vanish, according to

$$\beta_{jn,\omega'} = \frac{1}{\sqrt{\epsilon}} \int_{j\epsilon}^{(j+1)\epsilon} d\omega e^{2\pi i \omega n/\epsilon} \beta_{\omega\omega'} , \tag{4.17}$$

$$\langle N_{jn} \rangle = \int_0^\infty d\omega' |\beta_{jn,\omega'}|^2 \tag{4.18}$$

$$= \frac{1}{\epsilon} \int_{j\epsilon}^{(j+1)\epsilon} d\omega_1 e^{2\pi i \omega_1 n/\epsilon} \int_{j\epsilon}^{(j+1)\epsilon} d\omega_2 e^{-2\pi i \omega_2 n/\epsilon} \int_0^\infty d\omega' \beta_{\omega_1 \omega'} \beta^*_{\omega_2 \omega'} , \tag{4.19}$$

which results in the $\langle N_{jn} \rangle$ in Eqn. (4.13) and Eqn. (4.14) if you plug Eqn. (4.16) into Eqn. (4.19). If we wish to numerically verify this, we must compute (4.16) with sufficiently wide range of integration with respect to ω' to nullify the packetization term

$$e^{\frac{2\pi i n}{\epsilon}(\omega_1 - \omega_2)} . \tag{4.20}$$

Let us contemplate how this problem manifests itself for the other mirror trajectories. We know from Chapter 3 that the other mirror trajectories result in particles emitted that are only thermal at high frequency, $\omega' >> \omega$ and therefore only at late times, (large n) will a thermal character result. We expect n dependence for $\langle N_{jn} \rangle$ at earlier times. Proceeding along the same analytical route, we seek to solve Eqn. (4.15). For any of the mirrors that have Beta functions as their solutions for the beta coefficients, an integral of the form

$$\int_0^\infty d\omega' \, B(-i\omega_1, i(\omega_1 + \omega')) \times B(i\omega_2, -i(\omega_2 + \omega')) , \tag{4.21}$$

results. This is a challenging integral. Only the Omex and Proex mirrors do not involve Beta functions. We ignore Proex because packetization is shown later. The Omex mirror results in an integral for (4.15) of the form

$$\int_0^\infty d\omega' \, \omega'(\omega_1 + \omega')^{i\omega_1 - 1}(\omega_2 + \omega')^{-i\omega_2 - 1} . \tag{4.22}$$

This integral diverges, but if its solution is in terms of a delta function, $\delta(\omega_1 - \omega_2)$, this would negate '$n$' dependence, like the CW mirror, which we know is not the case. The indefinite form of Eqn. (4.22)

$$\frac{-i(\omega_1 + \omega')^{i\omega_1}(\omega_2 + \omega')^{-i\omega_2}}{\omega_1 - \omega_2} , \tag{4.23}$$

is however similar to the indefinite form of the CW mirror that results from Eqn. (4.15),

$$\int d\omega' \, \omega'^{i(\omega_1 - \omega_2) - 1} = \frac{-i\omega'^{i(\omega_1 - \omega_2)}}{\omega_1 - \omega_2} . \tag{4.24}$$

Placing the limits on Eqn. (4.24) gives the delta function

$$\int_0^\infty d\omega' \, \omega'^{i(\omega_1 - \omega_2) - 1} = 2\pi\delta(\omega_1 - \omega_2) . \tag{4.25}$$

Therefore, we are left with a difficult analytical task if we wish to solve for the particle localization of a trajectory like the Omex mirror, the task of solving Eqn. (4.22), which diverges (this is to be expected). If we wish to numerically solve for the particle localization of a trajectory like the Carlitz-Willey mirror we are faced with task of computing Eqn. (4.16) with a sufficiently wide range of ω' to cancel the packetization term $e^{\frac{2\pi in}{\epsilon}(\omega_1 - \omega_2)}$. For other diverging acceleration mirrors (like Omex) this numerical computation should avoid any cancelation of n, because they have an early time dependence of interest, i.e. they depend on n.

4.2 Energy Packets

4.2.1 Quanta Energy Summation

In this section we investigate the conditions for the failure of summing quanta. One might assume the total energy released by the mirror,

$$E = \int_{z(t)}^{\infty} \langle T^{00} \rangle dx = \int_{u_{min}}^{u_{max}} \langle T_{uu} \rangle \, du \, , \tag{4.26}$$

can be found by summing the energy of all quanta,

$$\int_{u_{min}}^{u_{max}} \langle T_{uu} \rangle \, du \;=\; \int_0^{\infty} \omega \langle N_\omega \rangle d\omega = \int_0^{\infty} dw \; w \int_0^{\infty} d\omega' |\beta_{\omega'\omega}|^2 \, . \tag{4.27}$$

A derivation of this is given in Fabbri and Navarro-Salas where the two-point function is used [23]. This was originally shown by Walker, who also pointed out that for mirrors with acceleration singularities, this is not always true [15]. The above summing method is derived from the definition of $\langle T_{uu} \rangle$ assuming no horizons. As a simple look at consistency, we can see how horizons allow particles to be created with zero or even negative energy. The familiar Davies-Fulling result, Eqn. (2.45),

$$\langle T_{uu} \rangle = \frac{1}{24\pi} \left[\frac{3}{2} \left(\frac{p''}{p'} \right)^2 - \frac{p'''}{p'} \right] \, , \tag{4.28}$$

is derived from the definition of $\langle T_{uu} \rangle$ as well, but makes no assumptions regarding horizons. We use it to see how the counting method might fail. We integrate Eqn. (4.28) by parts to give

$$E = -\frac{1}{24\pi} \frac{p''}{p'} \Big|_{-\infty}^{\infty} + \frac{1}{48\pi} \int_{-\infty}^{\infty} du \, \left(\frac{p''}{p'} \right)^2 \, . \tag{4.29}$$

128

Rewriting the boundary term in (4.29) using, $z(\tau_u) = \frac{1}{2}(p(u) - u)$ gives

$$-\frac{\alpha}{12\pi}\sqrt{\frac{1+\dot{z}}{1-\dot{z}}}\Bigg|_{\tau_u=-\infty}^{\tau_u=+\infty} \qquad \text{where} \qquad \alpha \equiv \frac{\ddot{z}}{(1-\dot{z}^2)^{3/2}} \; . \tag{4.30}$$

Here, α is the proper acceleration. Note that if $\alpha(\tau_u \to +\infty) \neq 0$ then we will have a v asymptote for $\dot{z} \to -1$. If there exists such a horizon, as first noticed by Walker [15], this boundary term does not vanish and energy production may be zero or negative. We will want to be careful using particle counting to find the energy, (i.e. (4.27)), as ultimately it is invalid if the mirror in question has a horizon. In particular, Proex has $\dot{z} \to -1$, yet $\alpha(\tau_u \to +\infty) = 0$. It has no u or v horizon. The above boundary term vanishes. For the Proex mirror, both calculations give (to within machine error for the summing method)

$$\int_0^\infty \omega \langle N_\omega \rangle d\omega = \int_{u_{min}}^{u_{max}} \langle T_{uu} \rangle \, du = \frac{\kappa}{96\pi} \; . \tag{4.31}$$

4.2.2 Summary of Energy Packet Summation

The energy in a packet is defined to be

$$E_{jn} = (j + \frac{1}{2})\epsilon \int_0^\infty d\omega' |\beta_{jn\omega'}|^2 \; . \tag{4.32}$$

The total energy will be found by

$$E = \sum_{jn} E_{jn} \; . \tag{4.33}$$

The total energy calculated is obtained by summing the many energy packets, particularly on the main $n = 0$ time window up to a high j. More energy packets can be summed, for $j = 0$ up to a particular maximum or minimum value of $\pm n$. A smaller ϵ

gives a more accurate result and requires more energy packets to be summed. Those packets which can be ignored should contribute only a negligible amount relative to the $n = 0$ time window packets and the $j = 0$ alternate time window packets.

4.3 Spectral Dynamics Using Packets

4.3.1 Numerical Packetizing for Spectral Count

Using the wavepacket localization procedure in Section 4.1, we examine the time evolution of the build up of particles from the asymptotically inertial mirrors. With the packetized beta coefficients, we obtain the detected particles

$$\langle N_{jn} \rangle = \int_0^\infty |\beta_{jn,\omega'}|^2 d\omega' \ . \tag{4.34}$$

This is done numerically and represents the counts of a particle detector. This quantity is plotted for a fixed n time window and a range of j's on the x-axis. The spectral graph shows an increase in the creation of particles and subsequent decrease as n is changed. The asymptotically inertial trajectories, Walker-Davies,Darcx, and Proex are analyzed. Figures 4.3, 4.4 and 4.5 show the particle counts for the spectral dynamics.

The procedure for localization of the particle creation in time throughout the trajectory motion is a straightforward numerical integration (packetization) of the normalized beta coefficient. Complex conjugation is then incorporated and numerical integration over all ω' is finally utilized.
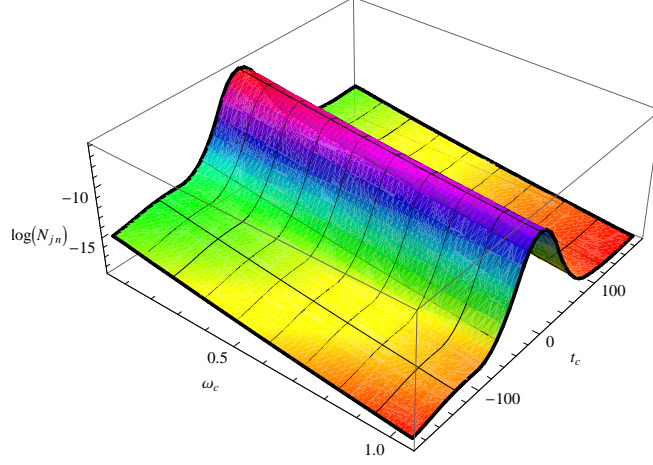
Figure 4.3: **WALKER-DAVIES**. A spectral build up in time and subsequent spectral diminishing for the Walker-Davies trajectory. $\epsilon = 0.1$, $B = 1$, $A = 2$ throughout. $t_c = 2\pi n/\epsilon$, $\omega_c = (j + 1/2)\epsilon$.

4.3.2 Summing Packets to Find Total Energy

A consistency check of this localization method is in order. Consider the Darcx trajectory with a final constant speed of $\xi = 0.99$. Using the stress tensor evaluation, Eqn (3.62), we determine the total energy to be

$$E_1 = \frac{\kappa}{96\pi} \left(\frac{13267 \ln 199}{6534} - \frac{26434}{6567} \right) = 0.0222901\kappa \ . \tag{4.35}$$

The globally-calculated, nonlocalized $\beta_{\omega\omega'}$ confirm this result as well. That is, we can computing the energy by summing up the energy of each quantum using the Bogolubov coefficients,

$$E_2 = \int_0^\infty dw \ w \int_0^\infty d\omega' |\beta_{\omega'\omega}|^2 = 0.0222901\kappa \ . \tag{4.36}$$

The modulus squared used here is Eqn. (3.60). A third confirmation via the time evolved packetization approach is possible. Using the localized betas one may numerically obtain,
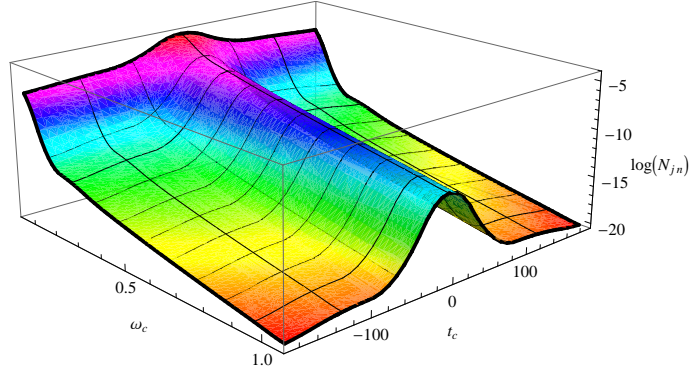
Figure 4.4: **DARCX**. A spectral build up in time and subsequent spectral diminishing for the Darcx trajectory. $\epsilon = 0.1$ and $\kappa = 1$ throughout. $t_c = 2\pi n/\epsilon$, $\omega_c = (j+1/2)\epsilon$.
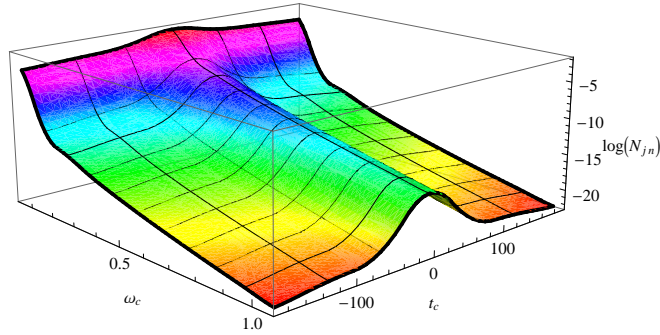
Figure 4.5: **PROEX**. A spectral build up in time and subsequent spectral diminishing for the Proex trajectory. $\epsilon = 0.1$ and $\kappa = 1$ throughout. $t_c = 2\pi n/\epsilon$, $\omega_c = (j + 1/2)\epsilon$.

$$E_3 = \sum_{jn} E_{jn} = 0.022291\kappa . \tag{4.37}$$

Here, we use energy packets, defined by

$$E_{jn} = (j + \frac{1}{2})\epsilon \int_0^\infty d\omega' |\beta_{jn\omega'}|^2 . \tag{4.38}$$

An $\epsilon = \frac{1}{1000}$ value was used, while summing continued until the last packet to be summed was about 10^{-3} of the largest energy packet. A smaller ϵ gives a more accurate result and requires more energy packets to be summed. The total energy

calculated in this check has a relative error of about 10^{-4}. The total value was obtained by summing the first 1175 energy packets on the main $n = 0$ time window up to $j = 1175$. As can be seen

$$E_1 = E_2 = E_3 \ . \tag{4.39}$$

We determined that the total energy of the Proex trajectory using the stress tensor in Eqn. (3.77) is

$$E_1 = \frac{\kappa}{96\pi} = 0.00331573\kappa \ . \tag{4.40}$$

We also determined the total energy by summing the number of particles Eqn. (3.79) and found it is the same,

$$E_2 = \frac{\kappa}{96\pi} = 0.00331573\kappa \ . \tag{4.41}$$

Localizing the particle creation via packetization numerically, we sum energy packets and obtain

$$E_3 = 0.00331281\kappa \ . \tag{4.42}$$

An $\epsilon = \frac{1}{20000}$ value was used, while summing continued until the last packet summed was less than about 10^{-4} (about 12000 packets in this case) of the largest energy packet. A smaller ϵ gives a more accurate result and requires more energy packets to be summed. The total energy calculated in this check has a relative error of about 0.08 percent. The total value was obtained by summing the first 12000 energy packets on the main $n = 0$ time window up to $j = 12000$.

This is confirmation that energy packets may accurately be used to calculate the energy flux carried by the particles during the corresponding times detected. This

confirms that the spectral packets are a successful way to partially time resolve the particle creation during strongly time dependent accelerated mirror motions.

4.4 Particle Creation Aspects

4.4.1 Dynamic Spacetime Particle Creation

In an expanding spacetime particles are created. This example that follows is exactly the calculation done in Section 3.4 of Birrell and Davies book [19]. The example presented here just fills in some of the details. This calculation was first carried out out by Bernard and Duncan [60]. In this section we review the simplest model of dynamic curved spacetime particle creation. This model is described here to exemplify several points: First, the transformation coefficients are similar expressions of gamma functions not unlike the new and simpler exactly solvable moving mirror trajectories in Chapter 3. Second, the expansion function used in this example is treated in Section 3.6 on heterogeneous mirror trajectories. Third, this example offers a preface for particle creation in curved spacetime, particularly for the more complex setting involving anisotropy treated in Chapter 5. Particles are created using the Minkowskian IN and OUT regions. The Robertson-Walker spacetime element for two dimensions is

$$ds^2 = dt^2 - a^2(t)dx^2 \ . \tag{4.43}$$

This metric allows for spatial expansion via the scalar function $a(t)$. A new time coordinate, η, called conformal time because our new element will be conformally flat, is defined by $d\eta = dt/a$ and thus $t = \int^t dt' = \int^\eta a(\eta')d\eta'$. The line element is therefore

$$ds^2 = C(\eta)(d\eta^2 - dx^2) \,, \tag{4.44}$$

where $C(\eta) = a^2(\eta)$. We will use the particular function

$$C(\eta) \equiv A + B\tanh(\rho\eta) \,, \tag{4.45}$$

where A, B, ρ are constants. In the past and future we obtain Minkowskian space-times because

$$C(\eta) \to A \pm B \quad \eta \to \pm\infty \,, \tag{4.46}$$

as $\tanh(\pm\infty) = \pm 1$. This function is considered for the moving mirror model in Section 3.6. Under these conditions, the formation of massive, minimally coupled ($\xi = 0$) scalar particles occurs. In two dimensions minimal coupling and conformal coupling are the same things. Conformal coupling is defined as $\xi = \frac{n-2}{4(n-1)}$. As $C(\eta)$ is not a function of the spatial coordinate x, spatial translation invariance is a symmetry, therefore separation of the variables in the modes is possible:

$$u_k(\eta, x) = (2\pi)^{-1/2} e^{ikx} \chi_k(\eta) \,. \tag{4.47}$$

The field in terms of the modes is

$$\phi(x) = \sum_i [a_i u_i(\eta, x) + a_i^\dagger u_i^*(\eta, x)] \,. \tag{4.48}$$

Using the metric (4.44), the modes (4.47) are placed into the wave equation

$$[\Box + m^2]\phi(x) = 0 \,, \tag{4.49}$$

and solved. The 'test' state, $|0\rangle$, is useful for this task. The condition

$$(g^{\mu\nu}\nabla_\mu\nabla_\nu + m^2)e^{-ikx}\chi_i(\eta) = 0 \ , \tag{4.50}$$

results, which resolves to an ordinary differential equation for $\chi_k(\eta)$,

$$d_\eta^2\chi_k(\eta) + (k^2 + C(\eta)m^2)\chi_k(\eta) = 0 \ . \tag{4.51}$$

This can be solved using hypergeometric functions. The normalized modes that correspond to the positive frequency Minkowski space modes in the far past are:

$$u_k^{in} = (4\pi\omega_{in})^{-1/2}e^{D(x,\eta)}{}_2F_1(a,b,c,z) \to (4\pi\omega_{in})^{-1/2}e^{ikx-i\omega_{in}\eta} \ , \tag{4.52}$$

and in the far future

$$u_k^{out} = (4\pi\omega_{out})^{-1/2}e^{D(x,\eta)}{}_2F_1(a,b,c',1-z) \to (4\pi\omega_{out})^{-1/2}e^{ikx-i\omega_{out}\eta} \ , \tag{4.53}$$

where I have defined several symbols to make notation easier, $\omega_{in}^2 = k^2 + m^2(A-B)$, $\omega_{out}^2 = k^2 + m^2(A+B)$, $\omega_\pm = \frac{1}{2}(\omega_{out}\pm\omega_{in})$, $D(x,\eta) \equiv ikx - i\omega_+\eta - (i\omega_-/\rho)\ln[2\cosh(\rho\eta)]$, and

$$a \equiv 1 + i\omega_-/\rho \ , \tag{4.54}$$

$$b \equiv i\omega_-/\rho \ , \tag{4.55}$$

$$c \equiv 1 - i\omega_{in}/\rho \ , \tag{4.56}$$

$$c' \equiv 1 + i\omega_{out}/\rho \ , \tag{4.57}$$

$$z \equiv \frac{1}{2}(1 + \tanh\rho\eta) \ , \tag{4.58}$$

$$1 - z = \frac{1}{2}(1 - \tanh\rho\eta) \ . \tag{4.59}$$

It is now possible to see that the creation of particles must occur. Since u_k^{in} and u_k^{out} are not equal, the β coefficient cannot be zero in

$$u_j^{in} = \sum_i (\alpha_{ji} u_i^{out} + \beta_{ji} u_i^{out*}) . \tag{4.60}$$

The properties $\alpha_{kk'} = \alpha_k \delta_{kk'}$, $\beta_{kk'} = \beta_k \delta_{-kk'}$ allow the relation

$$u_k^{in} = \alpha_k u_k^{out} + \beta_k u_{-k}^{out*} , \tag{4.61}$$

to hold. The linear transformation properties of hypergeometric functions,

$$
\begin{aligned}
{}_2F_1(a,b,c,z) &= \frac{\Gamma(c)\Gamma(c-a-b)}{\Gamma(c-a)\Gamma(c-b)} {}_2F_1(a,b,a+b+1-c,1-z) \\
&+ \frac{\Gamma(c)\Gamma(a+b-c)}{\Gamma(a)\Gamma(b)} (1-z)^{c-a-b} {}_2F_1(c-a,c-b,1+c-a-b,1-z)
\end{aligned} \tag{4.62}
$$

and

$$ {}_2F_1(a,b,c,z) = (1-z)^{c-a-b} {}_2F_1(c-a,c-b,c,z) , \tag{4.63}$$

allow the in-modes to be written in terms of the out-modes as,

$$u_k^{in}(\eta,x) = \alpha_k u_k^{out}(\eta,x) + \beta_k u_{-k}^{out*}(\eta,x) . \tag{4.64}$$

The coefficients are

$$\alpha_k = \left(\frac{\omega_{out}}{\omega_{in}} \right)^{\frac{1}{2}} \frac{\Gamma(c)\Gamma(c-a-b)}{\Gamma(c-a)\Gamma(c-b)} , \tag{4.65}$$

$$\beta_k = \left(\frac{\omega_{out}}{\omega_{in}} \right)^{\frac{1}{2}} \frac{\Gamma(c)\Gamma(a+b-c)}{\Gamma(a)\Gamma(b)} , \tag{4.66}$$

using our defined abc's Eqn. (4.54), etc. Squaring $|\beta_k|^2$, using $|\Gamma(ix)|^2 = \pi/x \sinh(\pi x)$, and $\Gamma(1+z) = z\Gamma(z)$, we find

$$|\beta_k|^2 = \frac{\sinh^2(\pi\omega_-/\rho)}{\sinh(\pi\omega_{in}/\rho)\sinh(\pi\omega_{out}/\rho)} \ . \tag{4.67}$$

If the quantum field resides in the vacuum state, $|0, in\rangle$ defined by $a_i|0\rangle_{in} = 0$, then in the remote past with a Minkowskian spacetime, inertial observers (detectors) will observe (register) no particles, i.e. an empty physical vacuum state. Now, working in the Heisenberg picture, we see that in the far future, the spacetime is also Minkowskian and the quantum field resides in the same state, $|0, in\rangle$. But here the role of the physical vacuum is assumed not by $|0, in\rangle$ but by $|0, out\rangle$. Therefore, particle detectors will register the presence of quanta in the out-region. In the mode k, the expected number of particles are given by Eqn. (4.67).

4.4.2 Statistics from Dynamics

The spin-statistics theorem can be derived from the use of quantum field theory under the influence of external conditions. The external conditions may include either curved spacetime or an accelerated boundary condition. The connection between the spin-statistics theorem and field dynamics for curved spacetime was previously discovered by Parker and Wang [61]. See Parker's and Tom's recent book [20] for more detail on the case of curved spacetime. Also see Wald [62] and Sorkin [63]. I present a new derivation of the spin-statistics theorem from the dynamics of an accelerated boundary in flat spacetime.

Moving Mirror Spin-Statistics Connection

The spin-statistics theorem can be derived from the use of an accelerated external boundary condition in flat spacetime. The field equation ,(2.31), and mirror dynamics, (2.32), dictate the relevant commutation relation. This is understood by the use

of the Bogolubov transformation for one of the two sets of creation-anniliation operators. Utilizing the conserved scalar product for the modes, the Wronskian relation for the Bogolubov coefficients holds. This Wronskian result is only a by-product of the dynamics of the mirror and field equation. The possible commutation relations are expressed in terms of the transformation coefficients. As long as $\beta_{\omega\omega'} \neq 0$, the mirror and equation of motion for the spin-0 field demand the negative sign in the possible commutation relations (from the Wronskian), implying particles at different times will obey the same statistics only in the case of Bose-Einstein statistics. If $\beta_{\omega\omega'} = 0$ this connection between dynamics and statistics disappears. An explicit derivation of how an accelerated mirror allows one to derive the relationship between spin and statistics is provided using the Carlitz-Willey conventions.

Spin-0 Case

The spin-statistics theorem can be derived from the use of the mirror in flat spacetime. In flat spacetime, statistics can be derived from dynamics, if an external boundary condition is present that gives a non-zero beta Bogolubov coefficient. The commutation relations of the creation operators determine the statistics:

$$\text{commuting} \quad \rightarrow \quad \text{Bose-Einstein}$$
$$\text{anticommuting} \quad \rightarrow \quad \text{Fermi-Dirac}$$

For the spin-0 field, only Bose-Einstein statistics is consistent with the flat spacetime dynamics that include an external boundary condition. Carlitz-Willey's conventions make this apparent. While the field motion is the Klein-Gordon equation $\Box\phi(u, v) = 0$, we can write

139

$$\phi(u, v) = \frac{1}{4\pi} \int_0^\infty \frac{d\omega}{\omega} \left[a_\omega \phi_\omega(u, v) + a_\omega^\dagger \phi_\omega^*(u, v) \right] , \qquad (4.68)$$

$$\phi(u, v) = \frac{1}{4\pi} \sum_I \int_0^\infty \frac{d\omega}{\omega} \left[a_\omega^I \phi_\omega^I(u, v) + a_\omega^{I\dagger} \phi_\omega^{I*}(u, v) \right] , \qquad (4.69)$$

where $I = R, L$ and for reference

$$\phi_{\omega'} = e^{-i\omega' v} - e^{-i\omega' p(u)} \qquad \begin{cases} \phi_\omega^R = e^{-i\omega V(v)} \Theta(-v) - e^{-i\omega u} \\ \phi_\omega^L = e^{-i\omega W(v)} \Theta(v) \end{cases} , \qquad (4.70)$$

$$p(u) = -\kappa^{-1} e^{-\kappa u} \qquad \begin{cases} V(v) = -\kappa^{-1} \ln(-\kappa v) & v < 0 \\ W(v) = +\kappa^{-1} \ln(+\kappa v) & v > 0 \end{cases} . \qquad (4.71)$$

The field equation along with this mirror imply that the Bogoliubov coefficients $\alpha_{\omega'\omega}^I$ and $\beta_{\omega'\omega}^I$ relate the operators $a_{\omega'}$ and $a_{\omega'}^\dagger$ to the operators a_ω^I and $a_\omega^{I\dagger}$:

$$a_{\omega'} = \frac{1}{4\pi} \sum_I \int_0^\infty \frac{d\omega}{\omega} \left(\alpha_{\omega'\omega}^I a_\omega^I + \beta_{\omega'\omega}^I a_\omega^{I\dagger} \right) , \qquad (4.72)$$

$$a_\omega^I = \frac{1}{4\pi} \int_0^\infty \frac{d\omega'}{\omega'} \left(\alpha_{\omega'\omega}^{I*} a_{\omega'} - \beta_{\omega'\omega}^I a_{\omega'}^\dagger \right) . \qquad (4.73)$$

Since we know the operators are related by a Bogolubov transformation, we may go further and look at the conserved scalar products, (where $J = L, R$),

$$(\phi_\omega, \phi_{\omega'}) \equiv i \int_{-\infty}^\infty dv \phi_{\omega'}^* \overset{\leftrightarrow}{\partial_v} \phi_\omega = 4\pi\omega\delta(\omega' - \omega) , \qquad (4.74)$$

$$i \int_0^\infty dv \phi_{\omega'}^{I*} \overset{\leftrightarrow}{\partial_v} \phi_\omega^J + i \int_{-\infty}^\infty du \phi_{\omega'}^{I*} \overset{\leftrightarrow}{\partial_u} \phi_\omega^J = 4\pi\omega\delta(\omega' - \omega)\delta^{IJ} . \qquad (4.75)$$

These imply

$$\frac{1}{4\pi} \sum_I \int_0^\infty \frac{d\omega}{\omega} \left(\alpha^I_{\omega'\omega} \alpha^{I*}_{\omega''\omega} - \beta^I_{\omega'\omega} \beta^{I*}_{\omega''\omega} \right) = 4\pi\omega' \delta(\omega'' - \omega') \,, \qquad (4.76)$$

$$\frac{1}{4\pi} \sum_I \int_0^\infty \frac{d\omega}{\omega} \left(\alpha^I_{\omega'\omega} \beta^I_{\omega''\omega} - \beta^I_{\omega'\omega} \alpha^I_{\omega''\omega} \right) = 0 \,, \qquad (4.77)$$

$$\frac{1}{4\pi} \int_0^\infty \frac{d\omega'}{\omega'} \left(\alpha^{I*}_{\omega'\omega} \alpha^J_{\omega'\omega''} - \beta^I_{\omega'\omega} \beta^{J*}_{\omega'\omega''} \right) = 4\pi\omega \delta(\omega - \omega'') \delta^{IJ} \qquad (4.78)$$

$$\frac{1}{4\pi} \int_0^\infty \frac{d\omega'}{\omega'} \left(\alpha^{I*}_{\omega'\omega} \beta^J_{\omega'\omega''} - \beta^I_{\omega'\omega} \alpha^{J*}_{\omega\omega''} \right) = 0 \,. \qquad (4.79)$$

These relations are derived consequences only of the field equation and the imposed Carlitz-Willey mirror trajectory.

Now consider the possible commutations relations

$$[a_\omega, a^\dagger_{\omega'}]_\pm = 4\pi\omega \delta(\omega' - \omega) \,, \qquad (4.80)$$

$$[a_\omega, a_{\omega'}]_\pm = [a^\dagger_\omega, a^\dagger_{\omega'}]_\pm = 0 \,. \qquad (4.81)$$

Here the $+$ sign corresponds to Fermi-Dirac statistics from the anticommutator, while the $-$ sign corresponds to Bose-Einstein statistics from the commutator. The possible left-right operators in terms of the transformation coefficients are

$$[a^I_\omega, a^{J\dagger}_{\omega'}]_\pm = \frac{1}{4\pi} \int_0^\infty \frac{d\omega'}{\omega'} \left(\alpha^{I*}_{\omega'\omega} \alpha^J_{\omega'\omega'} \pm \beta^I_{\omega'\omega} \beta^{J*}_{\omega'\omega'} \right) \,. \qquad (4.82)$$

The field equation result Eqn. (4.78) can be used to determine which of the possible commutation relations are implied to be used in (4.82). This implies the relations

using the $-$ sign,

$$[a_\omega^I, a_{\omega'}^{J\dagger}]_- = 4\pi\omega\delta(\omega - \omega')\delta^{IJ} .$$ (4.83)

Particles at different times will obey the same statistics only in the Bose-Einstein case. The Bose-Einstein case is then consistent with the dynamics of the field and mirror. In general, β is not zero so this result is a boundary condition in flat spacetime derivation of the relationship between spin and statistics.

Curved Spacetime Derivation of Spin-Statistics Connection

For completeness, I will derive the same connection between the dynamics and statistics that exists in curved spacetime, as it does for the mirror in flat spacetime. This calculation is in Parker and Toms [20]. The derivation here follows in essentially the same way. Consider a spin-0 field. The curved spacetime scalar field is described by the Lagrangian density

$$\mathcal{L} = \frac{1}{2}|g|^{1/2}(g^{\mu\nu}\partial_\mu\phi\partial_\nu\phi - m^2\phi^2 - \xi R\phi^2) ,$$ (4.84)

where $R \equiv g^{\mu\nu}R_{\mu\nu}$ is the scalar curvature of the spacetime and ξ is a dimensionless coupling constant. The notation is the standard used in Birrell and Davies [19]

$$\Box\phi + (m^2 + \xi R)\phi = 0 ,$$ (4.85)

The spatially flat isotropically changing metric

$$ds^2 = dt^2 - a^2(t)(dx^2 + dy^2 + dz^2) ,$$ (4.86)

142

has a cosmological scale factor, $a(t)$, that has an arbitrary time dependence. It will asymptotically approaches constant values at early and late time values of cosmic time t, i.e. proper time of a set of clocks on geodesic worldlines that remain at constant values of the spatial coordinates (x, y, z). $a(t)$ approaches a_1 as $t \to -\infty$ and $a(t)$ approaches a_2 as $t \to +\infty$. The scalar curvature, R is

$$R = 6 \left[\left(\frac{\dot{a}}{a} \right)^2 + \frac{\ddot{a}}{a} \right] , \tag{4.87}$$

which means the field equation takes the form

$$a^{-3} \partial_t (a^3 \partial_t \phi) - a^{-2} \sum_i \partial_i^2 \phi + (m^2 + \xi R)\phi = 0 . \tag{4.88}$$

The solutions take the form

$$\phi = \sum_{\vec{k}} \left[A_{\vec{k}} f_{\vec{k}}(x) + A_{\vec{k}}^\dagger f_{\vec{k}}^*(x) \right] , \tag{4.89}$$

$$\phi = \sum_{\vec{k}} \left[a_{\vec{k}} g_{\vec{k}}(x) + a_{\vec{k}}^\dagger g_{\vec{k}}^*(x) \right] . \tag{4.90}$$

The f and g reduce to positive frequency Minkowski spacetime solutions at early times and late times, respectively,

$$f_{\vec{k}} \sim \frac{1}{\sqrt{V a_1^3 2\omega_{1k}}} e^{i(\vec{k}\cdot\vec{x} - \omega_{1k}t)} \quad \text{early times} , \tag{4.91}$$

$$g_{\vec{k}} \sim \frac{1}{\sqrt{V a_2^3 2\omega_{2k}}} e^{i(\vec{k}\cdot\vec{x} - \omega_{2k}t)} \quad \text{late times} , \tag{4.92}$$

where

$$\omega_{1k} = [(k/a_1)^2 + m^2]^{1/2} , \qquad \omega_{2k} = [(k/a_2)^2 + m^2]^{1/2} . \qquad (4.93)$$

The late time asymptotic form of f is found from the field equation and takes the form

$$f_{\vec{k}} \sim \frac{1}{\sqrt{V a_2^3 2\omega_{2k}}} e^{i\vec{k}\cdot\vec{x}}[\alpha_k e^{-i\omega_{2k}t} + \beta_k e^{i\omega_{2k}t}] \qquad \text{(late times)} . \qquad (4.94)$$

The Bogolubov transformation is used to relate the annihilation operator for late times, $a_{\vec{k}}$, to the annihilation operator at early times, $A_{\vec{k}}$,

$$a_{\vec{k}} = \alpha_k A_{\vec{k}} + \beta_k^* A_{-\vec{k}}^\dagger . \qquad (4.95)$$

The Bogolubov coefficients only depend on $k = |\vec{k}|$ because only k^2 enters into the field equation. The scalar product, $(f_{\vec{k}}, f_{\vec{k}}) = 1$, is conserved and gives,

$$|\alpha_k|^2 - |\beta_k|^2 = 1 . \qquad (4.96)$$

Again, this is a result of just the field equation dynamics. The possible early time (IN vacuum) commutation relations are

$$[A_{\vec{k}}, A_{\vec{k}'}^\dagger]_\pm = \delta_{\vec{k},\vec{k}'} , \qquad (4.97)$$

$$[A_{\vec{k}}, A_{\vec{k}'}]_\pm = [A_{\vec{k}}^\dagger, A_{\vec{k}'}^\dagger]_\pm = 0 . \qquad (4.98)$$

The possible late time (OUT vacuum) commutation relations, expanded in terms of the Bogolubov coefficients are

$$[a_{\vec{k}}, a_{\vec{k}'}^\dagger]_\pm = (|\alpha_k|^2 \pm |\beta_k|^2)\delta_{\vec{k},\vec{k}'} , \qquad (4.99)$$

$$[a_{\vec{k}}, a_{\vec{k}'}]_{\pm} = (\alpha_k \beta_k^* \pm \alpha_k \beta_k^*)\delta_{\vec{k}, -\vec{k}'} .\tag{4.100}$$

For the particles at early times to obey the statistics of particles at late times, with $\beta_k \neq 0$, Bose-Einstein statistics must hold. As $a(t)$ can vary arbitrarily between early and late times and in the general case we have β_k not equal to zero, only Bose-Einstein statistics is consistent with the field equation dynamics of this spin-0 field. Like the mirror case, this connection between dynamics and statistics vanishes if we have $\beta_k = 0$ as when $a(t)$ is constant and spacetime is Minkowskian. Incidentally, Pauli said in his 1940 spin-statistics paper, 'according to our opinion the connection between spin and statistics is one of the most important applications of special relativity'. Using dynamics to explain the spin-statistics connection may be an important facet of quantum field theory under the influence of external conditions.

Chapter 5

Adiabatic Regularization in Anisotropic Spacetimes

5.1 Anisotropic Background with Adiabatic Subtraction

Consider a quantized massive (m) neutral scalar field, $\phi(\vec{x}, t)$ with arbitrary coupling ξ to the scalar curvature, R. The Lagrangian is

$$L = \frac{1}{2}(-g)^{1/2}(g^{\mu\nu}\partial_\mu\phi\partial_\nu\phi - \xi R\phi^2 - m^2\phi^2) , \tag{5.1}$$

and the wave equation is

$$g^{\mu\nu}\nabla_\mu\nabla_\nu\phi + \xi R\phi + m^2\phi = 0 . \tag{5.2}$$

A Bianchi Type I spacetime is an anisotropic homogeneous, spacetime with line element of the form

$$ds^2 = dt^2 - \sum_{i=1}^{3} a_i^2(t)(dx^i)^2 . \tag{5.3}$$

The wave Equation (5.2) for the metric in Equation (5.3) is

$$\partial_0^2 \phi + (\partial_0 a^3 / a^3) \partial_0 \phi - \sum_i a_i^{-2} \partial_i^2 \phi + (\xi R + m^2) \phi = 0 , \tag{5.4}$$

where $a^3 \equiv (-g)^{1/2} = a_1 a_2 a_3$.

The transition to quantum field theory is made by canonical quantization. The usual canonical commutation relations hold for the field and the conjugate momentum, $\pi \equiv \partial L / \partial(\partial_0 \phi) = a^3 \partial_0 \phi$,

$$[\phi(\vec{x}, t), \phi(\vec{x}', t)] = [\pi(\vec{x}, t), \pi(\vec{x}', t)] = 0 , \qquad [\phi(\vec{x}, t), \pi(\vec{x}', t)] = i\delta(\vec{x} - \vec{x}') . \tag{5.5}$$

The field is expanded in terms of mode functions such that

$$\phi = \int d^3 k (a_{\vec{k}} u_{\vec{k}} + a_{\vec{k}}^\dagger u_{\vec{k}}^*) . \tag{5.6}$$

Consider the new time variable $\eta = \int^t a^{-1} dt'$ where $u_k = a^{-1} \chi_k e^{-\vec{k} \cdot \vec{x}}$. The new time variable is such that η satisfies $d\eta = a^{-1} dt$ so that $\partial_0 = a^{-1} \partial_\eta$. Differentiation with respect to η is denoted by a prime or by ∂_η. The quantity χ_k is a solution to the equation

$$\chi_k'' + \left[\Omega^2 + (\xi - 1/6) a^2 R + Q\right] \chi_k = 0 , \tag{5.7}$$

with

$$Q = \frac{1}{18} \sum_{i<j} \left(\frac{a_i'}{a_i} - \frac{a_j'}{a_j}\right)^2 , \tag{5.8}$$

$$R = 6a^{-2} \left(Q + 4\frac{a'^2}{a^2} + 3\frac{a''}{a}\right) , \tag{5.9}$$

$$\Omega^2 \equiv a^2 \omega^2 = a^2 \left(\sum \frac{k_i^2}{a_i^2} + m^2\right) . \tag{5.10}$$

The $a_{\vec{k}}$ will satisfy canonical commutation relations, as long as $\chi_k'^* \chi_k - \chi_k^* \chi_k' = i$. The unrenormalized conformal energy-momentum tensor, $T_\mu{}^\nu$, has been given by Parker [45], while Nacier and Mazzitelli have given it for arbitrary coupling[64]. The expectation value of the energy density component of the generally coupled energy-momentum tensor, $T_\mu{}^\nu$, has been given by Parker [45], while Nacier and Mazzitelli have given it for arbitrary coupling[64]. The expectation value of the energy density component of the generally coupled energy-momentum tensor is

$$\langle T_\eta{}^\eta \rangle = \frac{1}{2a^4 (2\pi)^3} \int d^3k \; \left[|\chi_k'|^2 + (\Omega^2 - 6\xi Q)|\chi_k|^2 + \Xi \right] \; , \tag{5.11}$$

where

$$\Xi \equiv (\xi - \frac{1}{6}) \left[-6\frac{a'^2}{a^2}|\chi_k|^2 + 6\frac{a'}{a}\left(\chi_k' \chi_k^* + \chi_k \chi_k'^* \right) \right] \; . \tag{5.12}$$

Equation (5.11) is infinite and must be renormalized by subtracting the divergent terms. Adiabatic regularization is an efficient method and intuitively clear in physical interpretation. For a quantity such as $\langle T_\eta{}^\eta \rangle$, the subtraction is done mode by mode, for each k in the integrands of relevant quantities like Eqn. (5.11). The terms subtracted are leading terms in an asymptotic expansion of the integrands in powers of a large parameter that represents the "slowness" of the change of the metric. Effectively, one expands in terms of derivatives of the metric. There are three leading terms that suffice for the minimal number of subtractions to make ρ_0 converge to zero in the adiabatic limit, i.e. to make $\langle T_\eta{}^\eta \rangle$ finite. The order of a quantity can be determined by counting the number of derivatives with respect to η which it contains. The terms necessary to renormalize $\langle T_\eta{}^\eta \rangle$ contain zero, two and four time derivatives respectively.

Now we will go into more detail on the subtraction process. Adiabatic regularization calls for an approximate solution of Equation (5.7) of the positive-frequency generalized WKB form:

$$\chi_k(\eta) = \frac{1}{\sqrt{2a(\eta)W_k(\eta)}}\exp[-i\int^{\eta} a(\eta')W_k(\eta')d\eta'] \,. \qquad (5.13)$$

Following Parker, Fulling and Hu (FPH) [45], an appropriate positive function W_k is given by the Chakraborty-method [65], which we use here as well. The basic background method using conformal coupling involves letting a new variable $Y \equiv \Omega^2 + Q$. Later I will generalize to $\xi \neq 1/6$. The Chakraborty-method utilizes

$$W_k = a^{-1}[Y(1 + \underline{\epsilon_2})(1 + \underline{\epsilon_4})]^{1/2} \,, \qquad (5.14)$$

with

$$\underline{\epsilon_2} = -Y^{-3/4}\partial_\eta(Y^{-1/2}\partial_\eta Y^{1/4}) \,, \qquad (5.15)$$

$$\underline{\epsilon_4} = -Y^{-1/2}(1 + \underline{\epsilon_2})^{-3/4}\partial_\eta[Y(1 + \underline{\epsilon_2})]^{-1/2}\partial_\eta[(1 + \underline{\epsilon_2})^{1/4}] \,. \qquad (5.16)$$

Any function W_k which agrees with Eqn. (5.14) up to fourth order in time derivatives of the metric is acceptable. We follow FPH and write

$$\begin{aligned} W_k &= \omega(1 + \underline{\epsilon_2} + Q\Omega^{-2} + \underline{\epsilon_4} + \underline{\epsilon_2}Q\Omega^{-2})^{1/2} \\ &= \omega(1 + \epsilon_2 + \epsilon_4)^{1/2} \,, \end{aligned} \qquad (5.17)$$

where ω is defined in Eqn. (5.10), $\epsilon_2 = \underline{\epsilon_2} + Q\Omega^{-2}$ and $\epsilon_4 = \underline{\epsilon_4} + \underline{\epsilon_2}Q\Omega^{-2}$.

A generalized and improved method for computation with adiabatic regularization is given by Anderson and Eaker [66] and Molina-Paris, Anderson and Ramsey [49] (PAR). This technique involves an analytical approximation which is carried out

by expanding renormalization counterterms in inverse powers of k keeping only terms that are UV divergent. The resulting expressions are $\langle\phi^2\rangle_d$ and $\langle T_{\mu\nu}\rangle_d$, and the renormalized quantities are computed by subtracting and adding the UV divergent terms, for example

$$\langle\phi^2\rangle_R \equiv \langle\phi^2\rangle_n + \langle\phi^2\rangle_{an} \,, \tag{5.18}$$

$$\langle\phi^2\rangle_n \equiv \langle\phi^2\rangle_u - \langle\phi^2\rangle_d \,, \tag{5.19}$$

$$\langle\phi^2\rangle_{an} \equiv \langle\phi^2\rangle_d - \langle\phi^2\rangle_{ad} \,. \tag{5.20}$$

5.2 Fluctuations of a Scalar Field

In this section I derive the renormalization counterterms for $\langle\phi^2\rangle$ in anisotropic space-time with an arbitrary mass. I will also derive an analytical approximation for $\langle\phi^2\rangle$.

5.2.1 $\langle\phi^2\rangle_{ad}$ and Angular Integration of $\epsilon_{2(2)}$

The unrenormalized $\langle\phi^2\rangle_u$ is

$$\langle\phi^2\rangle_u = \frac{1}{(2\pi)^3}\frac{1}{a^2}\int d^3k|\chi|^2 \,. \tag{5.21}$$

In spherical coordinates, this becomes,

$$\langle\phi^2\rangle_u = \frac{1}{(2\pi)^3}\frac{1}{a^2}\int_0^\infty dk k^2 \int d\Omega|\chi|^2 \,, \tag{5.22}$$

where

$$k_i \;=\; k\lambda_i \;, \tag{5.23}$$

$$\sum \lambda_i^2 \;=\; 1 \;, \tag{5.24}$$

$$\lambda_1 \;=\; \sin\theta\cos\phi \;, \tag{5.25}$$

$$\lambda_2 \;=\; \sin\theta\sin\phi \;, \tag{5.26}$$

$$\lambda_3 \;=\; \cos\theta \;, \tag{5.27}$$

such that

$$\int d\Omega \equiv \int_0^{2\pi} \int_0^{\pi} \sin\theta d\theta d\phi \;. \tag{5.28}$$

The adiabatic counterterms $\langle\phi^2\rangle_{ad}$ are calculated by using the field $\chi(\eta)$,

$$\langle\phi^2\rangle_{ad} = \frac{1}{(2\pi)^3} \frac{1}{a^2} \int d^3k |\chi_{ad}|^2 \;. \tag{5.29}$$

We will drop the adiabatic subscripts on the χ field when there is no confusion on when the WKB approximation is being used. Up to second adiabatic order we have,

$$|\chi_{ad}|^2 \approx (2\Omega)^{-1}(1 - \frac{1}{2}\epsilon_{2(2)}) \;, \tag{5.30}$$

which is found in FPH (2.42). The renormalization counterterms are calculated only up to second adiabatic order. It is helpful to first have on hand, the angular integration of the second order terms. We utilize the notation by FPH [45]. We rely heavily on the framework developed in FPH and will commonly refer to their equations. We wish to integrate the angular pieces of $\epsilon_{2(2)}$, where the second subscript indicates adiabatic order. This is

$$\epsilon_{2(2)} = -\frac{1}{4}X^{-2}X'' + \frac{5}{16}X^{-3}(X')^2 + X^{-1}Q \ , \tag{5.31}$$

where

$$
\begin{aligned}
X &= a^2\omega^2 \ , \\
X' &= 2a^2[D\omega^2 + \frac{1}{2}\partial_\eta\omega^2] \ , \\
X'' &= 2a^2[(D' + 2D^2)\omega^2 + 2D\partial_\eta\omega^2 + \frac{1}{2}\partial_\eta^2\omega^2] \ ,
\end{aligned}
\tag{5.32}
$$

with $D \equiv a'/a$. Angular integration using the FPH method gives

$$\int d\Omega \epsilon_{2(2)} = \frac{1}{a^2}\left(\frac{p^4}{\omega^6}L_3 + \frac{p^2}{\omega^4}L_2 + \frac{1}{\omega^2}L_1\right) \ , \tag{5.33}$$

with

$$
\begin{aligned}
L_3 &= 5D^2\pi + 4\pi Q \ , \\
L_2 &= -6D^2\pi + 2D'\pi - 8\pi Q \ , \\
L_1 &= D^2\pi - 2D'\pi + 4\pi Q \ .
\end{aligned}
\tag{5.34}
$$

General coupling may be taken into account by using

$$\Omega_\xi = a(\omega^2 + (\xi - 1/6)R)^{1/2} \approx a\omega(1 + \frac{(\xi - 1/6)R}{2\omega^2}) \ , \tag{5.35}$$

where $\omega^2 = \sum \frac{k_i^2}{a_i^2} + m^2 = p^2 + m^2$ and $R = 6a^{-2}(D' + D^2 + Q)$, and substituting $\Omega \to \Omega_\xi$. Here $p_i = k_i/a_i$. R is second adiabatic order. Converting from k integration to p integration as is done in FPH, we have

$$\langle \phi^2 \rangle_{ad} = \frac{1}{(2\pi)^3} \frac{1}{a^2} a^3 \int_0^\infty dp p^2 \int d\Omega |\chi_{ad}|^2 \ . \tag{5.36}$$

Substituting Eqn. (5.30) and Eqn. (5.35) into Eqn. (5.36) gives

$$\langle \phi^2 \rangle_{ad} = \frac{1}{(2\pi)^3} \frac{1}{2} \int_0^\infty dp \ p^2 \int d\Omega \ (\frac{1}{w} - \frac{\epsilon_{2(2)}}{2\omega} - \frac{(\xi - 1/6)R}{2\omega^3}) \ . \tag{5.37}$$

After substitution of the angular terms as derived previously, and some simplification, one finds

$$\langle \phi^2 \rangle_{ad} = \frac{1}{4\pi^2} \int_0^\infty dp \left[\frac{p^2}{\omega} - \frac{(\xi - 1/6)R}{2} \frac{p^2}{\omega^3} - \frac{1}{8\pi a^2} \left(\frac{p^6}{\omega^7} L_3 + \frac{p^4}{\omega^5} L_2 + \frac{p^2}{\omega^3} L_1 \right) \right] \ . \tag{5.38}$$

5.2.2 Isotropic Limit of Adiabatic Counterterms, $\langle \phi^2 \rangle_{ad}$

In the Robertson-Walker limit, there are several key simplifications. The limit $Q \to 0$ is taken. In order to check with PAR [49] it is also helpful to note that in the isotropic limit, $p \to \frac{k}{a}$, $dp \to \frac{dk}{a}$ and $\omega \to \frac{\overline{\omega_k}}{a}$, where $\overline{\omega}_k^2 = k^2 + a^2 m^2$ is the definition used in PAR as opposed to FPH. It is important not to confuse the frequency notations. Converting ω definitions (which is an isotropic limit) ω (FPH) to $\overline{\omega_k}$ (PAR) and after making the above substitutions we find

$$\langle \phi^2 \rangle_{ad} = \frac{1}{4\pi^2 a^2} \int_0^\infty dk \ k^2 \left[\frac{1}{\overline{\omega_k}} - (\xi - \frac{1}{6}) \frac{a^2 R}{2\overline{\omega_k}^3} + \frac{m^2}{4\overline{\omega_k}^5}(a'^2 + aa'') - \frac{5a^2 a'^2 m^4}{8\overline{\omega_k}^7} \right] \ , \tag{5.39}$$

which is the form found in PAR, [49], for the $\langle \phi^2 \rangle_{ad}$ in the isotropic limit.

5.2.3 $\langle \phi^2 \rangle_{an}$ without Angular Integration

To calculate $\langle \phi^2 \rangle_{an}$ we need $\langle \phi^2 \rangle_d$ as in Eqn. (5.20). In terms of k, using Eqn. (5.29), the counterterms are

$$
\begin{aligned}
\langle \phi^2 \rangle_{ad} &= \frac{1}{(2\pi)^3} \frac{1}{2} \int_0^\infty dk \, k^2 \int d\Omega \, \left(\frac{1}{w} - \frac{\epsilon_{2(2)}}{2\omega} - \frac{(\xi - 1/6)R}{2\omega^3} \right) \\
&= \frac{1}{16a^3\pi^3} \int d\Omega \int_0^\infty dk \left(\frac{k^2}{\omega} + \frac{k^2}{\omega^3} N_1 + \frac{k^4}{\omega^5} N_2 + \frac{k^6}{\omega^7} N_3 \right) , \quad (5.40)
\end{aligned}
$$

where

$$
\begin{aligned}
N_1 &\equiv -\frac{D^2}{8a^2} + \frac{D'}{4a^2} - \frac{Q}{2a^2} - \frac{(\xi - 1/6)R}{2} , \\
N_2 &\equiv -\frac{DZZ'}{4a^2} + \frac{Z'^2}{4a^2} + \frac{ZZ''}{4a^2} , \\
N_3 &\equiv -\frac{5Z^2Z'^2}{8a^2} , \\
\omega^2 &\equiv k^2Z^2 + m^2 , \\
Z^2 &\equiv \sum \frac{\lambda_i^2}{a_i^2} . \quad (5.41)
\end{aligned}
$$

Expanding the integrand in inverse powers of k, and keeping only the divergent terms gives

$$
\langle \phi^2 \rangle_d = \frac{1}{16a^3\pi^3} \int d\Omega \, \frac{1}{Z} \left[\int_0^\infty dk \, k + \int_\epsilon^\infty dk \, \frac{N_4}{k} \right] , \quad (5.42)
$$

where

$$
\begin{aligned}
N_4 &\equiv -\frac{D^2}{8a^2Z^2} + \frac{D'}{4a^2Z^2} - \frac{m^2}{2Z^2} - \frac{Q}{2a^2Z^2} \\
&\quad -\frac{DZ'}{4a^2Z^3} - \frac{5Z'^2}{8a^2Z^4} + \frac{Z'^2 + ZZ''}{4a^2Z^4} - \frac{(\xi - 1/6)R}{2Z^2} . \quad (5.43)
\end{aligned}
$$

Here an introduction of a time independent cutoff, ϵ is used, following PAR. The angular and radial parts separate allowing us to treat the integrals separately. Then

154

using Eqn (5.20), Eqn. (5.40) and Eqn. (5.42), we obtain,

$$\langle \phi^2 \rangle_{an} = \frac{1}{16a^3\pi^3} \int d\Omega \left(M_2 + M_1 \left[1 - \ln\left(\frac{2Z\epsilon}{m}\right) \right] \right) , \tag{5.44}$$

with

$$
\begin{aligned}
M_1 &\equiv -\frac{D^2}{8a^2Z^3} + \frac{D'}{4a^2Z^3} - \frac{m^2}{2Z^3} - \frac{Q}{2a^2Z^3} - \frac{DZ'}{4a^2Z^4} - \frac{3Z'^2}{8a^2Z^5} + \frac{Z''}{4a^2Z^4} - \frac{(\xi - 1/6)R}{2Z^3} , \\
M_2 &\equiv \frac{m^2}{4Z^3} - \frac{DZ'}{12a^2Z^4} - \frac{Z'^2}{4a^2Z^5} + \frac{Z''}{12a^2Z^4} .
\end{aligned}
\tag{5.45}
$$

Isotropic Limit in k

To check the consistency of Eqn (5.44), one may look at the isotropic limit of the fluctuations. Using the isotropic limit for Z and its derivatives, one obtains the following simplifications:

$$M_1 = -\frac{1}{2}a^3(m^2 + (\xi - 1/6)R) , \tag{5.46}$$

$$M_2 = \frac{1}{12}(3a^3m^2 - a'') . \tag{5.47}$$

After the angular integration, we are left with

$$\langle \phi^2 \rangle_{an} = \frac{1}{16a^3\pi^3}[4\pi]\left(M_2 + M_1\left[1 - \ln\left(\frac{2\epsilon}{am}\right) \right] \right) . \tag{5.48}$$

Defining $s \equiv \ln\left[\frac{2\epsilon}{am}\right]$, the isotropic limit of Eqn. (5.44) is

$$\langle \phi^2 \rangle_{an} = -\frac{R}{288\pi^2} - \frac{(\xi - 1/6)R}{8\pi^2}(1 - s) - \frac{m^2}{16\pi^2}(1 - 2s) , \tag{5.49}$$

which is the equivalent to Equation (16a) of PAR.

5.2.4 Evaluation of $\langle\phi^2\rangle_{an}$ for $a_x = a_y$

For arbitrary Bianchi Type I metrics the angular integrations in Eqn. (5.44) are extremely difficult to do. However, they are manageable for spacetimes with $a_x = a_y$. One may perform angular integrations and still preserve anisotropy by setting $a_x = a_y$. The full integration of Eqn. (5.44) in both θ and ϕ gives:

$$\langle\phi^2\rangle_{an} = \frac{3}{288\pi^2 a^5} \frac{\left(T_1 + T_2\left(\ln\left[\frac{2\epsilon}{a_z m}\right]\right) + T_3\ln[G]\right)}{a_z(a_x^2 - a_z^2)^{5/2}} \;, \tag{5.50}$$

where

$$\begin{aligned}
T_1 &= a_x a_z \sqrt{a_x^2 - a_z^2}\left[-2a_x^4 a_x'' a_z + 3a_x a_x'^2 a_z^3 + 2a_x^2 a_x'' a_z^3 - 2a_x^4 a_x' a_z' \right.\\
&\quad - 4a_x' a_z^4 a_z' + a_x^3 a_z a_z'^2 + 2a_x a_z^3 a_z'^2 + 2a_x^3 a_z^2 a_z'' - 2a_x a_z^4 a_z''\\
&\quad + \left(2a_x^4 a_x' a_z - 2a_x^2 a_x' a_z^3 - 2a_x^3 a_z^2 a_z' + 2a_x a_z^4 a_z'\right)D\\
&\quad \left. + \left(6a^2 a_x^5 a_z - 12a^2 a_x^3 a_z^3 + 6a^2 a_x a_z^5\right)m^2\right] \;. \tag{5.51}
\end{aligned}$$

$$\begin{aligned}
T_2 &= \sqrt{a_x^2 - a_z^2}\left[B_2\left(-4a_x'^2 a_z^2 + 4a_x a_x'' a_z^2 + 4a_x a_x' a_z a_z' - 3a_x^2 a_z'^2 + 2a_x^2 a_z a_z''\right)\right.\\
&\quad + 3a_x^2(a_x - a_z)^2 a_z^2(a_x + a_z)^2 B_1\\
&\quad \left. + B_2\left(-4a_x a_x' a_z^2 - 2a_x^2 a_z a_z'\right)D\right] \;. \tag{5.52}
\end{aligned}$$

$$\begin{aligned}
T_3 &= 4a_x^5 a_x'^2 a_z^2 - 4a_x^6 a_x'' a_z^2 - 10a_x^3 a_x'^2 a_z^4 + 10a_x^4 a_x'' a_z^4 + 3a_x a_x'^2 a_z^6 - 6a_x^2 a_x'' a_z^6\\
&\quad - 4a_x^6 a_x' a_z a_z' + 10a_x^4 a_x' a_z^3 a_z' + 3a_x^7 a_z'^2 - 6a_x^5 a_z^2 a_z'^2 - 2a_x^7 a_z a_z'' + 2a_x^5 a_z^3 a_z''\\
&\quad - a_x\left(3a_x^6 a_z^2 - 6a_x^4 a_z^4 + 3a_x^2 a_z^6\right)B_1\\
&\quad + \left(4a_x^6 a_x' a_z^2 - 10a_x^4 a_x' a_z^4 + 6a_x^2 a_x' a_z^6 + 2a_x^7 a_z a_z' - 2a_x^5 a_z^3 a_z'\right)D \;. \tag{5.53}
\end{aligned}$$

$$B_1 = D^2 - 2D' + 4Q + 4a^2 \left[m^2 + (\xi - \frac{1}{6})R \right] . \tag{5.54}$$

$$B_2 = (a_x - a_z)^2 (a_x + a_z)^2 . \tag{5.55}$$

$$G = \frac{-a_z^2 + a_x(a_x + \sqrt{a_x^2 - a_z^2})}{a_z \sqrt{a_x^2 - a_z^2}} . \tag{5.56}$$

In the isotropic limit Eqn. (5.50) approaches Eqn. (5.49).

5.3   Energy Density of a Scalar Field

In this section I will calculate the renormalization counterterms for the energy density components of the stress tensor. This is done with general coupling to the scalar curvature, first to second adiabatic order then to fourth adiabatic order. I verify the result in the limit of conformal coupling and in the isotropic limit.

5.3.1   Adiabatic Regularization to Second Order

As an illustration of the calculation of the renormalization counterterms for the energy density to fourth order, we proceed by calculating up to second order first. The energy density component of the stress tensor, for an arbitrary coupled scalar field in a Bianchi Type I spacetime is given by (see Nacir-Mazzitelli 2007)[64]:

$$\langle T_\eta{}^\eta \rangle = \frac{1}{2a^4(2\pi)^3} \int d^3k \; \left[|\chi_k'|^2 + \Omega^2 |\chi_k|^2 + T_c \right] , \tag{5.57}$$

with

$$T_c = \left[-6\xi \left(\frac{a'^2}{a^2} + Q \right) + \frac{a'^2}{a^2} \right] |\chi_k|^2 + 6\frac{a'}{a} \left(\xi - \frac{1}{6} \right) \left(\chi_k' \chi_k^* + \chi_k \chi_k'^* \right) . \tag{5.58}$$

To second order, we will need (from FPH)

$$|\chi_k|^2 = (2aW)^{-1} \approx (2\Omega)^{-1}$$

$$\chi_k'\chi_k^* + \chi_k\chi_k'^* = -\frac{W_k'}{2W_k^2} \approx -\frac{\Omega'}{2\Omega^2} \,, \tag{5.59}$$

which is all that is required to obtain second adiabatic order. Substituting these expressions into Eqn. (5.58) and keeping terms up to and including second order, we find

$$T_c = \left[-6\xi\left(\frac{a'^2}{a^2} + Q\right) + \frac{a'^2}{a^2}\right](2\Omega)^{-1} - 6\frac{a'}{a}\left(\xi - \frac{1}{6}\right)\frac{\Omega'}{2\Omega^2} \tag{5.60}$$

$$= \left(\frac{a'^2}{a^3\omega} - \frac{6a'^2\xi}{a^3\omega} - \frac{3Q\xi}{a\omega}\right) + \partial_\eta\omega^2\left(\frac{a'}{4a^2\omega^3} - \frac{3a'\xi}{2a^2\omega^3}\right) \,, \tag{5.61}$$

having used $\Omega = a\omega$, Eqn (5.10). The contribution of this term to the energy density is

$$\langle T_\eta{}^\eta\rangle_c \equiv \frac{1}{2a(2\pi)^3}\int d^3p\, T_c \,, \tag{5.62}$$

with $d^3k = a^3 d^3p$. Performing the angular integration, using the FPH method, gives

$$\langle T_\eta{}^\eta\rangle_c \equiv -\frac{1}{4\pi^2a^2}\int_0^\infty dp\, p^2\left[\left(\xi - \frac{1}{6}\right)\left(\frac{3}{\omega}(Q + D^2) + \frac{3D^2m^2}{\omega^3}\right) + \frac{Q}{2\omega}\right] \,, \tag{5.63}$$

with mass, $\omega^2 = p^2 + m^2$. Combining these terms with the conformally coupled terms gives the fully generally coupled energy density of second order:

$$\rho_{0(2)} = -(96\pi^2)^{-1}m^4\int \omega^{-5}p^2 dp\, G_0{}^0$$

$$-(160\pi^2)^{-1}\int \omega^{-5}p^2(16p^4 + 40m^2p^2 + 15m^4)dp a^{-2}Q \tag{5.64}$$

$$-\frac{1}{4\pi^2a^2}\int_0^\infty dp\, p^2\left[\left(\xi - \frac{1}{6}\right)\left(\frac{3}{\omega}(Q + D^2) + \frac{3D^2m^2}{\omega^3}\right)\right] \,, \tag{5.65}$$

where $G_0{}^0 = 3a^{-2}(-D^2 + Q)$. The original derivation of the conformally coupled second order term was given by FPH [45], Equation (3.3).

5.3.2 Adiabatic Regularization to Fourth Order

This section contains the calculation of the fourth order piece of the energy density. I will only discuss terms which vanish in the $\xi \to 1/6$ limit because the other terms have been computed by FPH. Care must be given to keep track of the $|\chi_k'|^2 + \Omega^2|\chi_k|^2$ pieces, which include terms proportional to $(\xi - 1/6)$. The term $\Omega^2|\chi_k|^2$ up to fourth order is

$$\Omega^2|\chi_k|^2\Big|_{c(4)} = a^2 w^2 \left[\left(\frac{\epsilon_{2(2)}}{8a\omega^3} - \frac{1}{4a\omega^3} \right) (\xi - 1/6)R + \frac{3}{16a\omega^5}((\xi - 1/6)R)^2 \right] . \quad (5.66)$$

The term $|\chi_k'|^2$ up to fourth order with just the $(\xi - 1/6)$ terms is

$$\begin{aligned}
|\chi_k'|^2\Big|_{c(4)} &= \left(-\frac{a'^2}{16a^3\omega^3} + \frac{a}{4\omega} + \frac{a\epsilon_{2(2)}}{8\omega} - \frac{3a'\omega'}{8a^2\omega^4} - \frac{5\omega'^2}{16a\omega^5} \right) (\xi - 1/6)R \\
&\quad - \frac{a}{16\omega^3}((\xi - 1/6)R)^2 + \left(\frac{a'}{8a^2\omega^3} + \frac{\omega'}{8a\omega^4} \right) (\xi - 1/6)R' , \quad (5.67)
\end{aligned}$$

with

$$R' = \frac{1}{a^2} \left(-12D^3 + 6D'' - 12DQ + 6Q' \right) . \quad (5.68)$$

Next, we substitute χ_k into the first piece of T_c, Eqn (5.58), $\left[-6\xi \left(\frac{a'^2}{a^2} + Q \right) + \frac{a'^2}{a^2} \right] |\chi_k|^2$.
The relevant terms up to fourth order are

$$
\left[Q \left(\frac{3D^2}{2a^3\omega^3} + \frac{3D'}{2a^3\omega^3} - \frac{3}{a\omega} \right) + \epsilon_{2(2)} \left(\frac{3D^2}{2a\omega} + \frac{3Q}{2a\omega} \right) + \frac{3Q^2}{2a^3\omega^3} - \frac{3D^2}{a\omega} \right] (\xi - \frac{1}{6})
$$
$$
+ \left[Q \left(\frac{18D^2}{a^3\omega^3} + \frac{9D'}{a^3\omega^3} \right) + \frac{9D^4}{a^3\omega^3} + \frac{9D^2D'}{a^3\omega^3} + \frac{9Q^2}{a^3\omega^3} \right] (\xi - \frac{1}{6})^2 . \tag{5.69}
$$

It is also a tedious but straightforward matter to calculate the term

$$
6\frac{a'}{a} \left(\xi - \frac{1}{6} \right) \left(\chi'_k \chi_k^* + \chi_k \chi'^*_k \right) , \tag{5.70}
$$

to fourth order for the $(\xi - 1/6)$ terms only. Using the FPH angular integration method and combining all pieces, the terms proportional to $(\xi - 1/6)$ are

$$
\rho_0|_c = (32\pi^2 a^4)^{-1} \int_0^\infty dp \, \{
$$
$$
(\xi - 1/6) \left[\, p^8 \omega^{-9} \left(-105D^4 - 252D^2Q + 48DS \right) \right.
$$
$$
+ p^6 \omega^{-7} \left(210D^4 - 60D^2D' + 519D^2Q + 12Q^2 - 24DQ' - 96DS \right)
$$
$$
+ p^4 \omega^{-5} \left(-105D^4 + 96D^2D' + 6D'^2 - 12DD' \right)
$$
$$
+ p^4 \omega^{-5} \left(-330D^2Q' - 12D'Q - 48Q^2 + 30DQ' + 48DS \right)
$$
$$
+ p^4 \omega^{-3} \left(24a^2D^2 \right)
$$
$$
+ p^2 \omega^{-3} \left(-36D^2D' - 6D'^2 + 12DD'' + 63D^2Q + 12D'Q + 36Q^2 - 6DQ' \right)
$$
$$
+ p^2 \omega^{-1} \left(-48a^2D^2 - 24a^2Q \right) \,]
$$
$$
+ (\xi - 1/6)^2 \left[\, p^4 \omega^{-5} \left(-216D^4 - 216D^2D' - 216D^2Q \right) \right.
$$
$$
+ p^2 \omega^{-3} \left(324D^4 + 216D^2D' + 36D'^2 - 72DD'' \right)
$$
$$
+ p^2 \omega^{-3} \left(+432D^2Q + 144D'Q + 108Q^2 - 72DQ' \right) \,] \, \} . \tag{5.71}
$$

These are only the terms that vanish in the conformal limit. I have also computed the terms, ρ_0^{FPH}, which do not vanish in the conformal limit to fourth order. I have checked that they agree with those derived by FPH, but the result is too long to show here. The energy density counterterms are

$$\langle T_\eta{}^\eta \rangle_{ad} = \rho_0^{FPH} + \rho_0\big|_c \ . \tag{5.72}$$

5.3.3 Isotropic Limit of Fourth Order Energy Density Terms

In the isotropic limit it is clear that the quantities, $Q, Q', Q'', U, S, S' \to 0$. Converting to k-momentum via $p \to k/a$ and making the correct frequency conversion $\omega \to \overline{\omega_k}/a$ gives

$$\rho_0^{iso}\big|_c = \frac{1}{4\pi^2 a^4} \int_0^\infty dk \ k^2 \bigg\{ \tag{5.73}$$

$$(\xi - 1/6)^2 \left[\frac{27a'^2 a'' m^2}{a\overline{\omega_k}^5} - \frac{9}{2\overline{\omega_k}^3} \left(\frac{2a''' a'}{a^2} - \frac{a''^2}{a^2} - \frac{4a'' a'^2}{a^3} \right) \right] \tag{5.74}$$

$$+ (\xi - 1/6) \left[\frac{105a^2 a'^4 m^6}{8\overline{\omega_k}^9} - \frac{15m^4 a^4}{8\overline{\omega_k}^7} \left(\frac{4a'' a'^2}{a^3} + 3\frac{a'^4}{a^4} \right) \right. \tag{5.75}$$

$$\left. + \frac{3m^2 a^2}{4\overline{\omega_k}^5} \left(\frac{2a''' a'}{a^2} - \frac{a''^2}{a^2} - \frac{a'^4}{a^4} \right) - \frac{3}{\overline{\omega_k}} \frac{a'^2}{a^2} - \frac{3m^2 a'^2}{\overline{\omega_k}^3} \right] \bigg\} \ . \tag{5.76}$$

In the isotropic limit of the coupled terms, $\rho_0\big|_c$, this agrees with that of the Anderson and Parker [48] Eqn. (2.10a). I have confirmed that ρ_0^{FPH} and my expression for the conformal energy density up to fourth order are in agreement. I have confirmed that $\rho_0\big|_c$, give the Robertson-Walker energy density terms in the isotropic limit as first presented by Bunch in [50].

Chapter 6

Conclusions

In this thesis, quantum effects under the influence of external conditions have been studied. These external conditions include moving mirror and curved spacetime with anisotropy. A focus on the tools within the quantum field theory in curved spacetime framework has made it possible to scrutinize the basic nature of particle and energy production for moving mirrors. The same tools have helped identify the stress-energy-momentum tensor of the quantized field which acts as the source of gravity in the anisotropic case. The main results in this thesis include: (1) two analytically known COAST mirror trajectories, (2) particle localization in time and frequency from the COAST mirror trajectories, (3) explicit Carlitz-Willey trajectory and acceleration, (4) three exact diverging-acceleration mirror trajectories, (5) renormalization counterterms for $\langle \phi^2 \rangle$ in an arbitrary Bianchi Type I anisotropic spacetime, (6) renormalization counterterms for energy density $\langle T_\eta{}^\eta \rangle$ and (7) an analytical approximation for $\langle \phi^2 \rangle$ for a limited class of Bianchi Type I spacetimes.

First, two COAST mirrors have been introduced, i.e. asymptotically inertial moving mirror trajectories which attain a constant, coasting velocity at late times (Darcx

and Proex). These un-spliced trajectories (COnstant-velocity ASymptotic Trajectories) avoid delta function spikes in energy production. Their Bogolubov transformation coefficients, energy flux, and total energy production have been exactly and analytically computed. Particle production is computed numerically, by computing the occupation number in these non-trivial cases. These are the first coasting moving mirror solutions to be introduced and studied. I have solved for other relevant physical quantities associated with the motion of these trajectories. These non-asymptotically static, yet still asymptotically inertial trajectories produce negative energy flux.

Consider some characteristics of importance that these COAST mirror solutions have: (1) COAST trajectories mimic a type of backreaction, as the total energy emitted is finite. A principal consequence of back reaction effects of the radiated energy on the background geometry of a black hole should be to provide a finite result for the total radiated energy. (2) These COAST mirrors provide a model in which particle production is similar in nature to that of a black hole that forms and then evaporates. The possible end-phase of the evaporating black hole leaves a left-over entity that red-shifts field modes. This object has no horizon and saps the evaporating particle energy, reducing particle production to zero. This left-over object asymptotically delays the creation of particles indefinitely, and may be called a 'black hole remnant' [35][67]. (3) By construction, the COAST mirror geometry allows all incident waves from I_R^- to be reflected to I_R^+, preserving unitarity and preserving information. (4) The emitted energy flux is not always positive. Both Darcx and Proex exhibit extended periods of negative energy flux emission. (5) From the general properties of COAST trajectories, it is known that there are correlations in the stress-tensor of the quantum field larger than the vacuum ones in connection with unitarity and negative fluxes [23]. Work is in progress to compute the correlations

associated with Darcx and Proex.

Second, the spectrum of particle creation from these trajectories has been examined in a time evolved way by utilizing wavepackets. The total energy production is confirmed in three ways: by calculating total energy production via the stress tensor energy flux, by summing quanta, and by summing energy packets. The time analysis of the emitted spectrum is verified by the agreement of the total summation of energy packets with the total energy produced. The time-evolution of the particle spectra reveals an onset of particle creation that builds up to a maximum emission and then settles down, ceasing to radiate in the far future.

The importance of being able to time evolve COAST mirror trajectories manifests itself through the discovery that particle creation can be partially localized at all times during motion, including early times. No late-time assumptions are made and therefore no questionable approximations (i.e. disregarding boundary terms, asymptotic trajectory forms or high frequency integral boundary limits) are needed. As a possible extension for this program the time evolution may give insight into the particle/energy connection during periods of negative energy flux.

I presented the 'never-before-seen' explicit forms of both the trajectory and the acceleration of the Carlitz-Willey trajectory that results in a constant energy flux and thermal emission for all times. I have used wavepackets to obtain time-resolved spectra and found them to be Planckian. The Planck spectrum has been obtained for the first time using this approach on the Carlitz-Willey trajectory, in contrast to the Planck spectrum result from the density matrix or correlation calculations.

The importance of the results of the explicit Carlitz-Willey trajectory include: (1)

The connection to the Unruh effect is further distinguished. As is shown, time-dependent acceleration is responsible for the thermal dynamical Casimir effect. Compare this to the time-*independent* acceleration of the thermal Unruh effect. (2) Attention is given to the mathematical relevance of the product log function for the physically relevant constant energy flux and thermal emission due to the mirror's motion. (3) Transcendental inversions (necessary for the Carlitz-Willey Trajectory) are analytically tractable for some ray-tracing functions relevant to the moving mirror model.

I found three static-start future-horizon mirrors whose beta coefficients and energy flux can be computed exactly: Arcx, Logex, Omex. This is in contrast to the Davies-Fulling trajectory which is solved only for late times and is spliced (non-smooth joining or C^1 joining with a resulting δ-function pulse in the energy flux). These mirror trajectories have added a number of new refinements to the moving mirror model (no splicing, no δ pulses, no late-time approximations). Each of the three trajectories acts as a model in which the Bogoliubov transformation, which is induced by the moving boundary, can be computed explicitly. These exactly soluble trajectories with acceleration singularities (a proper acceleration that approaches infinity in the far future that results in the Plankian spectrum) mimic the particle production that occurs when a black hole forms from gravitational collapse but backreaction effects are not taken into account.

There are several reasons why these trajectories with asymptotically diverging acceleration are important: (1) They have potential for particle production to be localized with an appropriate packetization procedure. (2) They provide characteristic exact, simple solutions for asymptotic thermal radiation in the moving mirror model. (3) It may be possible to map to dilaton black hole spacetimes. Identifying the center of collapse of the black hole as the location of the moving mirror, one may

165

precisely formulate gravitational collapse in the mirror framework [67]. (4) They avoid δ-function pulses in flux from joined trajectories or non-smooth splicing. (5) These diverging acceleration mirrors have no vanishing flux (as in the hyperbolic case) and (6) no approximations (obscure or otherwise) are needed for either the transformation coefficients or the energy flux because these are not solely late-time trajectories.

In curved spacetime, I have two main results. I found an analytical approximation for $\langle \phi^2 \rangle$ for a scalar field with arbitrary mass and curvature coupling in Bianchi Type I anisotropic spacetimes with $a_x = a_y \neq a_z$. I have calculated the renormalization counter terms for the energy density in the case of arbitrary curvature coupling ξ for an arbitrary Bianchi Type I spacetime. Previously, this had just been done for $\xi = 1/6$. Extensions of this work could be (1) an analytic approximation for the energy density when $a_x = a_y$. (2) A numerical computation of the full renormalized energy density in any specific Bianchi Type I spacetime is now possible. (3) Renormalization counterterms could be calculated for the pressure in various directions. Then these quantities could be computed numerically, and one could solve the semi-classical backreaction equations to investigate the dissipation of anisotropy due to particle production[37] [39] [40] [41] [42].

Extensions for the moving mirror model include calculations of the energy emission correlation ratios as discussed briefly in subsection 2.1.5. These are straightforward calculations that could reveal interesting behavior of the energy emission that the stress-energy-momentum tensor and particle count alone could not tell us. One may also compute the production of entropy using correlations with the Wilczek definition [35] or using the trajectories themselves with the Mukohyama-Israel definition [13]. Exact, trajectory-specific calculations of vacuum-excess (subsection 2.1.5)

correlations during negative energy flux emission may reveal more about an entropy interpretation. Possible divergences of energy correlations could point to a breakdown of the semiclassical approximation. Mapping these COAST mirror trajectories to dilaton black hole geometries could give insight into the effects of particle production for these models.

Bibliography

[1] H. B. G. Casimir. On the Attraction Between Two Perfectly Conducting Plates. *Indag. Math.*, 10:261–263, 1948.

[2] Gerald T. Moore. Quantum theory of the electromagnetic field in a variable-length one-dimensional cavity. *Journal of mathematical physics, 1970.*

[3] S. W. Hawking. Particle Creation by Black Holes. *Commun. Math. Phys.*, 43:199–220, 1975.

[4] Bryce S. DeWitt. Quantum Field Theory in Curved Space-Time. *Phys. Rept.*, 19:295–357, 1975.

[5] P. C. W. Davies and S. A. Fulling. Radiation from a moving mirror in two-dimensional space- time conformal anomaly. *Proc. Roy. Soc. Lond.*, A348:393–414, 1976.

[6] P. C. W. Davies and S. A. Fulling. Radiation from Moving Mirrors and from Black Holes. *Proc. Roy. Soc. Lond.*, A356:237, 1977.

[7] W. G. Unruh. Notes on black hole evaporation. *Phys. Rev.*, D14:870, 1976.

[8] P. Candelas and D. Deutsch. On the vacuum stress induced by uniform acceleration or supporting the ether. *Proc. Roy. Soc. Lond.*, A354:79–99, 1977.

[9] L. H. Ford and Alexander Vilenkin. Quantum Radiation by Moving Mirrors. *Phys. Rev.*, D25:2569, 1982.

[10] W. G. Unruh and Robert M. Wald. Acceleration Radiation and Generalized Second Law of Thermodynamics. *Phys. Rev.*, D25:942–958, 1982.

[11] Robert D. Carlitz and Raymond S. Willey. Reflections on Moving Mirrors. *Phys. Rev.*, D36:2327, 1987.

[12] Ramin Golestanian and Mehran Kardar. Path Integral Approach to the Dynamic Casimir Effect with Fluctuating Boundaries. *Phys. Rev.*, A58:1713–1722, 1998.

[13] Shinji Mukohyama and Werner Israel. Moving-mirror entropy. *Phys. Rev.*, D62:121501, 2000.

[14] Don N. Page. Black Hole Configurations with Total Entropy Less than A/4, gr-qc/0101009. 2000.

[15] W. R. Walker. Particle and Energy Creation by Moving Mirrors. *Phys. Rev.*, D31:767, 1985.

[16] Adam D. Helfer. Moving mirrors and thermodynamic paradoxes. *Phys. Rev.*, D63:025016, 2001.

[17] W. R. Walker. Negative Energy Fluxes and Moving Mirrors in Curved Space. *Class. Quant. Grav.*, 2:L37, 1985.

[18] P. C. W. Davies. Can Moving Mirrors Violate the Second Law of Thermodynamics? *Phys. Lett.*, B113:215, 1982.

[19] N. D. Birrell and P. C. W. Davies. Quantum Field in Curved Space. Cambridge, Uk: Univ. Pr. (1982) 340p.

[20] Leonard Parker and David Toms. Quantum field theory in curved spacetime: quantized fields and gravity. Cambridge Univ. Press, Cambridge, 2009.

[21] Robert M. Wald. Quantum field theory in curved space-time and black hole thermodynamics. Chicago, USA: Univ. Pr. (1994) 205 p.

[22] S. A. Fulling. Aspects of Quantum Field Theory in Curved Space-time. *London Math. Soc. Student Texts*, 17:1–315, 1989.

[23] A. Fabbri and J. Navarro-Salas. Modeling black hole evaporation. London, UK: Imp. Coll. Pr. (2005) 334 p.

[24] C. Braggio, G. Bressi, G. Carugno, C. Del Noce, G. Galeazzi, A. Lombardi, A. Palmieri, G. Ruoso, and D. Zanello. A novel experimental approach for the detection of the dynamical casimir effect. *EPL (Europhysics Letters)*, 70(6):754, 2005.

[25] Woo-Joong Kim, James Hayden Brownell, and Roberto Onofrio. Detectability of dissipative motion in quantum vacuum via superradiance. *Phys. Rev. Lett.*, 96(20):200402, May 2006.

[26] Kimball A. Milton and Y. Jack Ng. Observability of the bulk Casimir effect: Can the dynamical Casimir effect be relevant to sonoluminescence? *Phys. Rev.*, E57:5504–5510, 1998.

[27] C.M. et al. Wilson. Observation of the Dynamical Casimir Effect in a Superconducting Circuit, arXiv:1105.4714v1[quant-ph]. 2011.

[28] Kimball A. Milton. The Casimir effect: Recent controversies and progress. *J.Phys.A*, A37:R209, 2004.

[29] S. A. Fulling. Review of some recent work on acceleration radiation. *Journal of Modern Optics*, 52:2207–2213, 2005.

[30] A. Calogeracos. Radiation from perfect mirrors starting from rest and accelerating forever and the black body spectrum. *J. Phys.*, A35:3435–3446, 2002.

[31] A. Calogeracos. Radiation from accelerated perfect or dispersive mirrors following prescribed relativistic asymptotically inertial trajectories. 2001.

[32] A. Calogeracos. Radiation from perfect mirrors following prescribed relativistic trajectories. *Int. J. Mod. Phys. ,A17*, page 1018, 2002.

[33] P G Grove. On the detection of particle and energy fluxes in two dimensions. *Classical and Quantum Gravity*, 3(5):793, 1986.

[34] W R Walker and P C W Davies. An exactly soluble moving-mirror problem. *Journal of Physics A: Mathematical and General*, 15(9):L477, 1982.

[35] Frank Wilczek. Quantum purity at a small price: Easing a black hole paradox, hep-th/9302096 . 1993.

[36] M. Dorca and E. Verdaguer. Wave packet quantization in flat space with a moving mirror. Prepared for Proceedings of the Relativity Meeting '93: Relativity in General, Salas, Spain, 7-10 Sep 1993.

[37] B. L. Hu and L. Parker. Anisotropy Damping Through Quantum Effects in the Early Universe. *Phys. Rev.*, D17:933–945, 1978.

[38] Ya.B. Zeldovich and Alexei A. Starobinsky. Particle production and vacuum polarization in an anisotropic gravitational field. *Sov.Phys.JETP*, 34:1159–1166, 1972.

[39] J.B. Hartle and B.L. Hu. Quantum Effects in the Early Universe. III. Dissipation of Anisotropy by Scalar Particle Production . *Phys.Rev.*, D21:2756–2769, 1980.

[40] J.B. Hartle and B.L. Hu. Quantum Effects in the Early Universe. 2. Effective Action for Scalar Fields in Homogeneous Cosmologies with Small Anisotropy. *Phys.Rev.*, D20:1772–1782, 1979.

[41] J.B. Hartle. Quantum Effects in the Early Universe. IV. *Phys.Rev.*, D22:2091–2095, 1980.

[42] E. Calzetta and B.L. Hu. Closed Time Path Functional Formalism in Curved Space-Time: Application to Cosmological Back Reaction Problems. *Phys.Rev.*, D35:495, 1987.

[43] L. Parker. PhD. Thesis. *Harvard University.*, 1966.

[44] S.A. Fulling and L. Parker. Renormalization in the theory of a quantized scalar field interacting with a robertson-walker spacetime. *Annals Phys.*, 87:176–204, 1974.

[45] S.A. Fulling, Leonard Parker, and B.L. Hu. Conformal energy-momentum tensor in curved spacetime: Adiabatic regularization and renormalization. *Phys.Rev.*, D10:3905–3924, 1974.

[46] Leonard Parker and S.A. Fulling. Adiabatic regularization of the energy momentum tensor of a quantized field in homogeneous spaces. *Phys.Rev.*, D9:341–354, 1974.

[47] N.D. Birrell. The Application of Adiabatic Regularization to Calculations of Cosmological Interest. *Proc. Roy. Soc. London*, B361:513, 1978.

[48] Paul R. Anderson and Leonard Parker. Adiabatic Regularization in Closed Robertson-Walker Universes. *Phys.Rev.*, D36:2963, 1987.

[49] Carmen Molina-Paris, Paul R. Anderson, and Stephen A. Ramsey. One-loop $\lambda\phi^4$ field theory in Robertson-Walker spacetimes: Adiabatic regularization and analytic approximations. *Phys.Rev.*, D61:127501, 2000.

[50] T S Bunch. Adiabatic regularisation for scalar fields with arbitrary coupling to the scalar curvature. *Journal of Physics A: Mathematical and General*, 13(4):1297, 1980.

[51] M. Reuter and C. T. Hill. Moving Mirrors in Schrodinger Picture. *Ann. Phys.*, 195:190, 1989.

[52] A. Zee. Quantum field theory in a nutshell. *Princeton University Press*, 2003.

[53] Charles W. Misner, K.S. Thorne, and J.A. Wheeler. Gravitation. *W. H. Freeman; First Edition edition*, 1974.

[54] W. Rindler. Relativity: Special, general, and cosmological. *Clarendon Press, Oxford*, 2006.

[55] W. Rindler. Kruskal Space and the Uniformly Accelerated Frame. *Am.J.Phys.*, 34:1174, 1966.

[56] H. Nyquist. Thermal Agitation of Electric Charge in Conductors. *Phys. Rev.*, 32:110–113, 1928.

[57] H. Epstein, V. Glaser, and A. Jaffe. Nonpositivity of the energy density in quantized field theories. *Il Nuovo Cimento (1955-1965)*, 36:1016–1022, 1965. 10.1007/BF02749799.

[58] N. Obadia and R. Parentani. Uniformly accelerated mirrors. I: Mean fluxes. *Phys. Rev.*, D67:024021, 2003.

[59] A. Fabbri, J. Navarro-Salas, and Gonzalo J. Olmo. Particles and energy fluxes from a CFT perspective. *Phys. Rev.*, D70:064022, 2004.

171

[60] Claude W. Bernard and Anthony Duncan. Regularization and Renormalization of Quantum Field Theory in Curved Space-Time. *Ann. Phys.*, 107:201, 1977.

[61] Leonard Parker and Yi Wang. Statistics from dynamics in curved spacetime. *Phys. Rev. D*, 39(12):3596–3605, Jun 1989.

[62] Robert M. Wald. Existence of the S Matrix in Quantum Field Theory in Curved Space-time. *Annals Phys.*, 118:490–510, 1979.

[63] Rafael Sorkin. Particle Statistics in Three-Dimensions. *Phys.Rev.*, D27:1787, 1983.

[64] Diana Lopez Nacir and Francisco D. Mazzitelli. New counterterms induced by trans-Planckian physics in semiclassical gravity. *Phys.Rev.*, D78:044001, 2008.

[65] B. Chakraborty. The mathematical problem of reflection solved by an extension of the wkb method. *Journal of Mathematical Physics*, 14(2):188–190, 1973.

[66] Paul R. Anderson and Wayne Eaker. Analytic approximation and an improved method for computing the stress energy of quantized scalar fields in Robertson-Walker space-times. *Phys.Rev.*, D61:024003, 2000.

[67] M. Hotta, M. Shino, and M. Yoshimura. Moving mirror model of Hawking evaporation. *Prog. Theor. Phys.*, 91:839–870, 1994.